THE EFFECT OF THE GALAXY-HALO CONNECTION ON GALAXY CLUSTERING IN THE ADVENT OF STAGE-IV EXPERIMENTS

SANTIAGO ÁVILA

LINEA WEBINAR, 8-APR-2021

INDEX

PART 1.
LSS, MOTIVATION

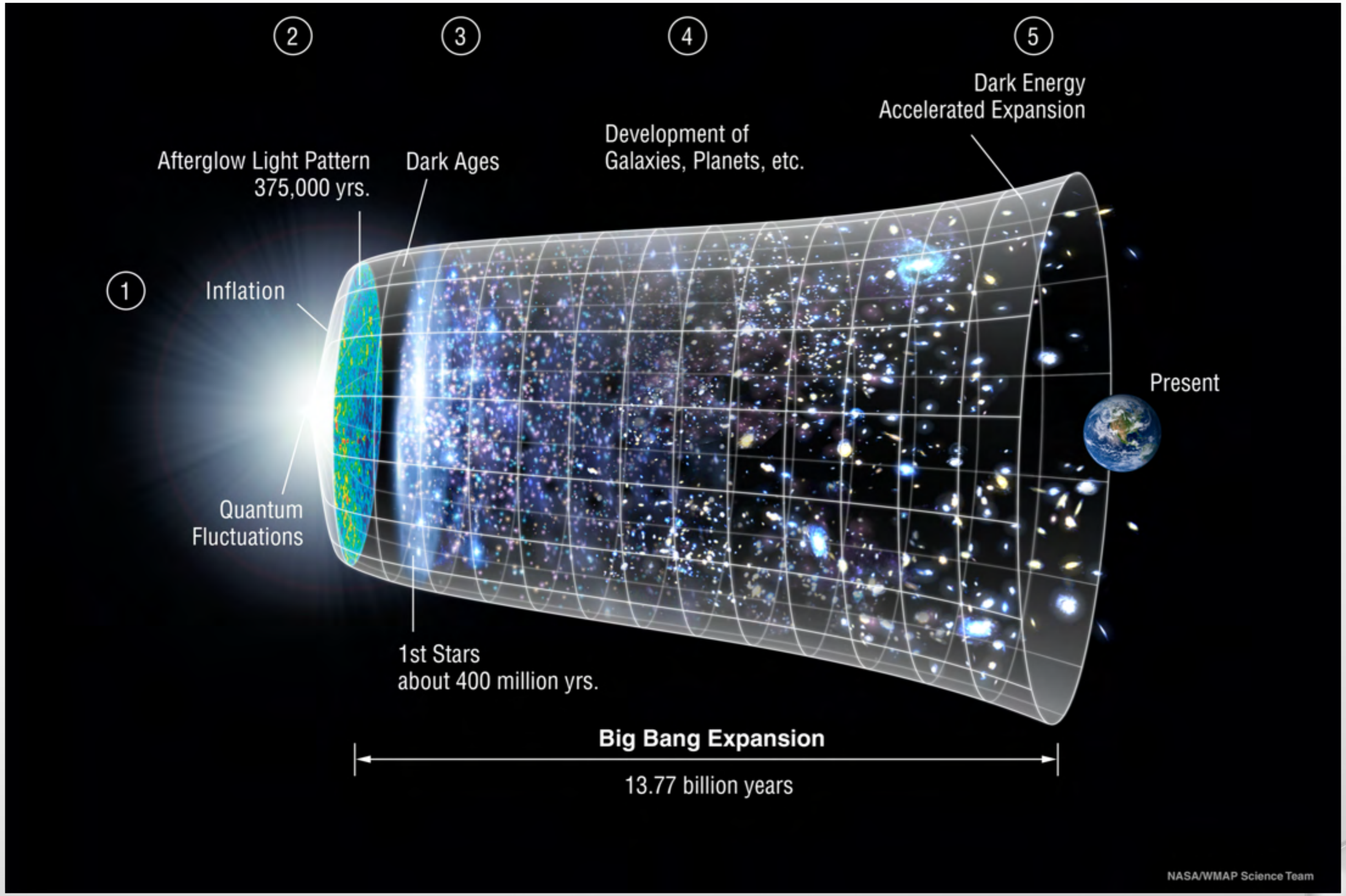

BARYONIC ACOUSTIC OSCILLATIONS

- The early universe is made of a hot baryon-photon plasma
- Untill the temperature drops below 13.6ev and matter becomes neutral

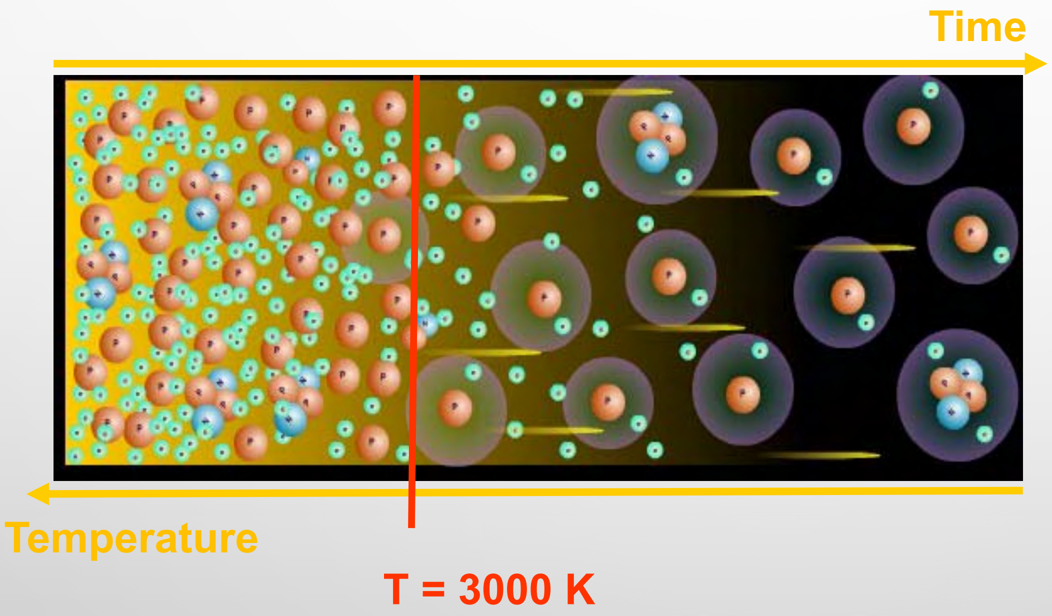

BARYONIC ACOUSTIC OSCILLATIONS

- The early universe is made of a hot baryon-photon plasma
- Untill the temperature drops below 13.6ev and matter becomes neutral

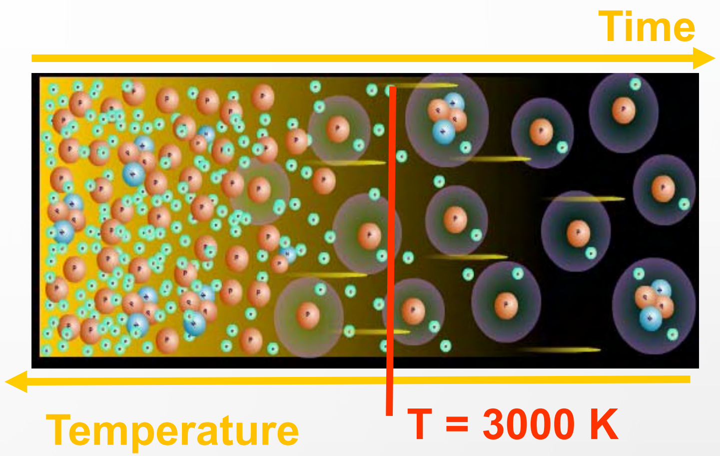

- Sound waves propagate in the primordial plasma
  untill baryons decouple: the Baryonic Accoustic Oscillations.
- This leaves a preferred scale in the distribution of matter in the Universe.
- From decoupling, the BAO simply evolves with the expanding Universe

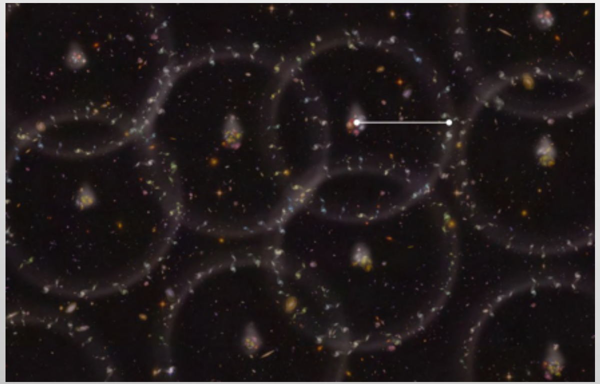

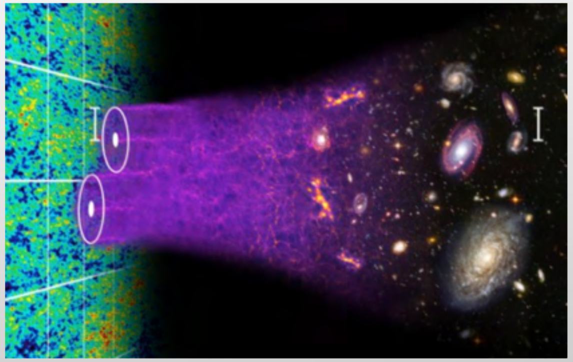

BARYONIC ACOUSTIC OSCILLATIONS

- BAO can be found in the 2PCF of the CMB or the distribution of galaxies in the Universe (LSS)
- For galaxies, BAO is seen as an excess of pairs separated by ~100Mpc/h

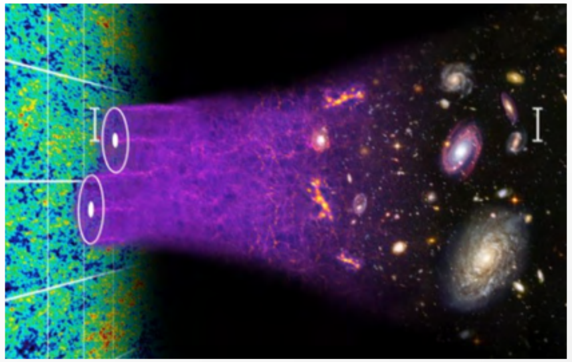

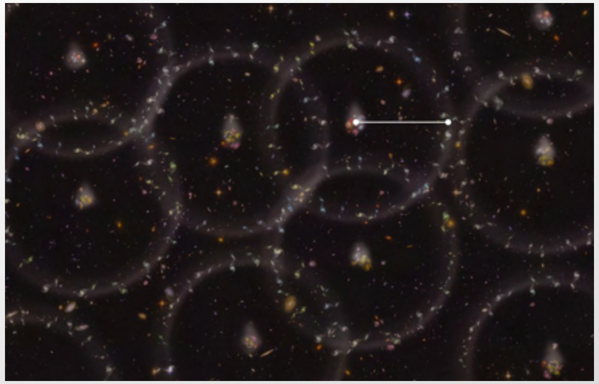

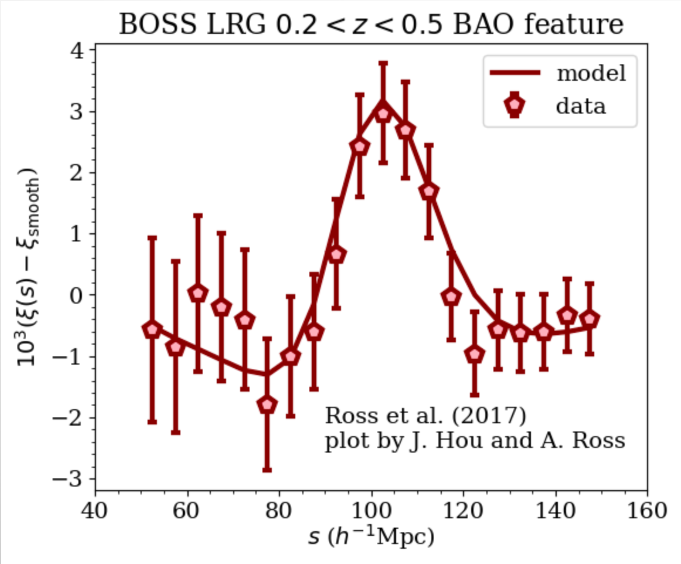

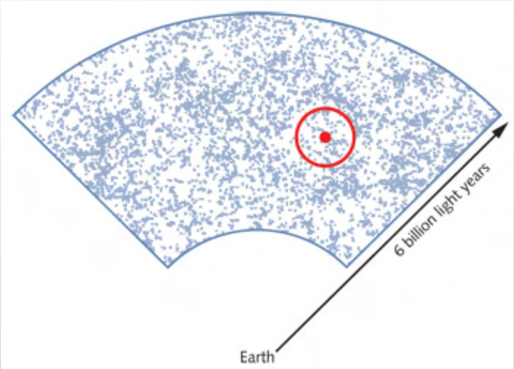

BARYONIC ACOUSTIC OSCILLATIONS

- BAO can be used as a **standard ruler**
  in a similar way SNIa are used as standard candles
  to constrain the expansion history of the Universe

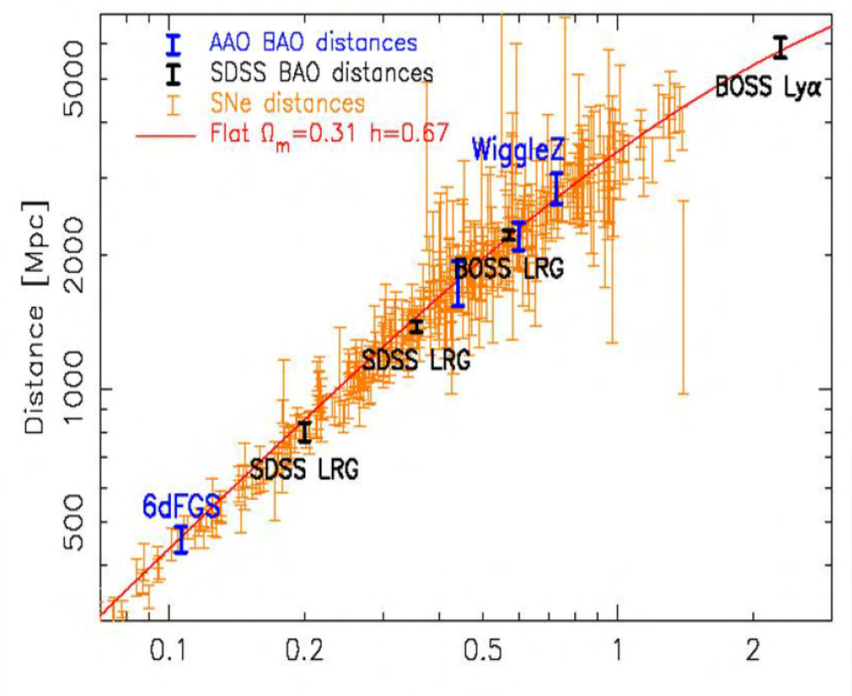

Credit: C. Blake

- Angular BAO constrains angular distances

$$D_M(z) = \frac{c}{H_0} S_k\left(\frac{D_C(z)}{c/H_0}\right)$$

$$S_k(x) = \begin{cases} \sin(\sqrt{-\Omega_k}x)/\sqrt{-\Omega_k} & \Omega_k < 0, \\ x & \Omega_k = 0, \\ \sinh(\sqrt{\Omega_k}x)/\sqrt{\Omega_k} & \Omega_k > 0. \end{cases}$$

- Radial BAO constrains Hubble rate $H(z)$

$$H^2(z) = H_0^2\left[\Omega_r(1+z)^4 + \Omega_m(1+z)^3 + \Omega_k(1+z)^2 + \Omega_X(1+z)^{3(1+w_0+w_1)}\exp\left(\frac{-3w_1 z}{1+z}\right)\right]$$

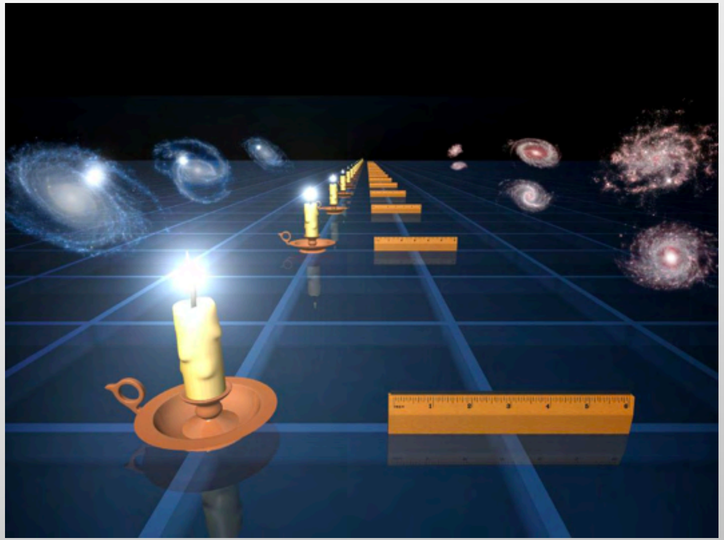

EXPANSION RATE $H(z)$

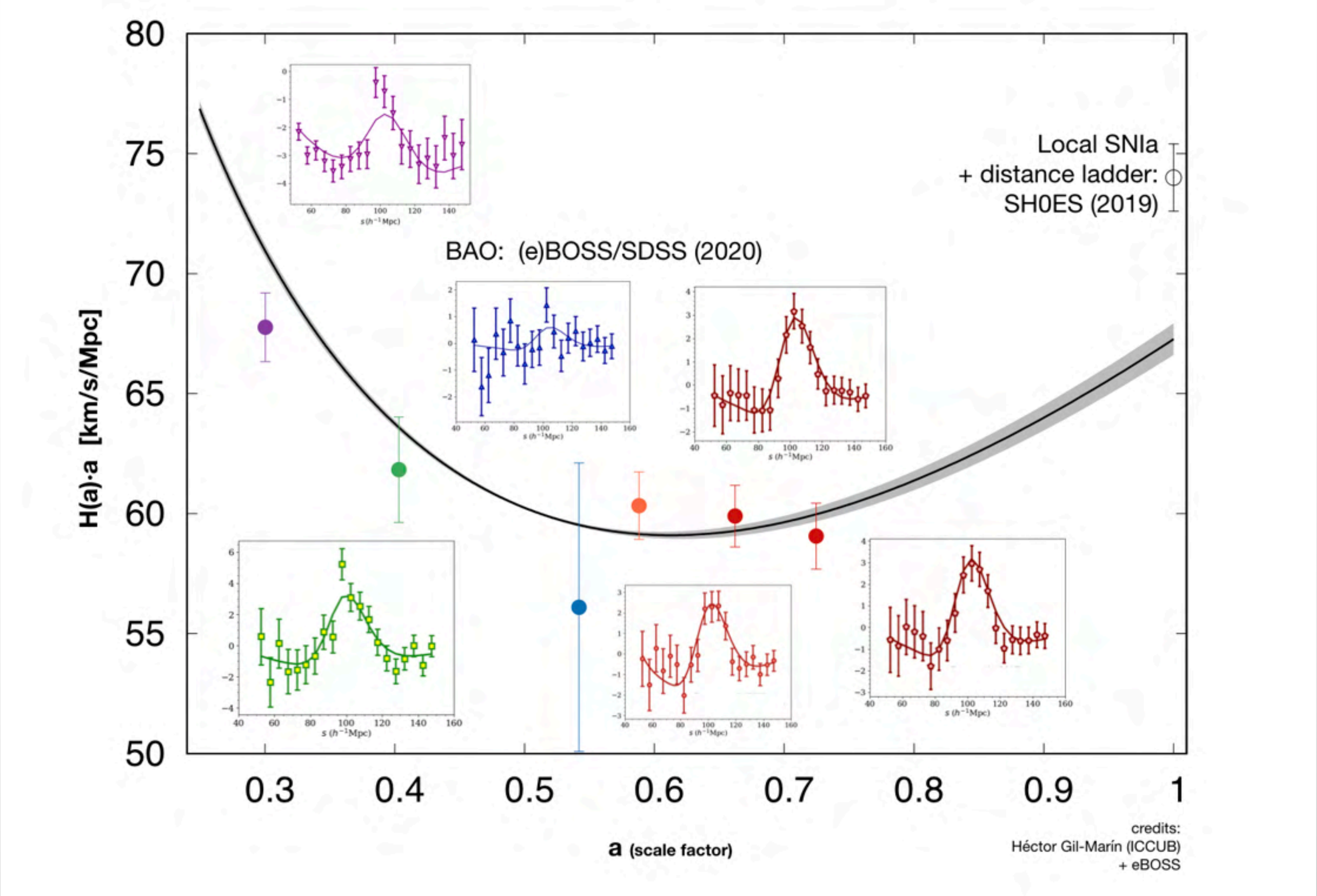

BAO AS A PILLAR OF ΛCDM

- BAO contributed to the settlement of LCDM as a standard model

~2010

2020

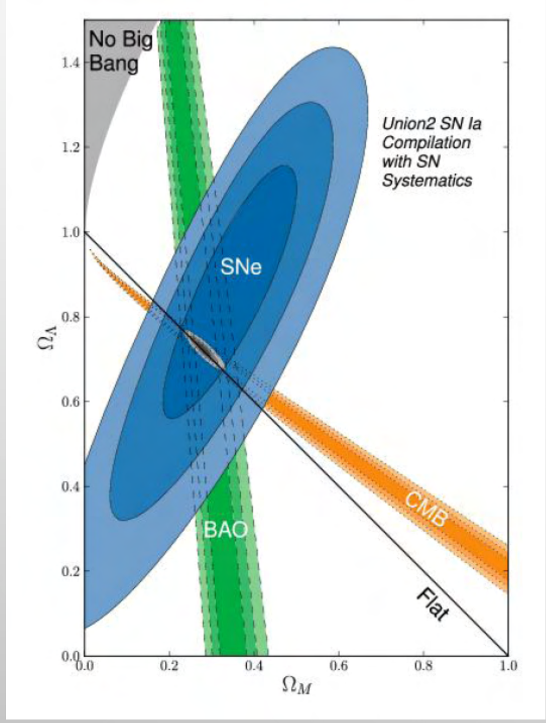

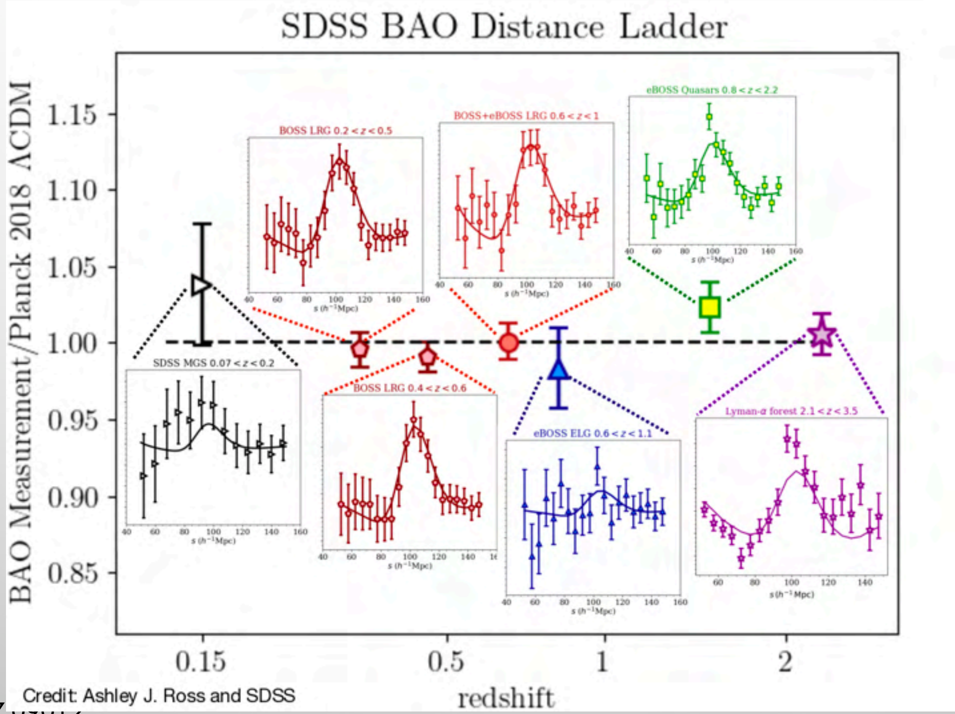

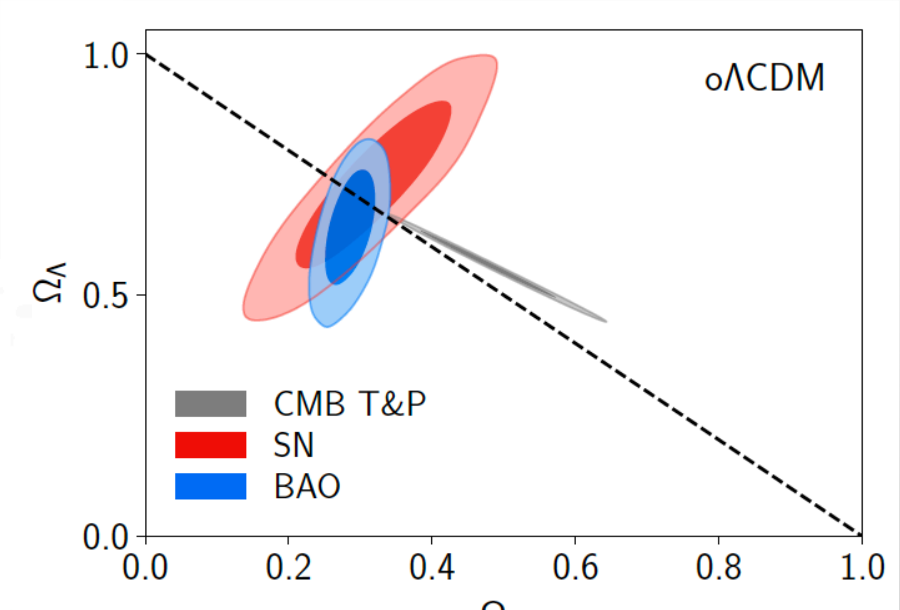

THE DARK ENERGY SURVEY

BAO WITH DES-Y1

- BAO ANGULAR DISTANCE MEASUREMENT WITH 4% ACCURACY, WITH Y3/Y5: <2%

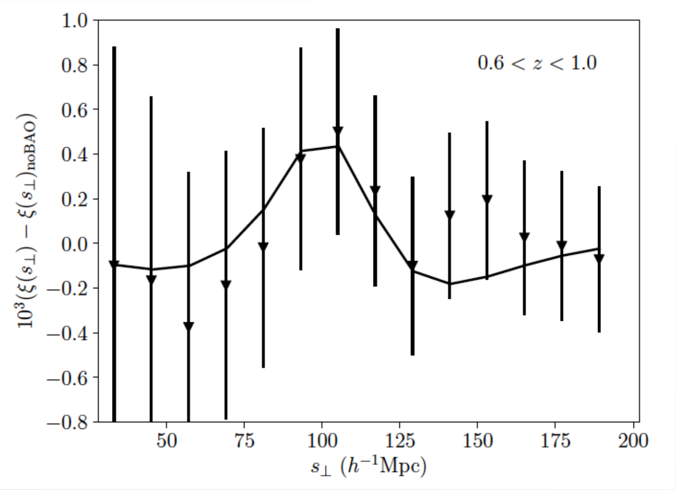

BAO signal!

Standard Ruler: Angular distance

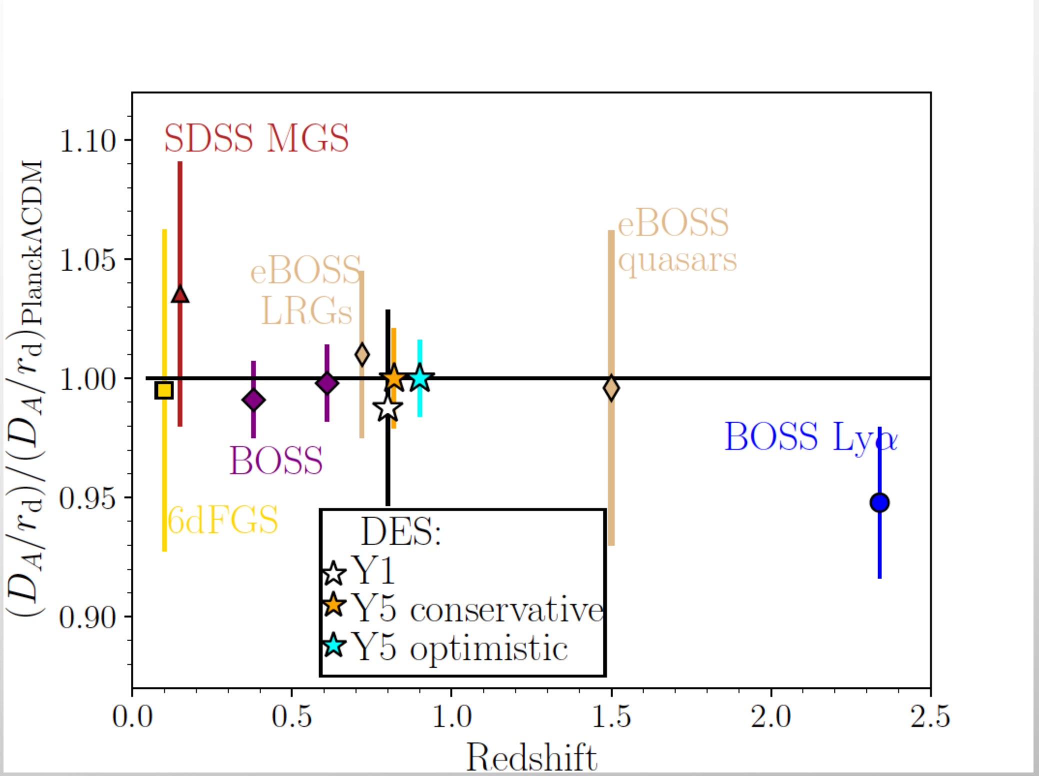

Best fit

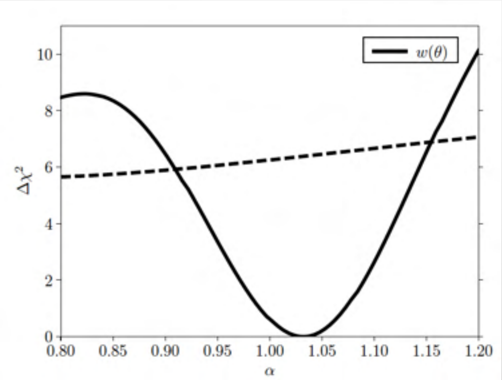

BAO WITH DES-Y1

- BAO ANGULAR DISTANCE MEASUREMENT WITH 4% ACCURACY, WITH Y3/Y5: <2%

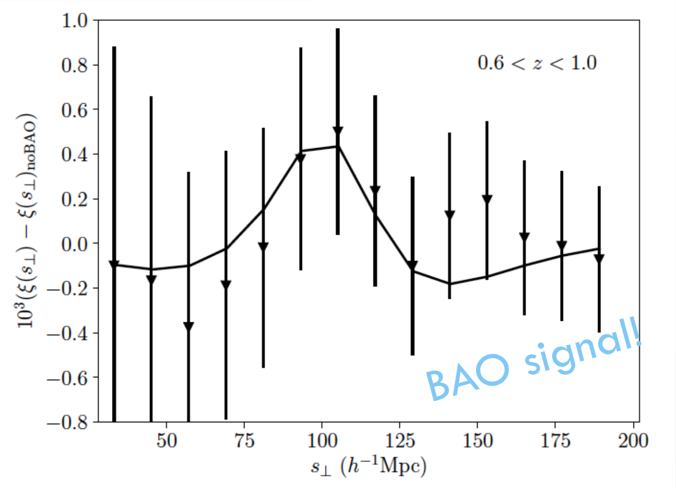

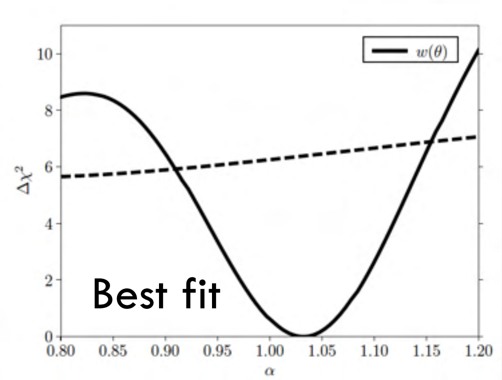

Standard Ruler: Angular distance

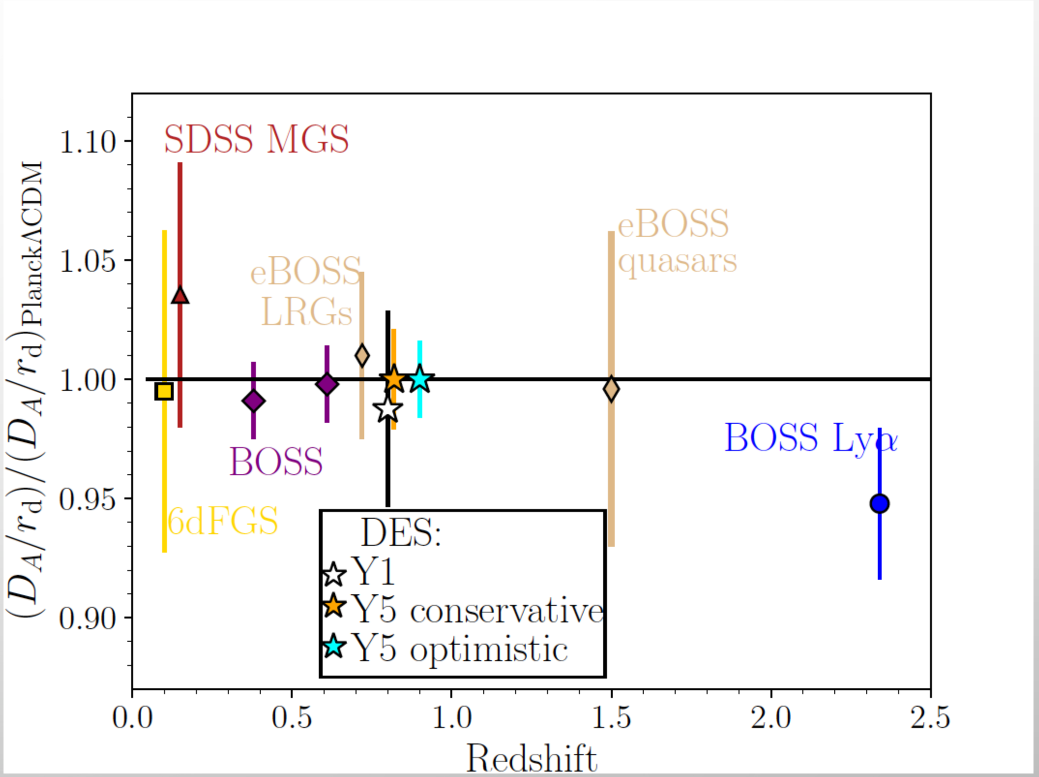

References:
- Ross et al. 2017. (methods 3D 2PCF)
- Avila et al. 2018 (simulations)
- Chan et al. 2018 (methods, angular 2PCF)
- Camacho et al. 2019 (methods C_l)
- Crocce et al. 2019 (sample selection)
- DES et al. 2019 (main paper)

Year-3 coming up soon!!

CLUSTERING STATISTICS

Isotropic 2-Point Correlation Function (2PCF)

$$\xi(r)) = \frac{\langle N_{g,\mathrm{pairs}}(r \pm dr/2) \rangle}{\langle n \rangle dV} - 1$$

“excess probability of finding 2 galaxies separated by a distance r with respect to a random distribution”

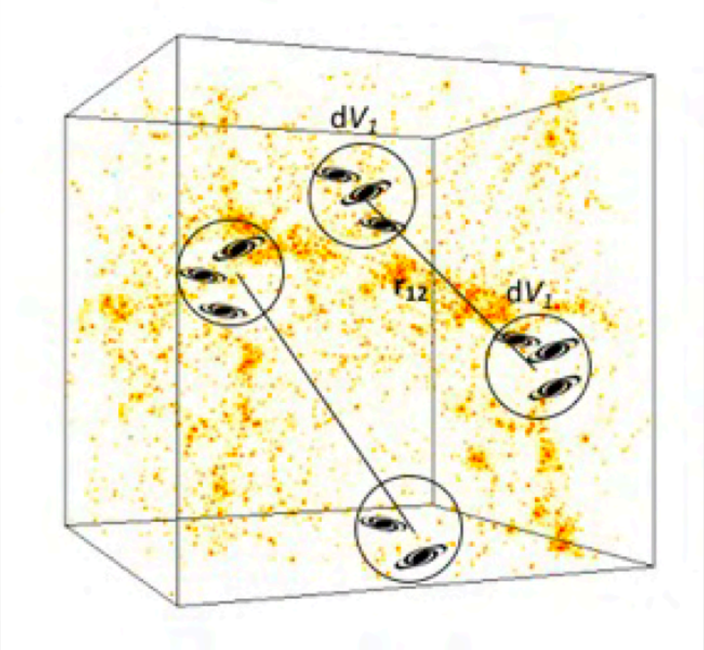

CLUSTERING STATISTICS

Isotropic 2-Point Correlation Function (2PCF)

$$\xi(r)) = \frac{\langle N_{g,\mathrm{pairs}}(r \pm dr/2)\rangle}{\langle n\rangle dV} - 1$$

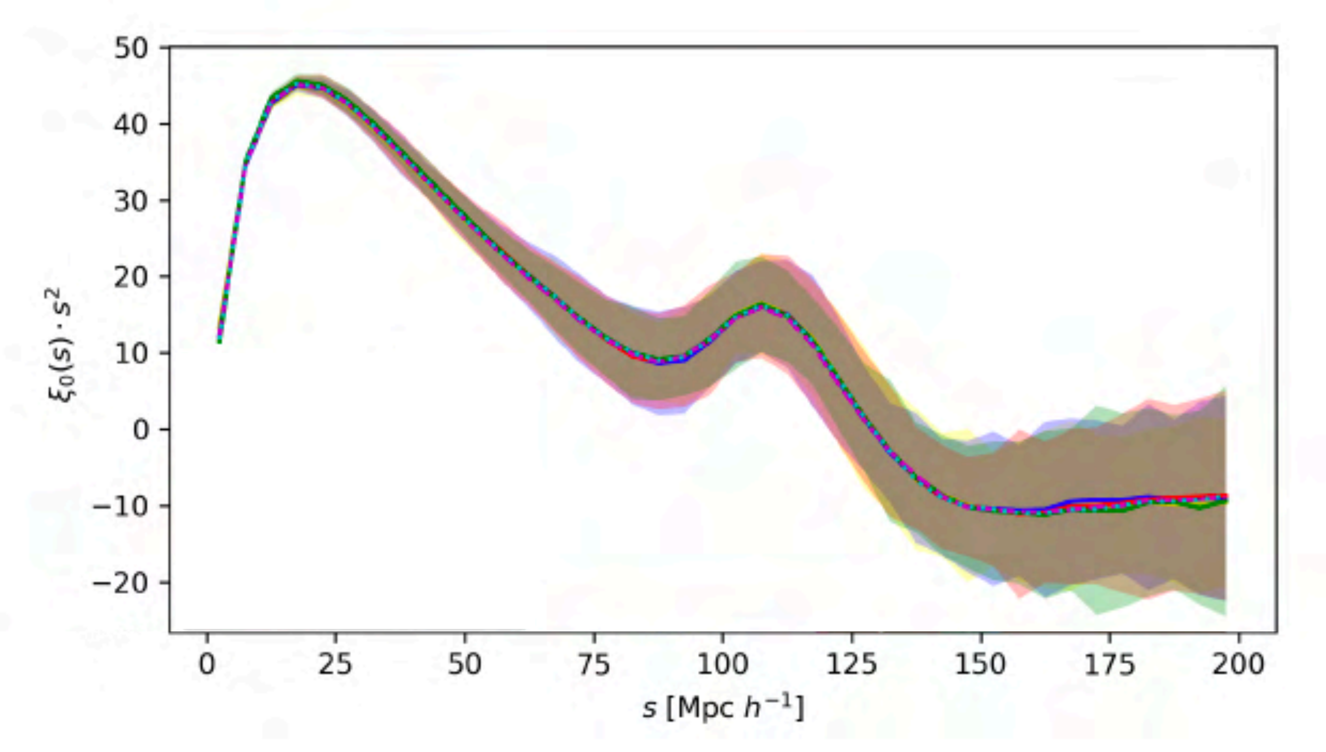

"excess probability of finding 2 galaxies separated by a distance r with respect to a random distribution"

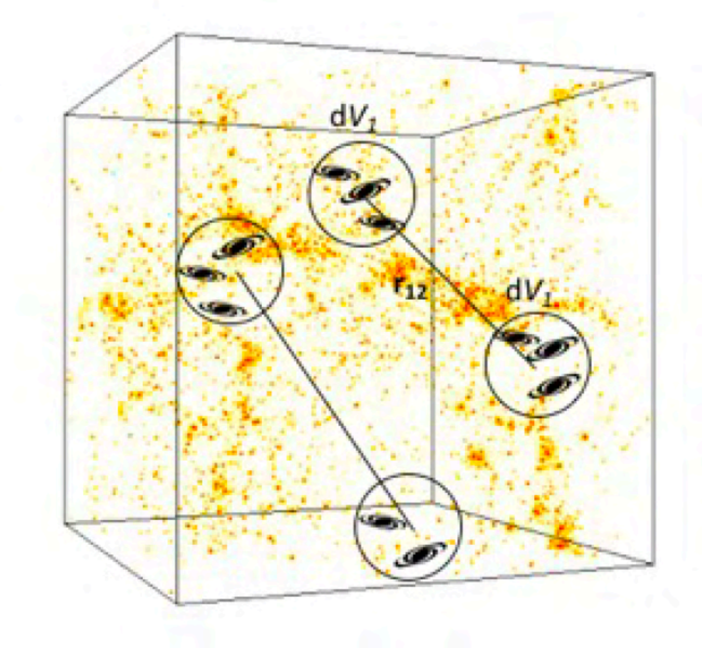

CLUSTERING STATISTICS

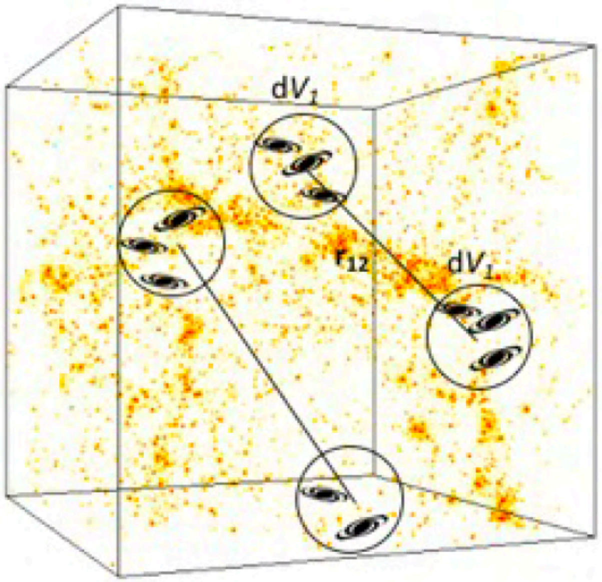

"excess probability of finding 2 galaxies separated by a distance r with respect to a random distribution"

Isotropic 2-Point Correlation Function (2PCF)

$$\xi(r)) = \frac{\langle N_{g,\mathrm{pairs}}(r \pm dr/2) \rangle}{\langle n \rangle dV} - 1$$

2D 2PCF, consider two "distances":

- angular + radial

$$\xi(r_\perp, r_\|) = \xi(r_p, r_l) = \xi(\sigma, \pi)$$

- distance + orientation

$$\xi(r, \mu) = \xi(s, \mu)$$

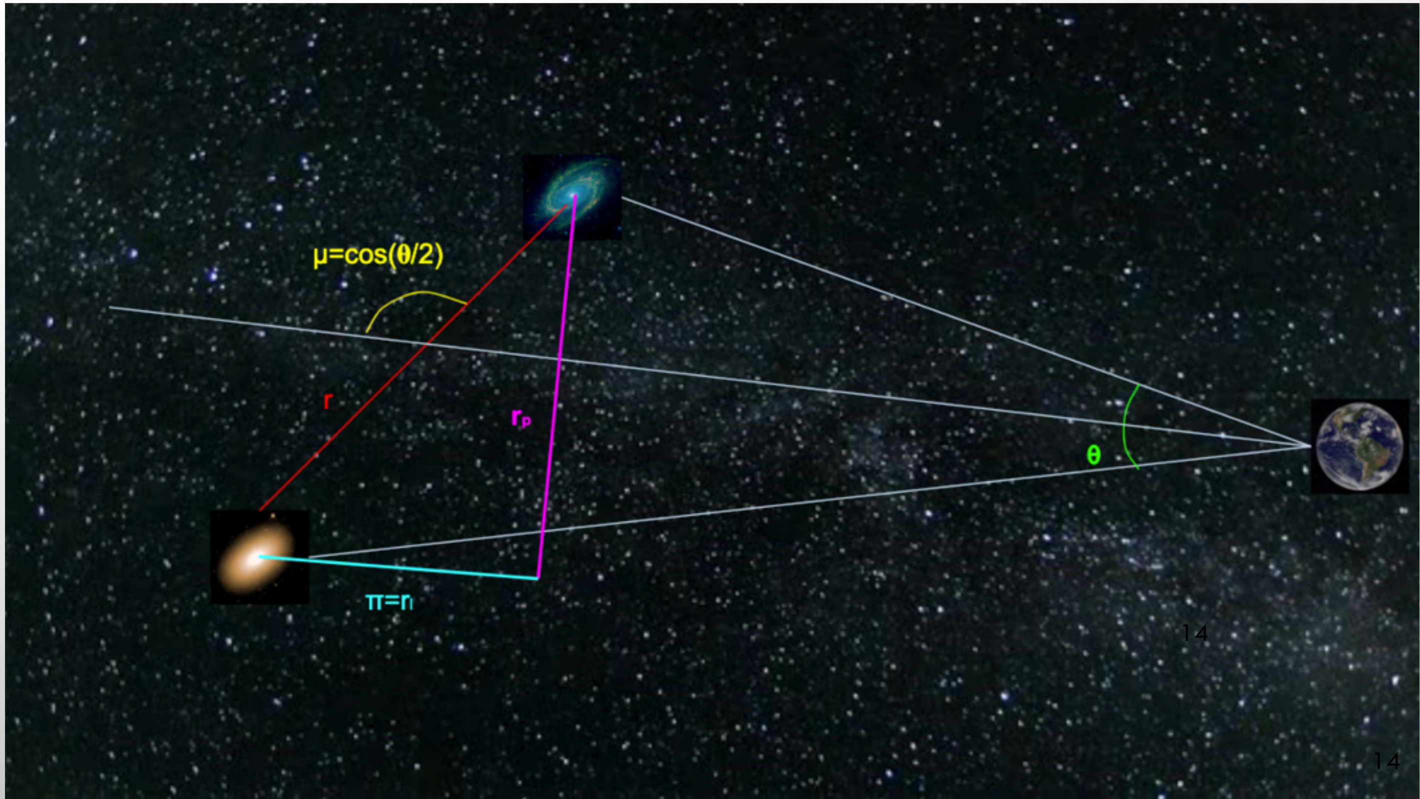

CLUSTERING STATISTICS

Isotropic 2-Point Correlation Function (2PCF)

$$\xi(r)) = \frac{\langle N_{g,\mathrm{pairs}}(r \pm dr/2)\rangle}{\langle n \rangle dV} - 1$$

2D 2PCF, consider two "distances":

- angular + radial

$$\xi(r_\perp, r_\parallel) = \xi(r_p, r_l) = \xi(\sigma, \pi)$$

- distance + orientation

$$\xi(r, \mu) = \xi(s, \mu)$$

2PCF multipoles:

$$\xi_\ell(s) = (2\ell + 1)\int_0^1 \xi(s, \mu) L_\ell(\mu) d\mu$$

Monopole l=0

Quadrupole l=2

Isotropic

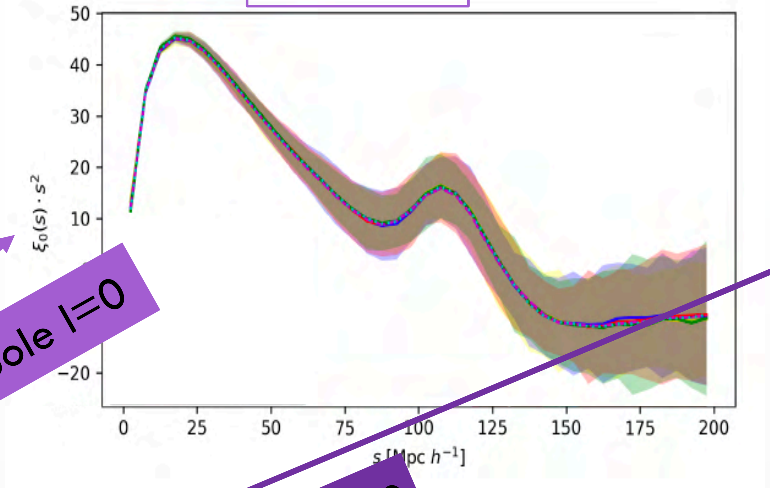

Sensitive to line-of-sight velocities

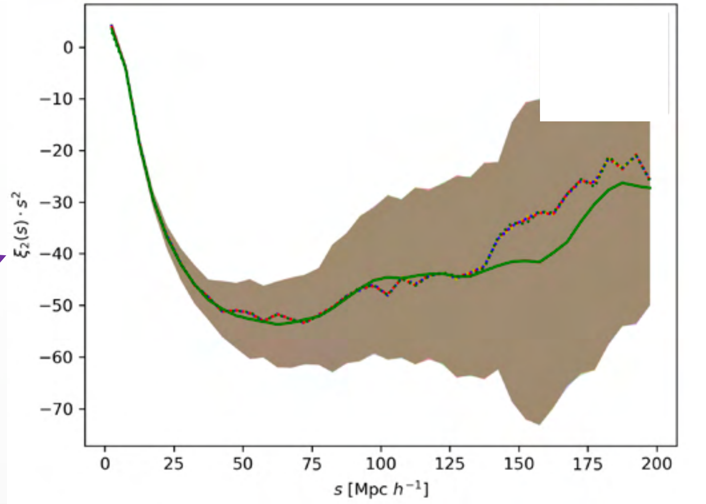

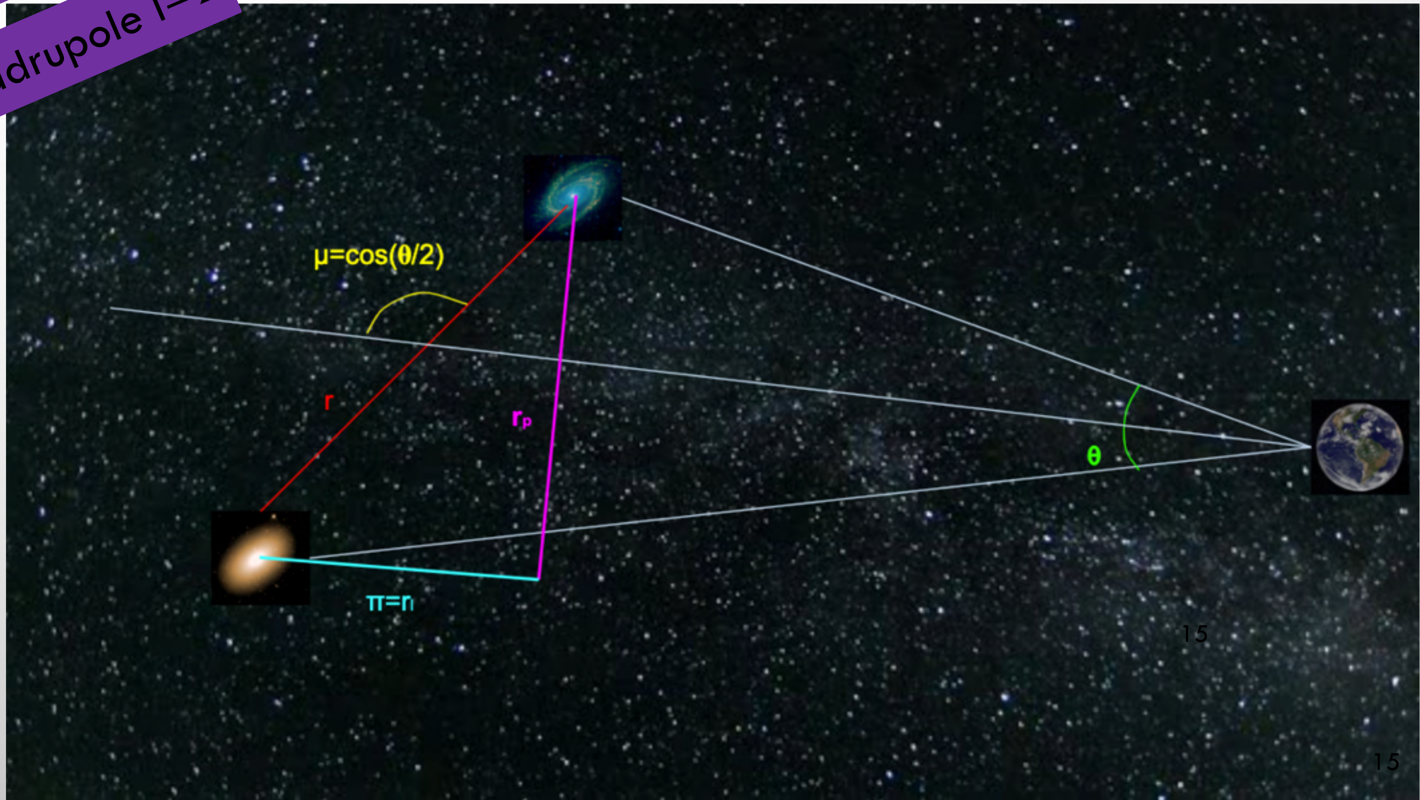

CLUSTERING STATISTICS

Isotropic 2-Point Correlation Function (2PCF)

$$\xi(r)) = \frac{\langle N_{g,\mathrm{pairs}}(r \pm dr/2)\rangle}{\langle n\rangle dV} - 1$$

2D 2PCF, consider two "distances":

- angular + radial

$$\xi(r_\perp, r_\parallel) = \xi(r_p, r_l) = \xi(\sigma, \pi)$$

- distance + orientation

$$\xi(r,\mu) = \xi(s,\mu)$$

2PCF multipoles:

$$\xi_\ell(s) = (2\ell + 1)\int_0^1 \xi(s,\mu) L_\ell(\mu) d\mu$$

Projected Correlation Function

$$w_p(r_p) = 2\int_0^{\pi_{\max}} \xi(r_p, \pi) d\pi$$

Isotropic

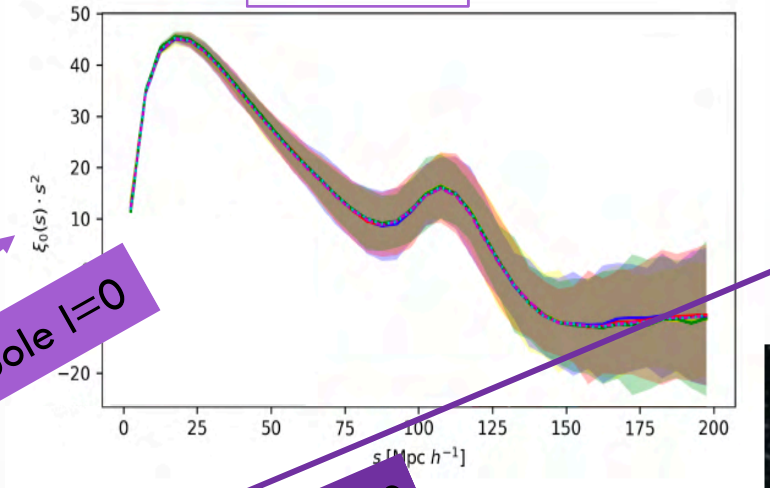

Monopole l=0

Sensitive to line-of-sight velocities

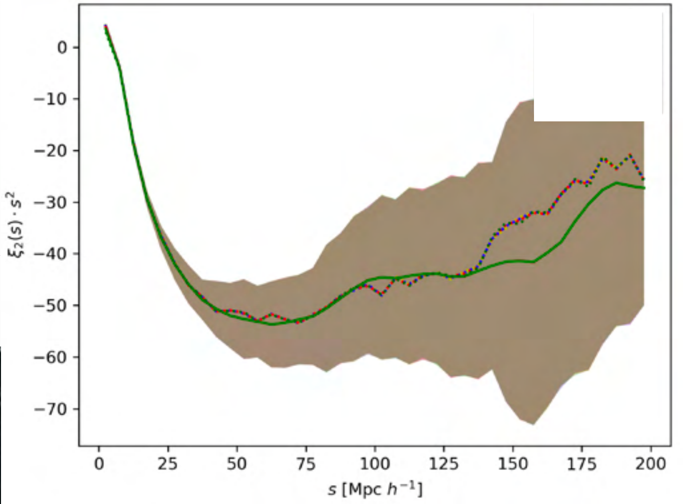

Quadrupole l=2

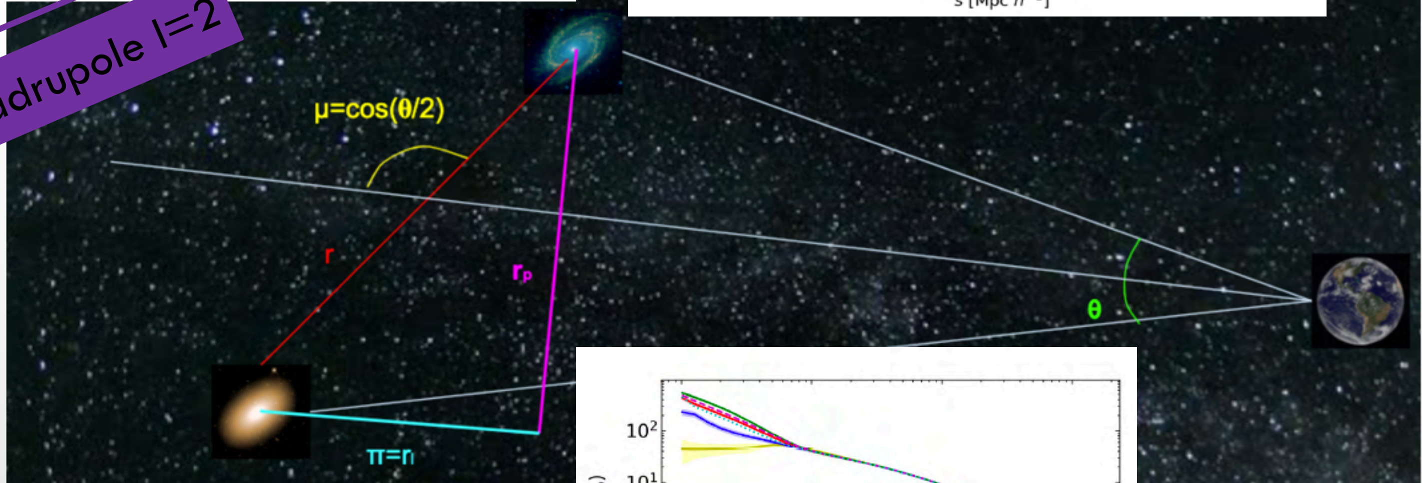

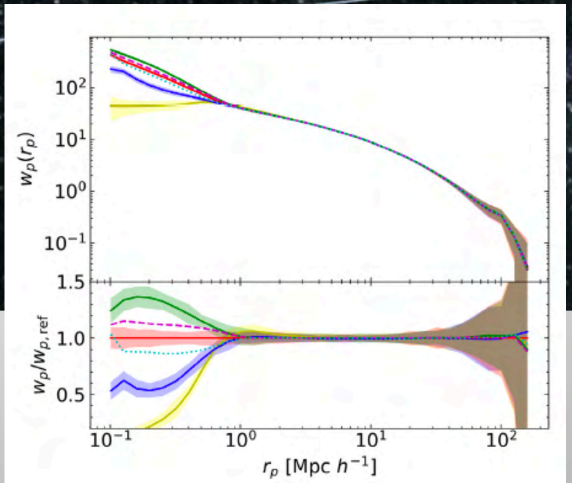

Projected correlation

REDSHIFT SPACE DISTORTIONS

- MATTER OVERDENSITIES CREATE VELOCITY DIVERGENCES DUE TO GRAVITY

$$\vec{\nabla} \cdot \vec{v} = -a\delta \frac{\dot{D}}{D} = -a\delta H$$

- WE MEASURE GALAXY POSITIONS IN REDSHIFT-SPACE: PECULIAR VELOCITIES WILL AFFECT THEIR APPARENT POSITION.

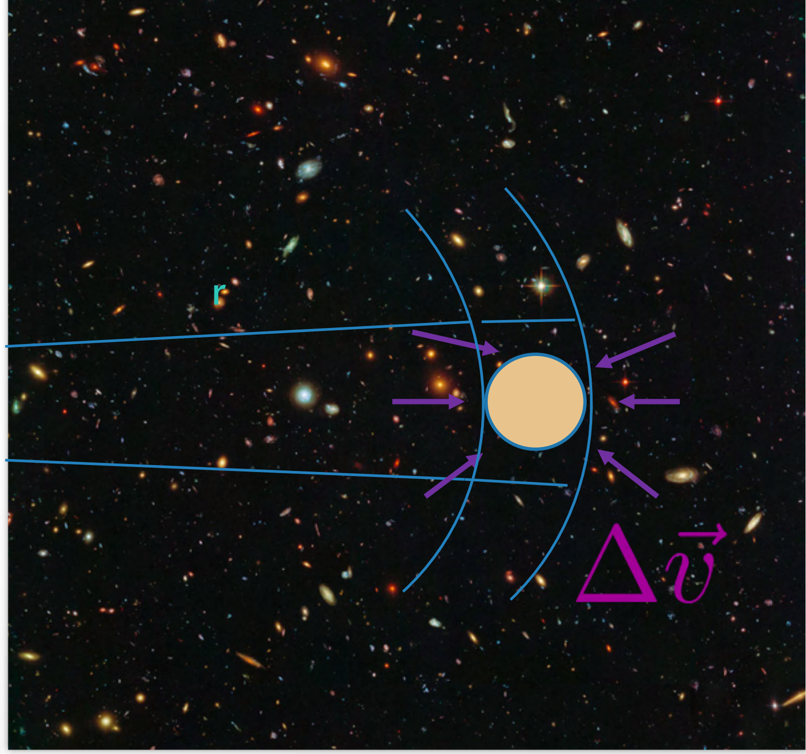

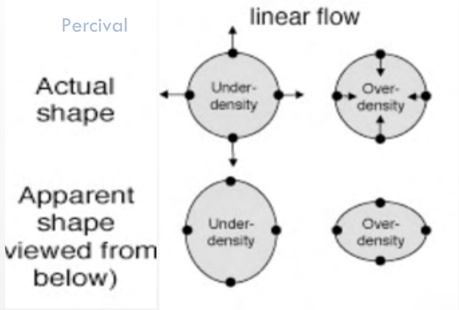

- THIS WILL ENHANCE APPARENT OVERDENSITIES, AND INDUCE AN ANISOTROPY IN GALAXY CLUSTERING (KAISER 1987)

$$P_0(k) = \left(b^2 + \frac{2}{3} f b + \frac{1}{5} f^2\right) P_m(k)$$

$$P_{gal}(k, \mu) = (b + f \cdot \mu^2)^2 P_{DM}(k)$$

WITH $f(a) = \frac{\mathrm{d}\,\log D(a)}{\mathrm{d}\,\log a}$ THE GROWTH RATE OF STRUCTURE FORMATION.

THIS TELLS ABOUT THE **STRENGTH OF GRAVITY** AT COSMOLOGICAL SCALES

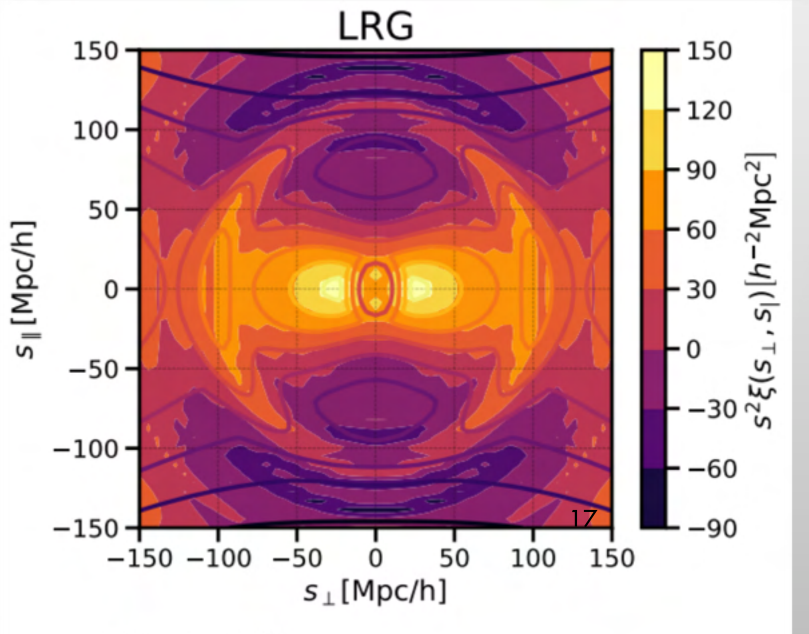

Bautista et al. (2020)
(plot by Jiamin Hou, MPE)

REDSHIFT SPACE DISTORTIONS

- Anisotropic Clustering due to RSD

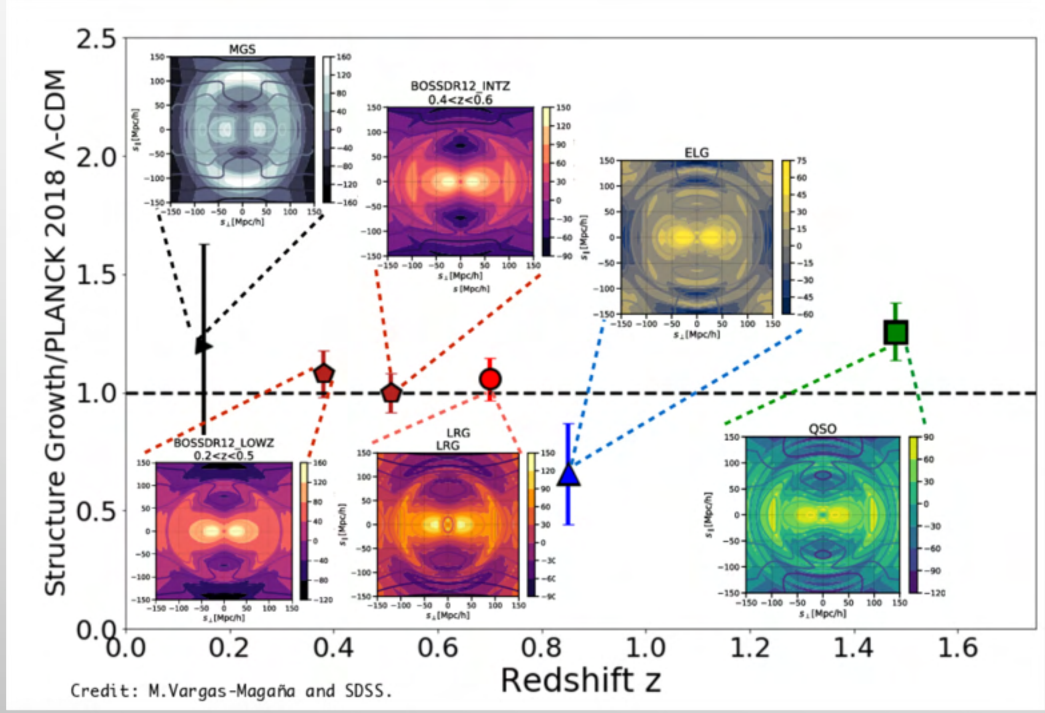

- Constraints on Modified Gravity

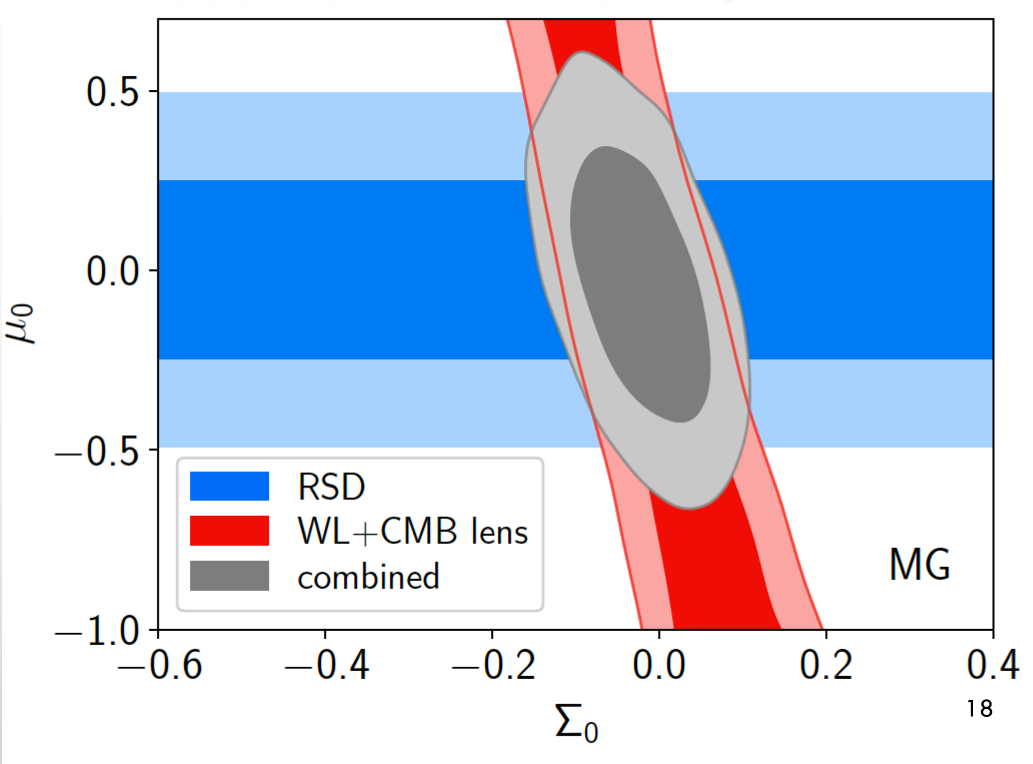

[eBOSS: 2007.08991](https://arxiv.org/abs/2007.08991)

SDSS / BOSS / EBOSS

- SLOAN DIGIGITAL SKY SURVEY
- (EXTENDED) BARYONIC ACOUSTIC OSCILLATION **SPECTROSCOPIC** SURVEY

- MAIN GOAL:
  - TO MEASURE BAO AT DIFFERENT EPOCHS
  - TO MEASURE REDSHIFT SPACE DISTORTIONS

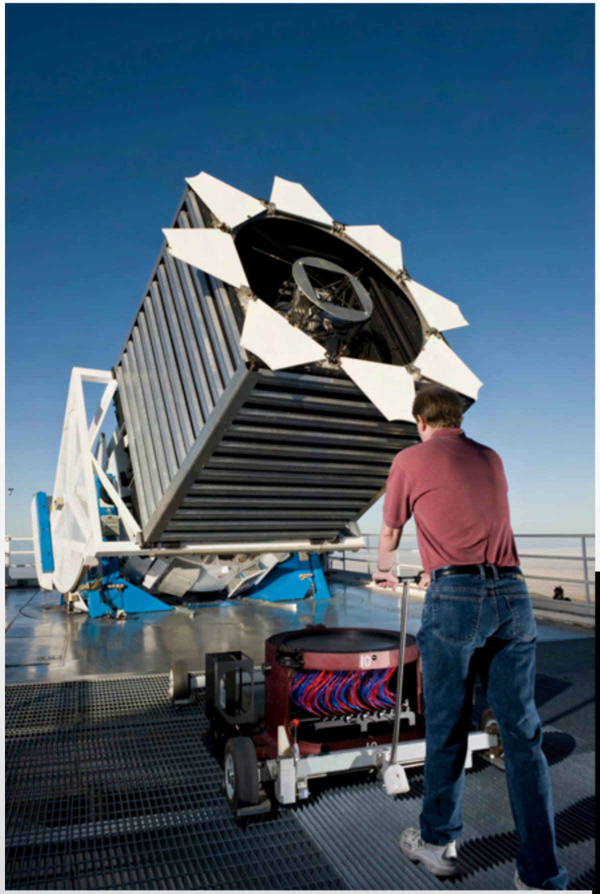

Apache Point Observatory, US

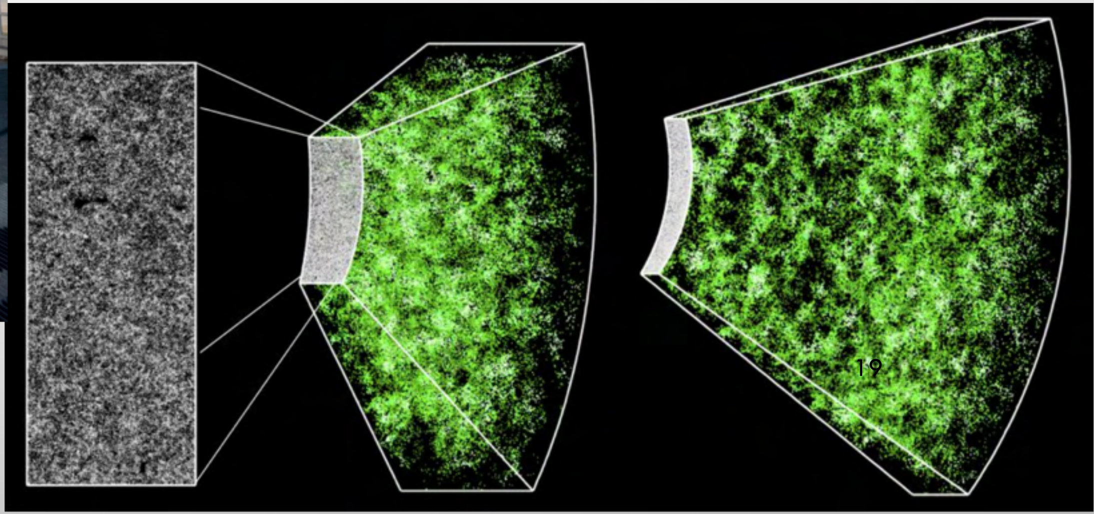

[eBOSS: 2007.08991](https://arxiv.org/abs/2007.08991)

EBOSS RESULTS

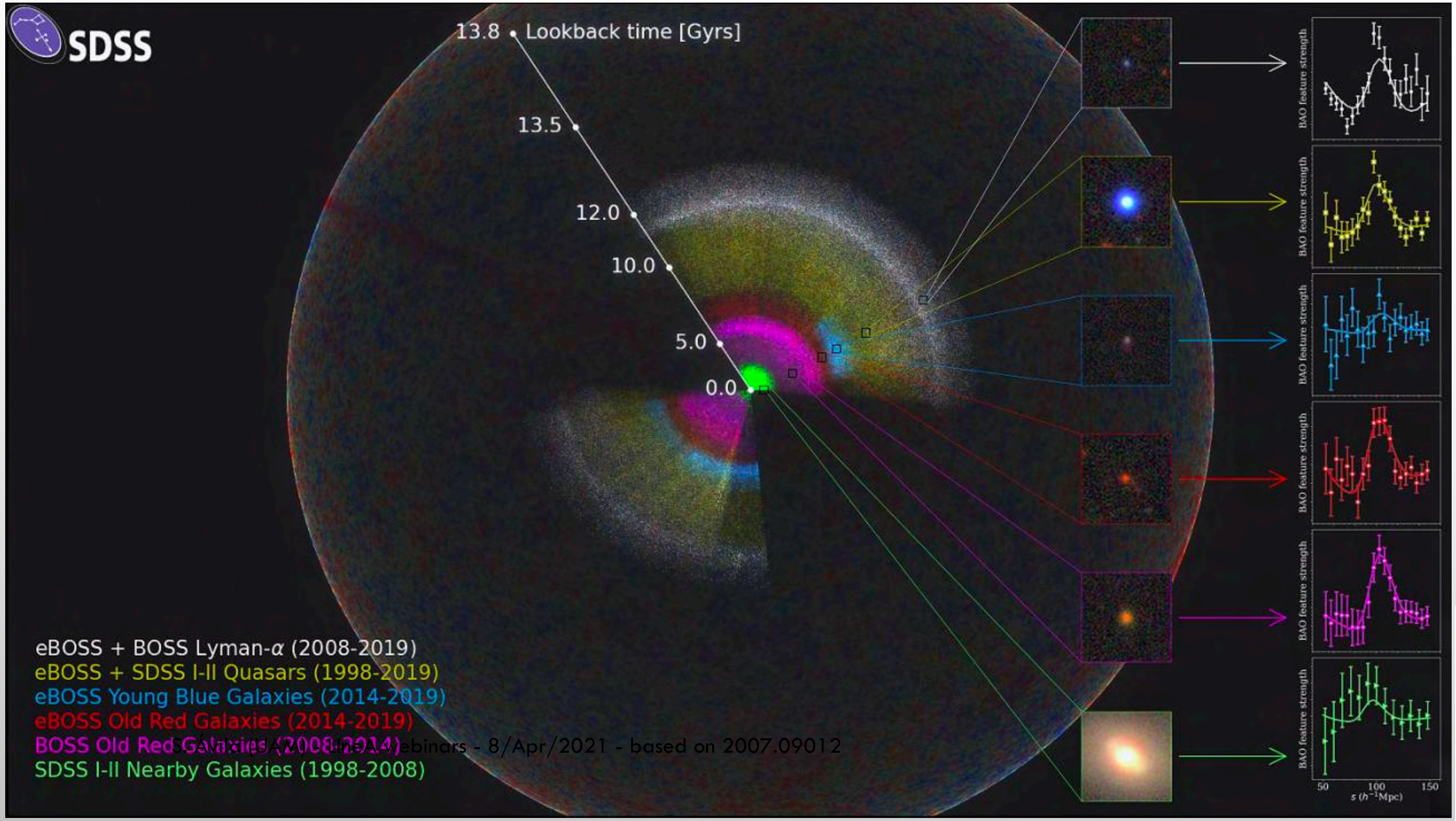

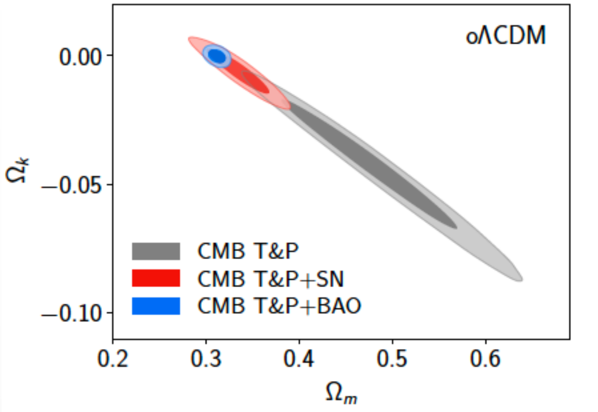

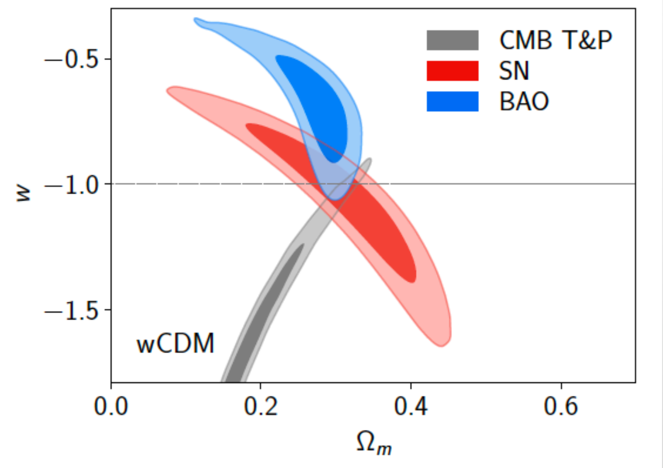

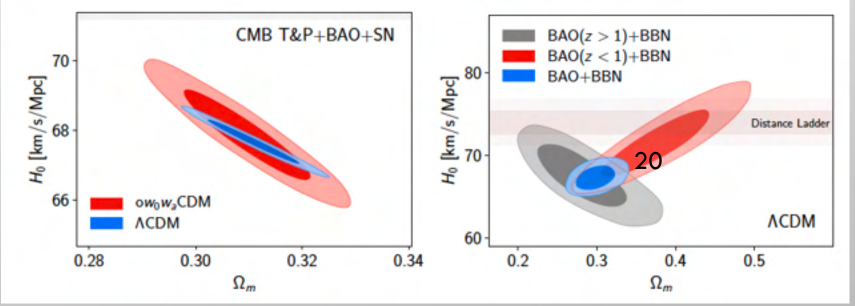

SDSS

eBOSS: 2007.08991

EBOSS RESULTS

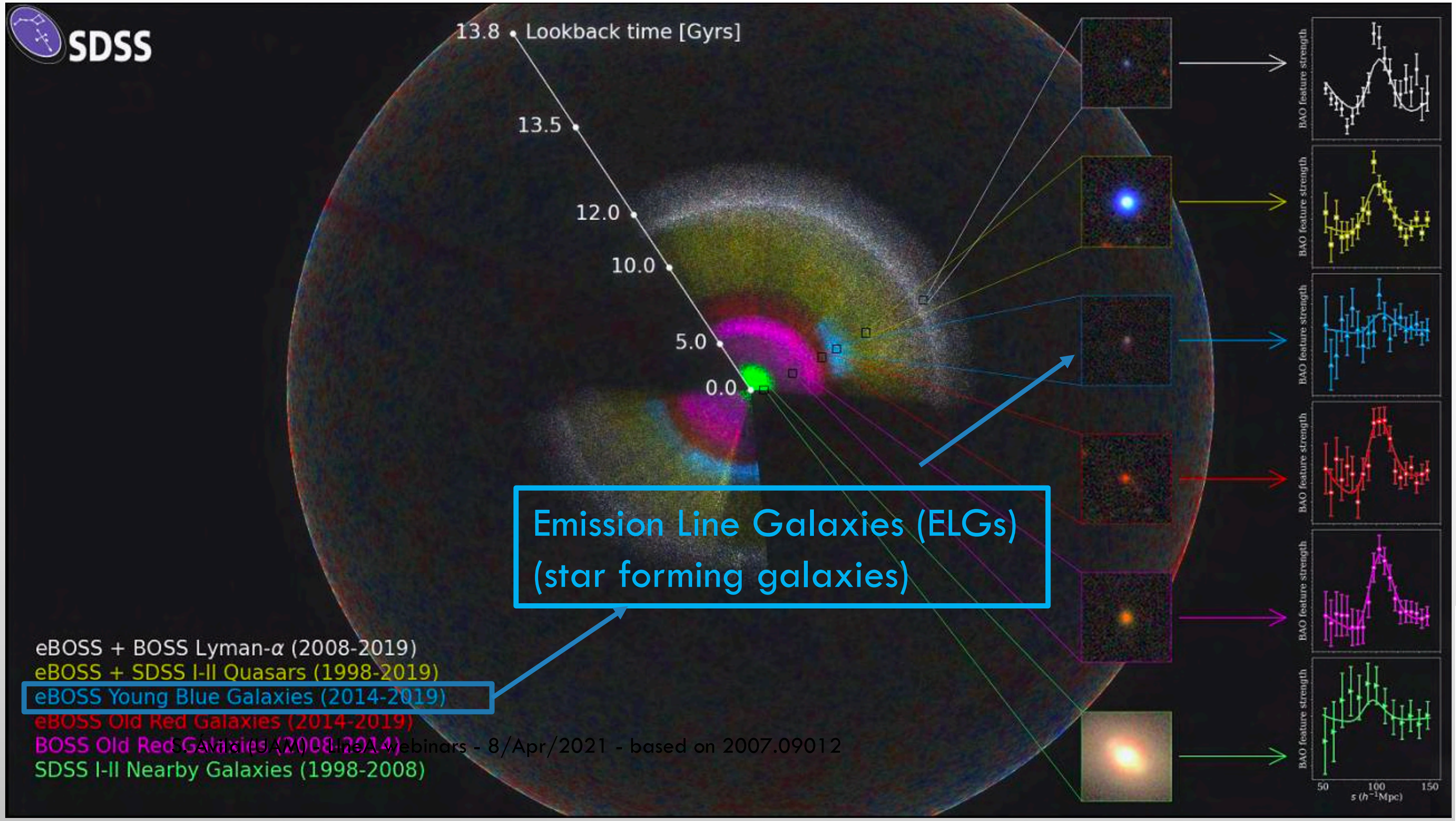

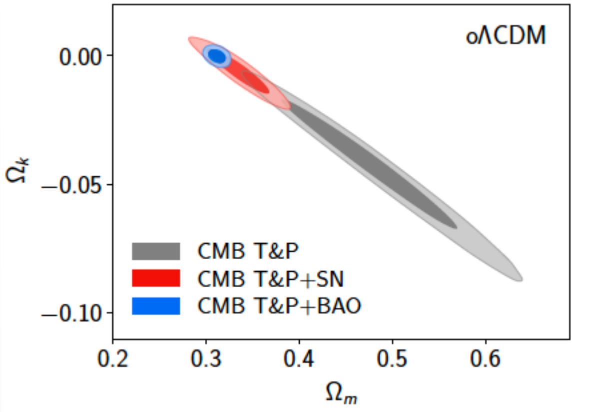

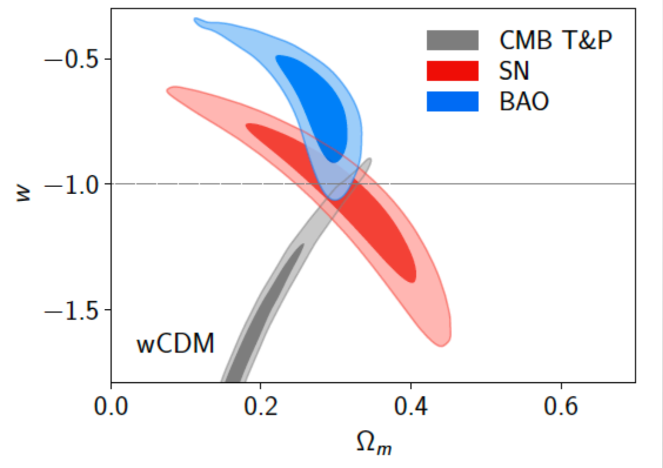

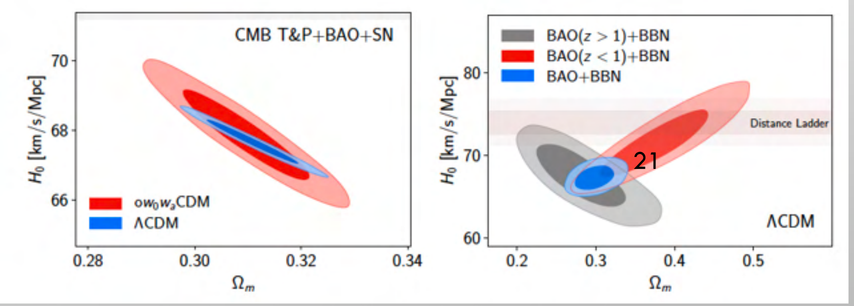

REFERENCES

Parameter	Main Galaxy Sample (MGS)	BOSS Galaxy	BOSS Galaxy	eBOSS LRG	eBOSS ELG	eBOSS Quasar	Lyα-Lyα	Lyα-Quasar
Imaging, Target Selection, and Spectroscopic Properties of Each Sample								
Imaging for Target Selection	SDSS	SDSS	SDSS	SDSS + WISE	DECaLS	SDSS + WISE	SDSS + WISE + MISC	SDSS + WISE + MISC
Target Selection	g,r	g,r,i	g,r,i	g,r,i,z,W1	g,r,z	u,g,r,i,z,W1, W2	misc	misc
Spectroscopic Program	SDSS-I and - II	BOSS	BOSS	BOSS and eBOSS	eBOSS	primarily eBOSS	BOSS and eBOSS	BOSS and eBOSS
redshift range	0.07 < z < 0.20	0.2 < z < 0.5	0.4 < z < 0.6	0.6 < z < 1.0	0.6 < z < 1.1	0.8 < z < 2.2	z > 2.1	z > 1.77
Number of Tracers	63,163	604,001	686,370	377,458	173,736	343,708	210,005	341,468
Effective Redshift	0.15	0.38	0.51	0.70	0.85	1.48	2.33	2.33
Effective Volume (Gpc^3)	0.24	3.7	4.2	2.7	0.6	0.6		
Clustering Catalog Documentation	Ross et al. (2020)	Reid et al. (2016)	Reid et al. (2016)	Ross et al. (2020)	Raichoor et al. (2020)	Ross et al. (2020), Lyke et al. (2020)	du Mas des Bourbuox et al. (2020), Lyke et al. (2020)	du Mas des Bourbuox et al. (2020), Lyke et al. (2020)
N-body and Mock Catalogs		Kitaura et al. (2016)	Kitaura et al. (2016)	Zhao et al. (2020), Rossi et al. (2020)	Zhao et al. (2020), Lin et al. (2020), Alam et al. (2020), Avila et al. (2020)	Zhao et al. (2020), Smith et al. (2020)	Farr et al. (2020)	Farr et al. (2020)

RSD Measurements								
Correlation Function Measurement	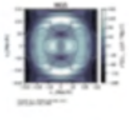	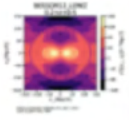	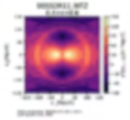	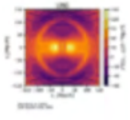	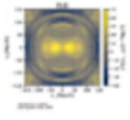	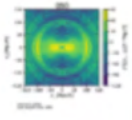		
$f\sigma_8(z)$	0.53 +/- 0.16	0.500 +/- 0.047	0.455 +/- 0.039	0.448 +/- 0.043	0.315 +/- 0.095	0.462 +/- 0.045		
BAO+RSD Measurements								
Correlation Function Multipoles	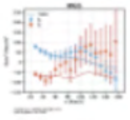	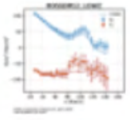	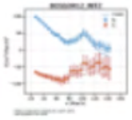	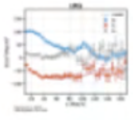	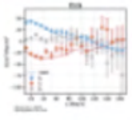	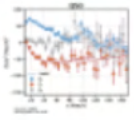		
Power Spectrum Multipoles		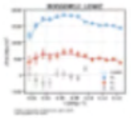	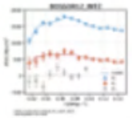	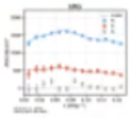	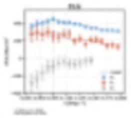	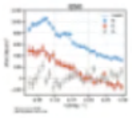		
$D_V(z)/r_d$	4.51 +/- 0.14							
$D_M(z)/r_d$		10.27 +/- 0.15	13.38 +/- 0.18	17.65 +/- 0.30	19.5 +/- 1.0	30.21 +/- 0.79	37.6 +/- 1.9	37.3 +/- 1.7
$D_H(z)/r_d$		24.89 +/- 0.58	22.43 +/- 0.48	19.78 +/- 0.46	19.6 +/- 2.1	13.23 +/- 0.47	8.93 +/- 0.28	9.08 +/- 0.34
$f\sigma_8$	0.53 +/- 0.16	0.497 +/- 0.045	0.459 +/- 0.038	0.473 +/- 0.041	0.315 +/- 0.095	0.462 +/- 0.045		
Reference for final results	Howlett et al. (2015)	BOSS Collaboration (2017)	BOSS Collaboration (2017)	Bautista et al. (2020), Gil-Marin et al. (2020)	Tamone et al. (2020), de Mattia et al. (2020)	Hou et al. (2020), Neveux et al. (2020)	du Mas des Bourbuox et al. (2020)	du Mas des Bourbuox et al. (2020)

REFERENCES

WORK BASED ON [ARXIV:2007.09012]

Monthly Notices of the ROYAL ASTRONOMICAL SOCIETY

MNRAS **499,** 5486–5507 (2020) doi:10.1093/mnras/staa2951
Advance Access publication 2020 September 25

The Completed SDSS-IV extended Baryon Oscillation Spectroscopic Survey: exploring the halo occupation distribution model for emission line galaxies

S. Avila,[1,2,3★] V. Gonzalez-Perez,[3,4★] F. G. Mohammad,[5,6] A. de Mattia,[7] C. Zhao,[8] A. Raichoor,[8] A. Tamone,[8] S. Alam,[9] J. Bautista,[3] D. Bianchi,[10,11] E. Burtin,[7] M. J. Chapman,[5,6] C.-H. Chuang,[12] J. Comparat,[13] K. Dawson,[14] T. Divers,[3] H. du Mas des Bourboux,[14] H. Gil-Marin,[10,11] E. M. Mueller,[15] S. Habib,[16] K. Heitmann,[16] V. Ruhlmann-Kleider,[7] N. Padilla,[17] W. J. Percival,[5,6,18] A. J. Ross,[19] H. J. Seo,[19] D. P. Schneider[20] and G. Zhao[3,21]

PART II. INGREDIENTS

HOD model

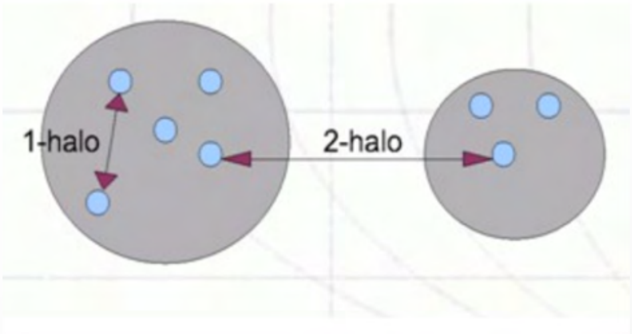

Outerrim Simulation

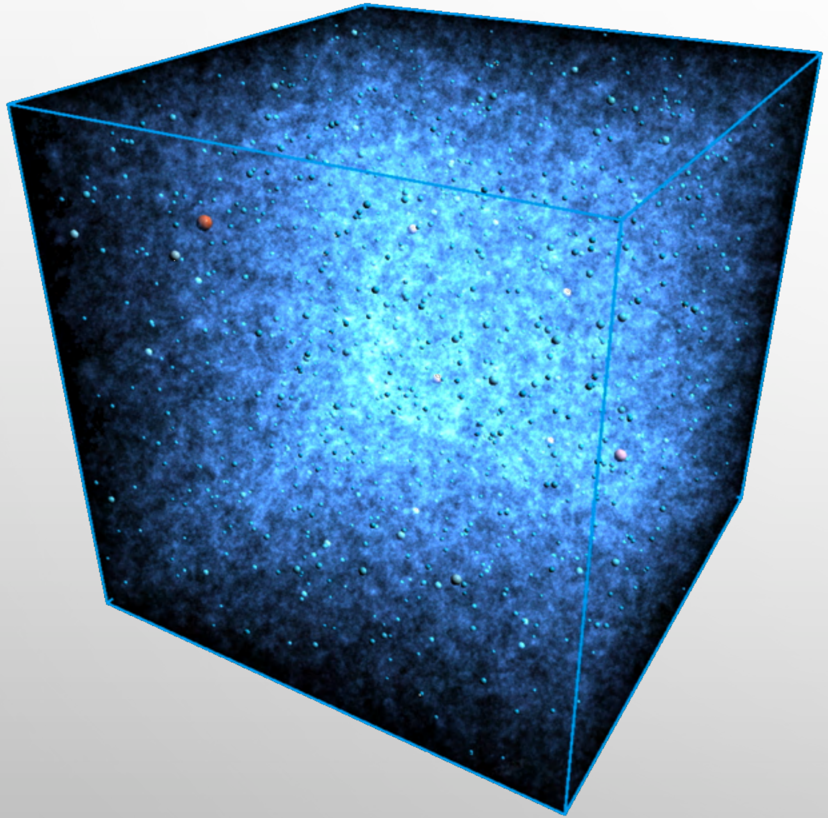

eBOSS ELG data

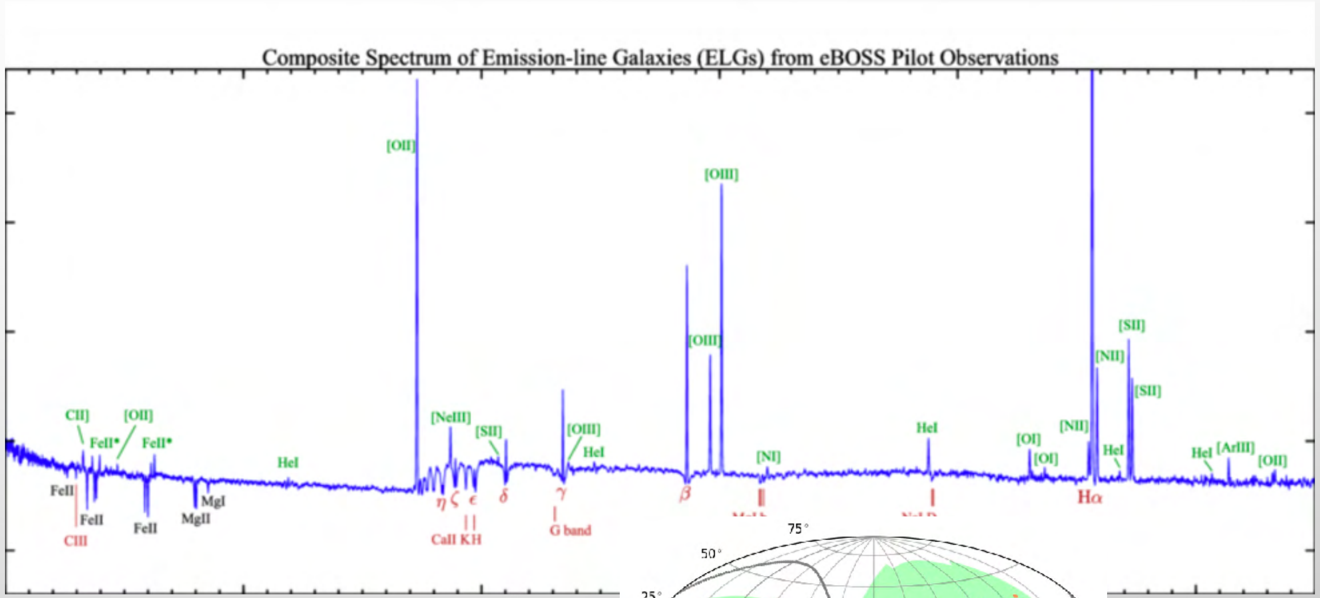

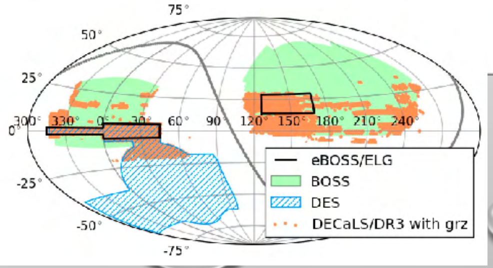

ELGS WITH EBOSS: THE SAMPLE

- N(Z)

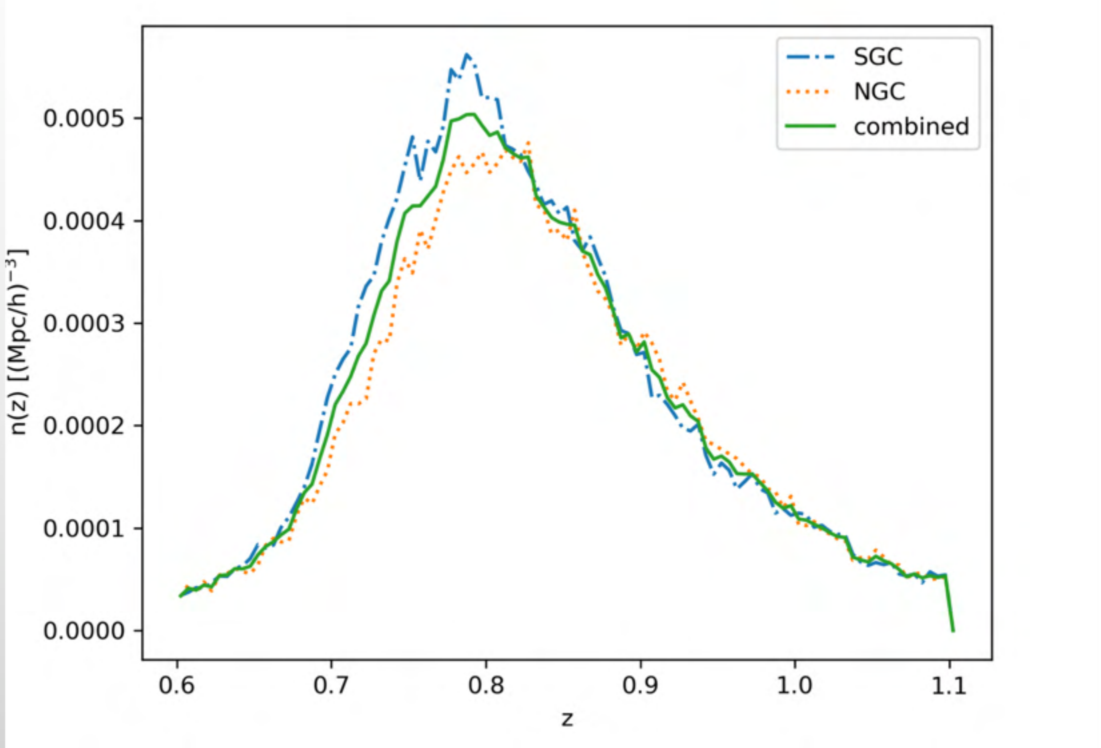

N_{eff} = 201,122

$$\bar{n} = \frac{N_{\rm eff}}{V_{\rm eff}} \qquad \bar{n}_{\rm eBOSS} = 2.187 \cdot 10^{-4} (\mathrm{Mpc}/h)^{-3}$$

$$\bar{n}_{\rm SGC} = 2.267 \cdot 10^{-4} (\mathrm{Mpc}/h)^{-3}, \ \bar{n}_{\rm NGC} = 2.110 \cdot 10^{-4} (\mathrm{Mpc}/h)^{-3}$$

- Footprint

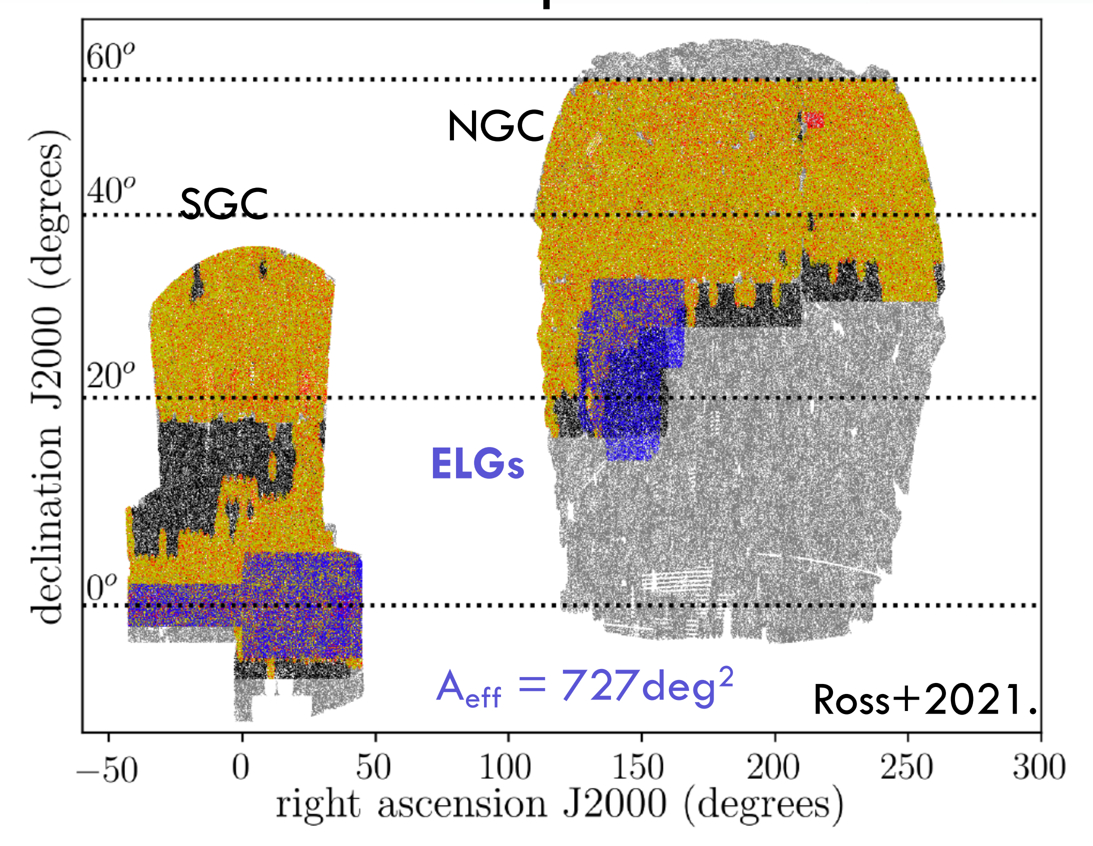

V_{eff} = (972.4 Mpc/h)^3

DARK MATTER HALOS

- GALAXIES LIVE IN DARK MATTER HALOS
- DARK MATTER HALOS ARE BETTER UNDERSTOOD FROM THE THEORETICAL POINT-OF-VIEW:
  - SPHERICAL TOP-HAT COLLAPSE
  - PRESS-SCHECHTER
  - PEAK-BACKGROUND SPLIT MODEL
  - HALO MODEL, ETC.
- LARGE SIMULATIONS USED FOR VERY LARGE SCALES ONLY INCLUDE DARK MATTER.
- WE WILL USE HALOS FROM OUTERRIM SIMULATION
- WE WILL STUDY HOW THE RELATION BETWEEN DARK MATTER AND GALAXIES AFFECTS GALAXY CLUSTERING

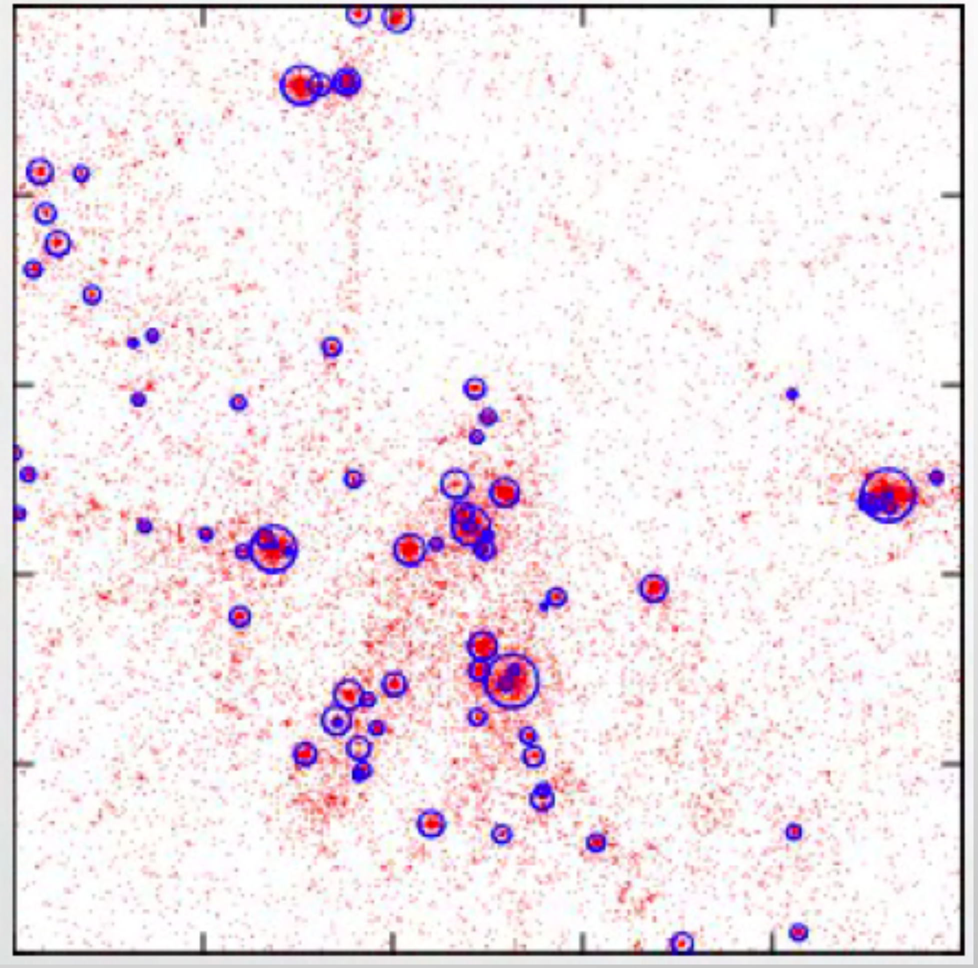

OUTERRIM SIMULATION

- N-Body simulation

  Using snapshot z=0.865

(Heitman et al. 2019)

$$L = 3000\mathrm{Mpc}/h$$
$$N = 10240^3$$
$$m_{\mathrm{DM}} = 1.9 \times 10^9 M_{\mathrm{sun}}/h$$

Ω_{cdm}	0,22
Ω_b	0,0448
n_s	0,963
h	0,71
σ_8	0,8

- Halo Clustering

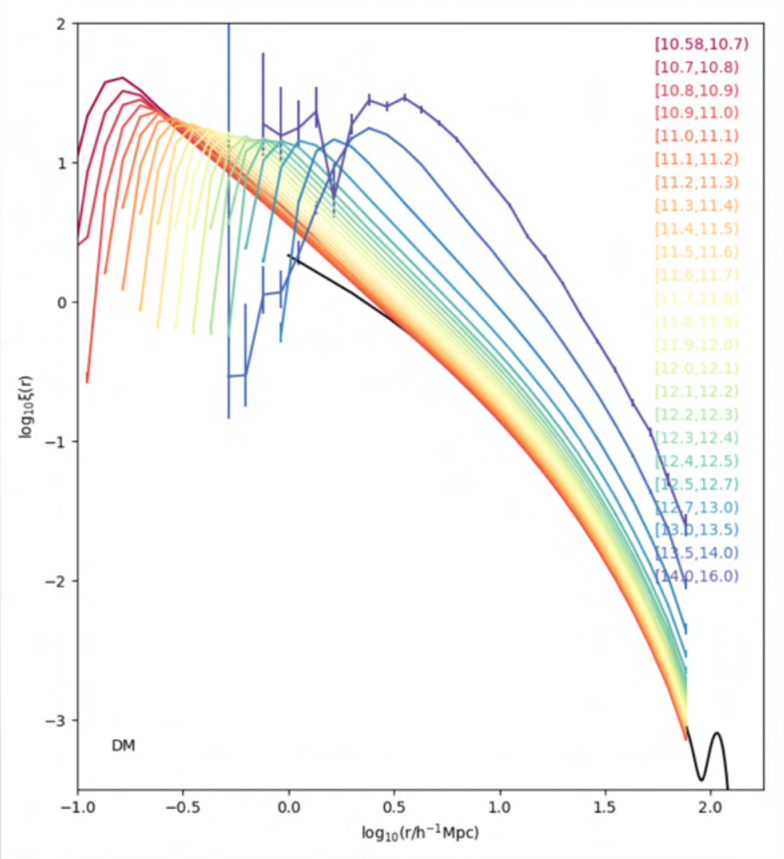

- Halo Mass Function

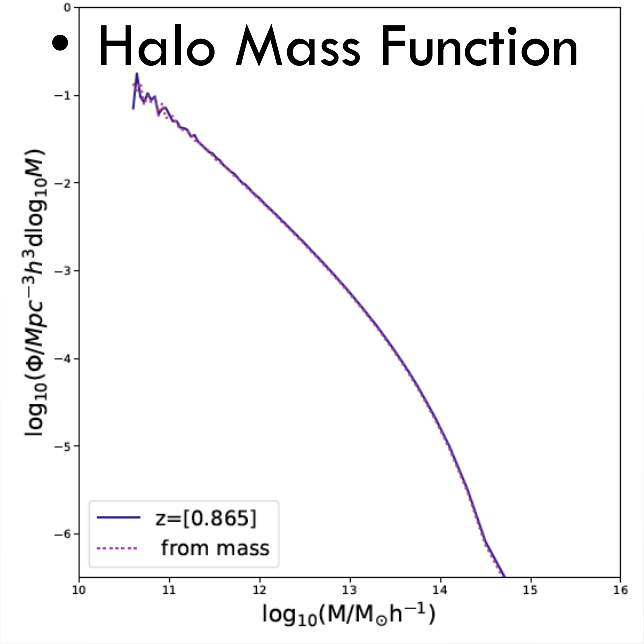

- Bias function

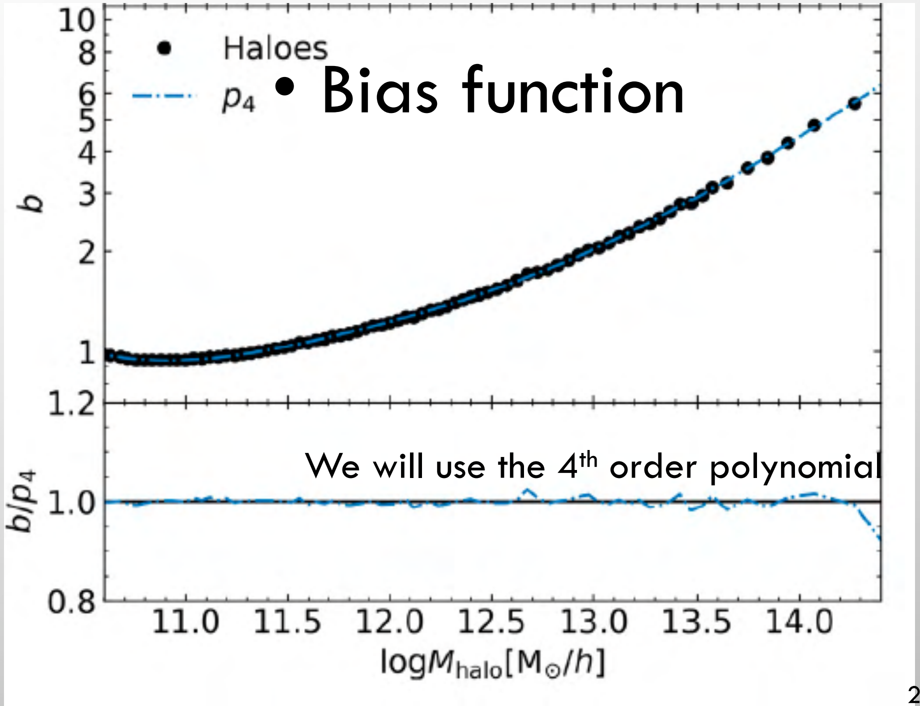

We will use the 4th order polynomial

OUTERRIM SIMULATION

- N-Body simulation

  Using snapshot z=0.865

(Heitman et al. 2019)

$$L = 3000\mathrm{Mpc}/h$$
$$N = 10240^3$$
$$m_{\mathrm{DM}} = 1.9 \times 10^9 M_{\mathrm{sun}}/h$$

Ω_{cdm}	0,22
Ω_b	0,0448
n_s	0,963
h	0,71
σ_8	0,8

- Halo Clustering

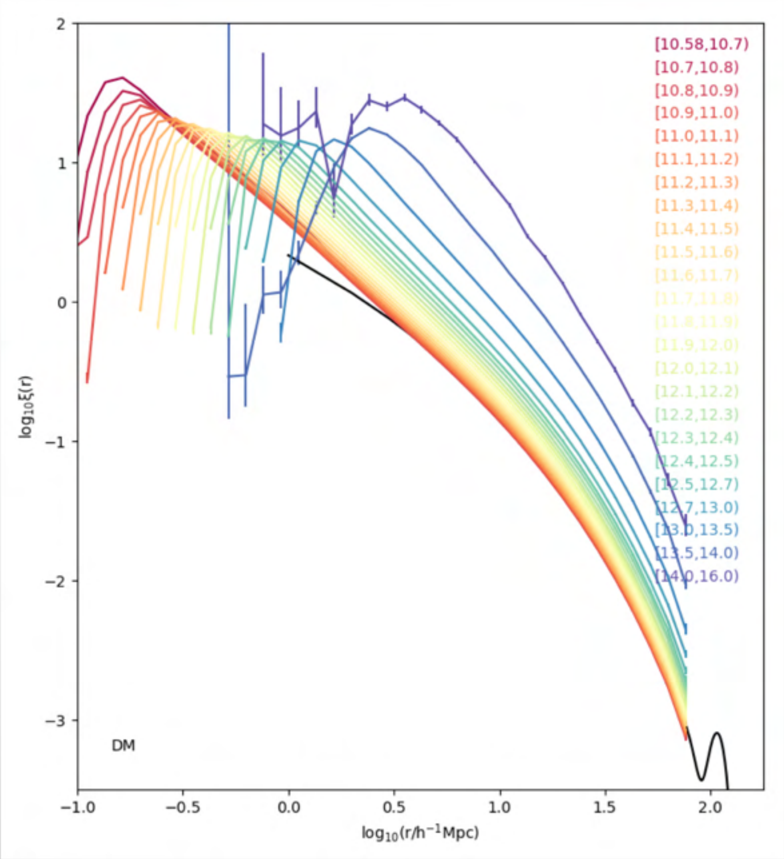

- Halo Mass Function

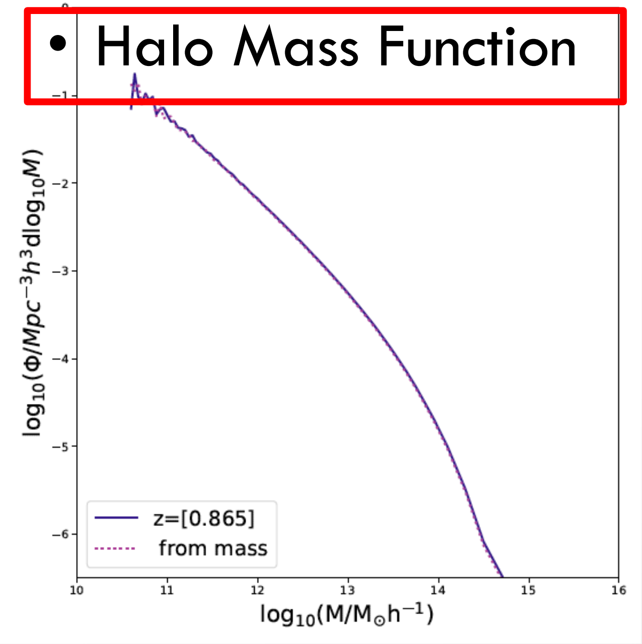

- Bias function

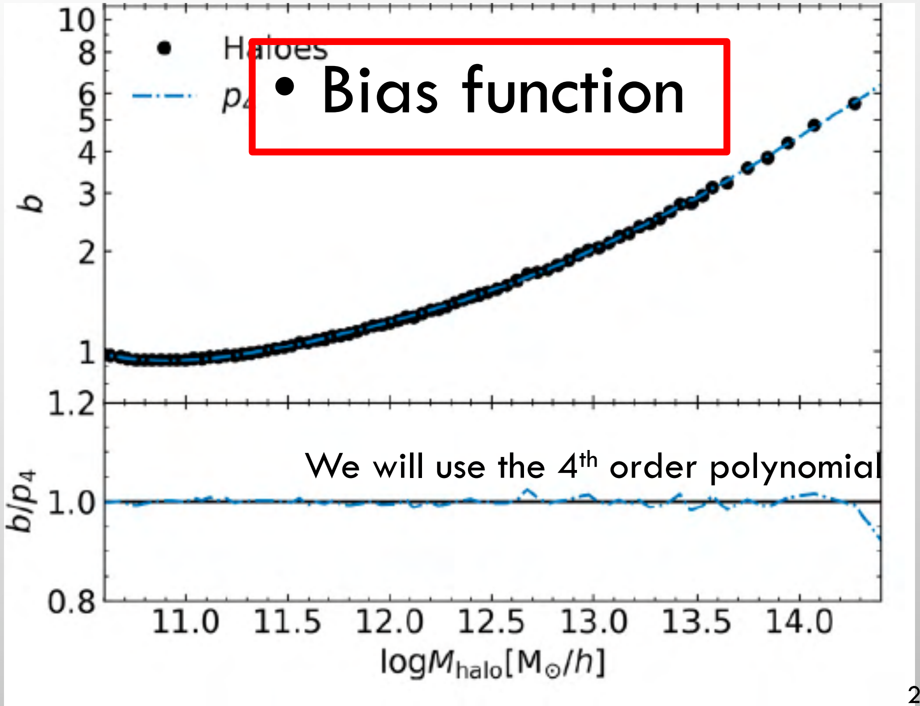

We will use the 4^{th} order polynomial

THE HALO OCCUPATION DISTRIBUTION MODEL

- The clustering of galaxies has 2 component: 1-halo and 2-halo terms

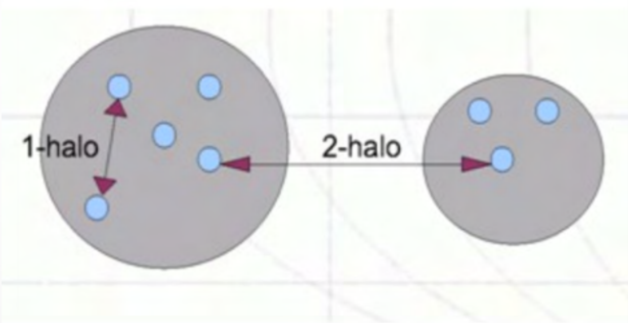

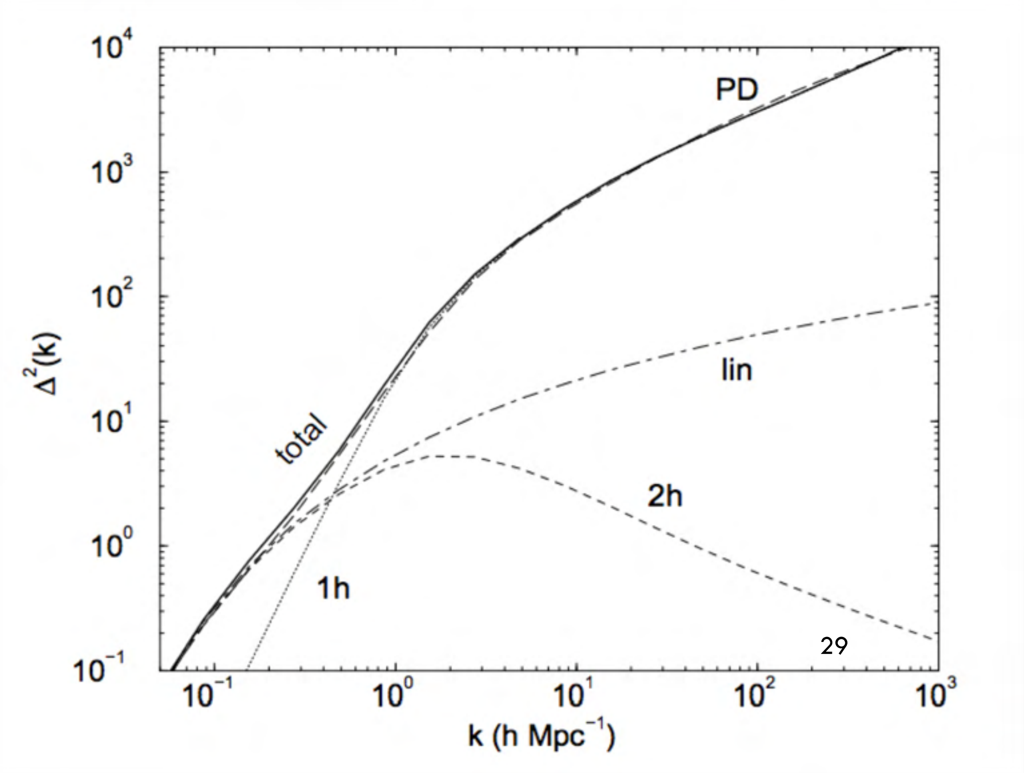

Model: Peacock & Dodds 96; Source: Cooray & Seth 2002

THE HALO OCCUPATION DISTRIBUTION MODEL

- The clustering of galaxies has 2 component: 1-halo and 2-halo terms

- How a certain galaxy sample populates the DM halos of different masses will determine the clustering of the galaxies.
  It will depend on five properties (Berlind & Weinberg 2002):

2-halo

  - 1. Mean halo Occupation <N(M)> $\langle N(M_h) \rangle$

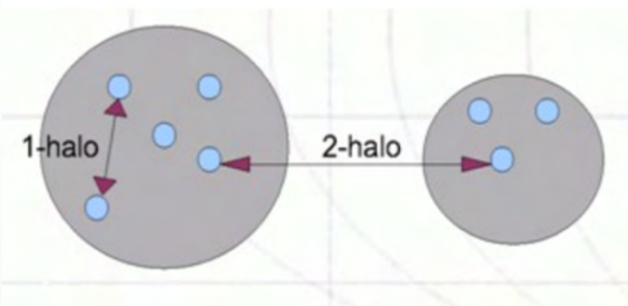

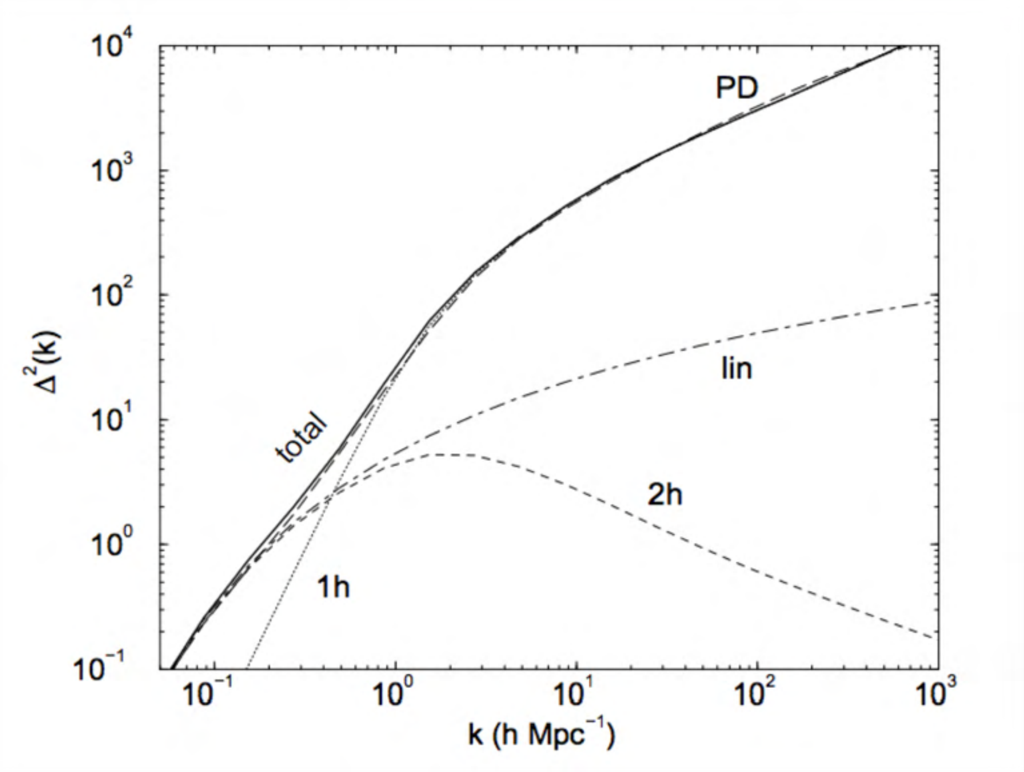

Model: Peacock & Dodds 96; Source: Cooray & Seth 2002

THE HALO OCCUPATION DISTRIBUTION MODEL

- The clustering of galaxies has 2 component: 1-halo and 2-halo terms

- How a certain galaxy sample populates the DM halos of different masses will determine the clustering of the galaxies.
  It will depend on five properties (Berlind & Weinberg 2002):

2-halo

- 1. Mean halo Occupation <N(M)> $\langle N(M_h) \rangle$
- 2. Probability distribution $P(N|\langle N \rangle)$
- 3. Central-Satellite split:
  $$\langle N_{\rm tot}(M_h) \rangle = \langle N_{\rm cen}(M_h) \rangle + \langle N_{\rm sat}(M_h) \rangle$$
- 4. Satellite profile distribution $\rho_g(r)$
- 5. Satellite velocity distribution $P(v_t)$

1-halo

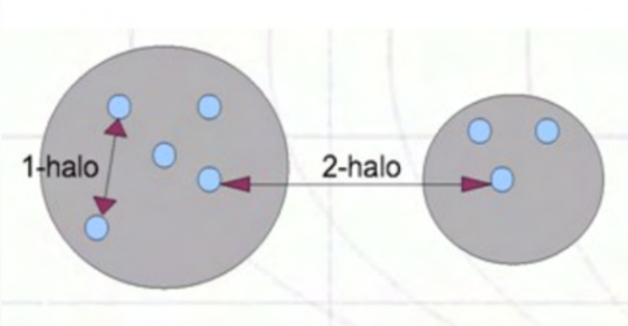

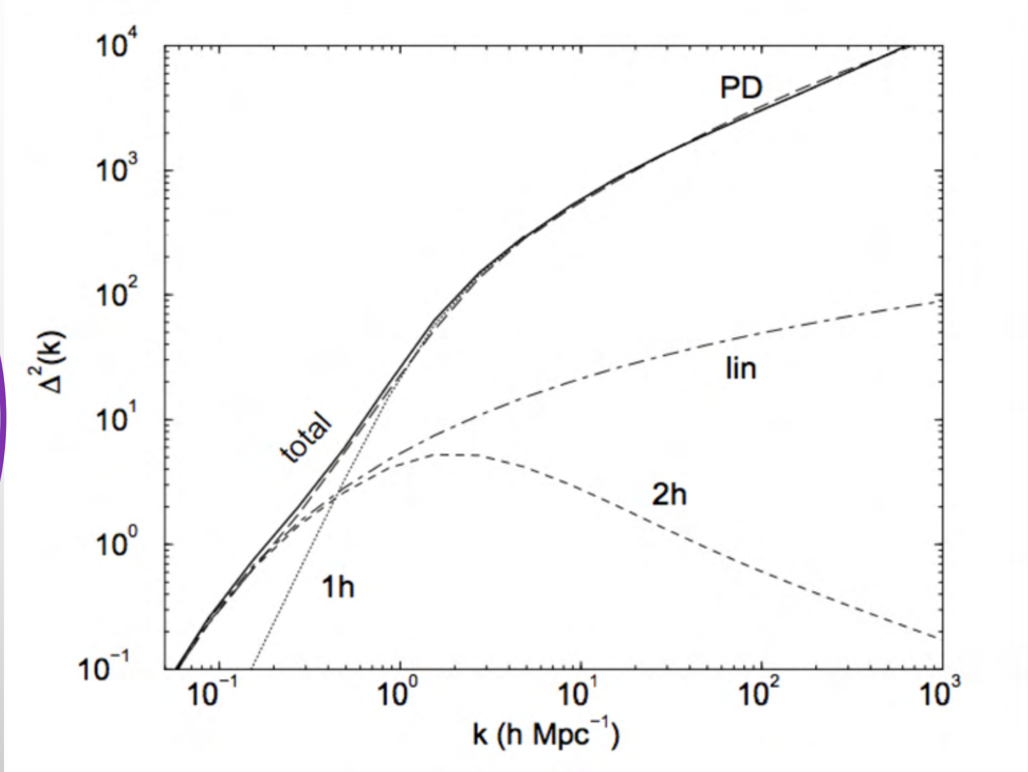

Model: Peacock & Dodds 96; Source: Cooray & Seth 2002

THE HALO OCCUPATION DISTRIBUTION MODEL

- The clustering of galaxies has 2 component: 1-halo and 2-halo terms

- How a certain galaxy sample populates the DM halos of different masses will determine the clustering of the galaxies.
  It will depend on five properties (Berlind & Weinberg 2002):

2-halo

- 1. Mean halo Occupation <N(M)> $\langle N(M_h) \rangle$
- 2. Probability distribution $P(N|\langle N \rangle)$
- 3. Central-Satellite split:
  $$\langle N_{\rm tot}(M_h) \rangle = \langle N_{\rm cen}(M_h) \rangle + \langle N_{\rm sat}(M_h) \rangle$$
- 4. Satellite profile distribution $\rho_g(r)$
- 5. Satellite velocity distribution $P(v_t)$

1-halo

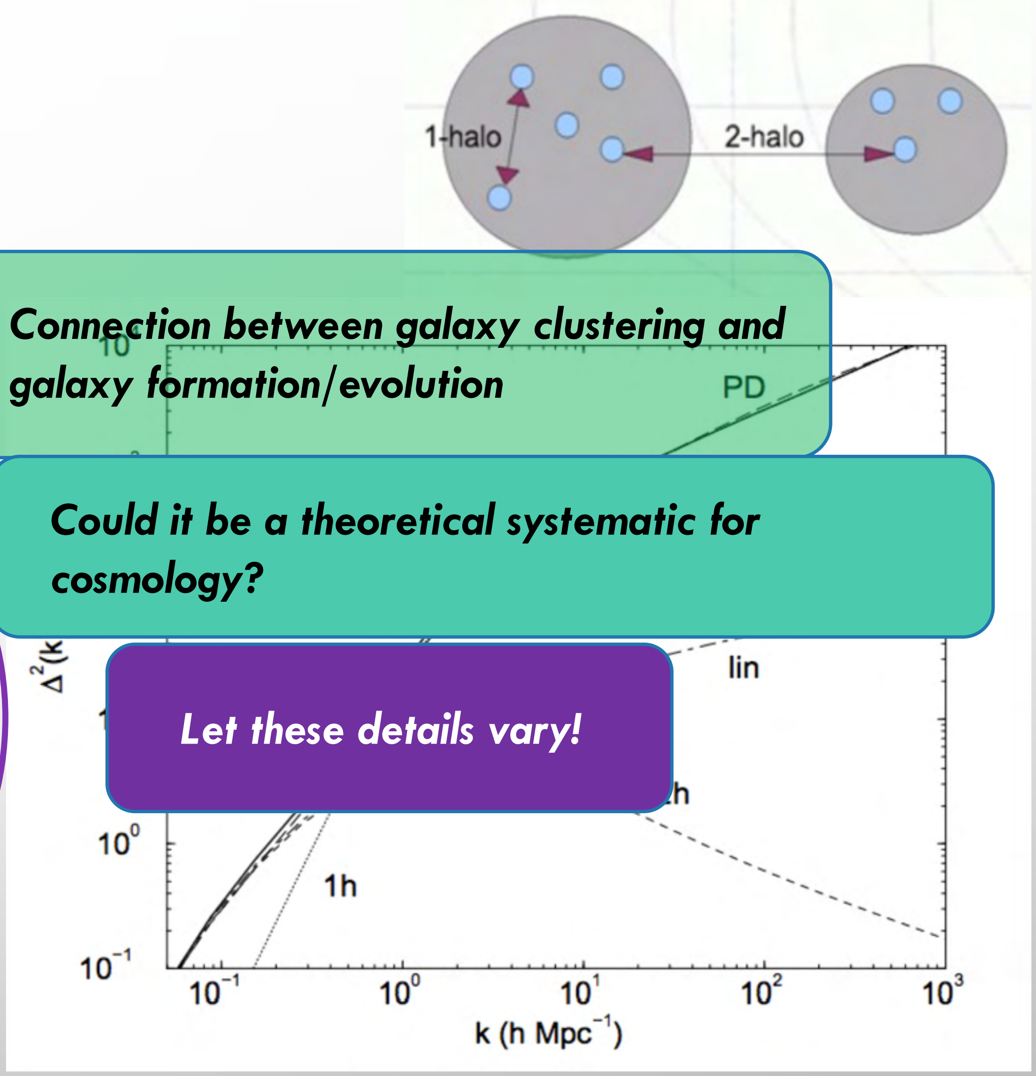

Connection between galaxy clustering and galaxy formation/evolution

Could it be a theoretical systematic for cosmology?

Let these details vary!

Model: Peacock & Dodds 96; Source: Cooray & Seth 2002

“CANONICAL” HOD SHAPE

Zehavi 2005

- Typically, a smooth step function for centrals

- And a power law for the satellites

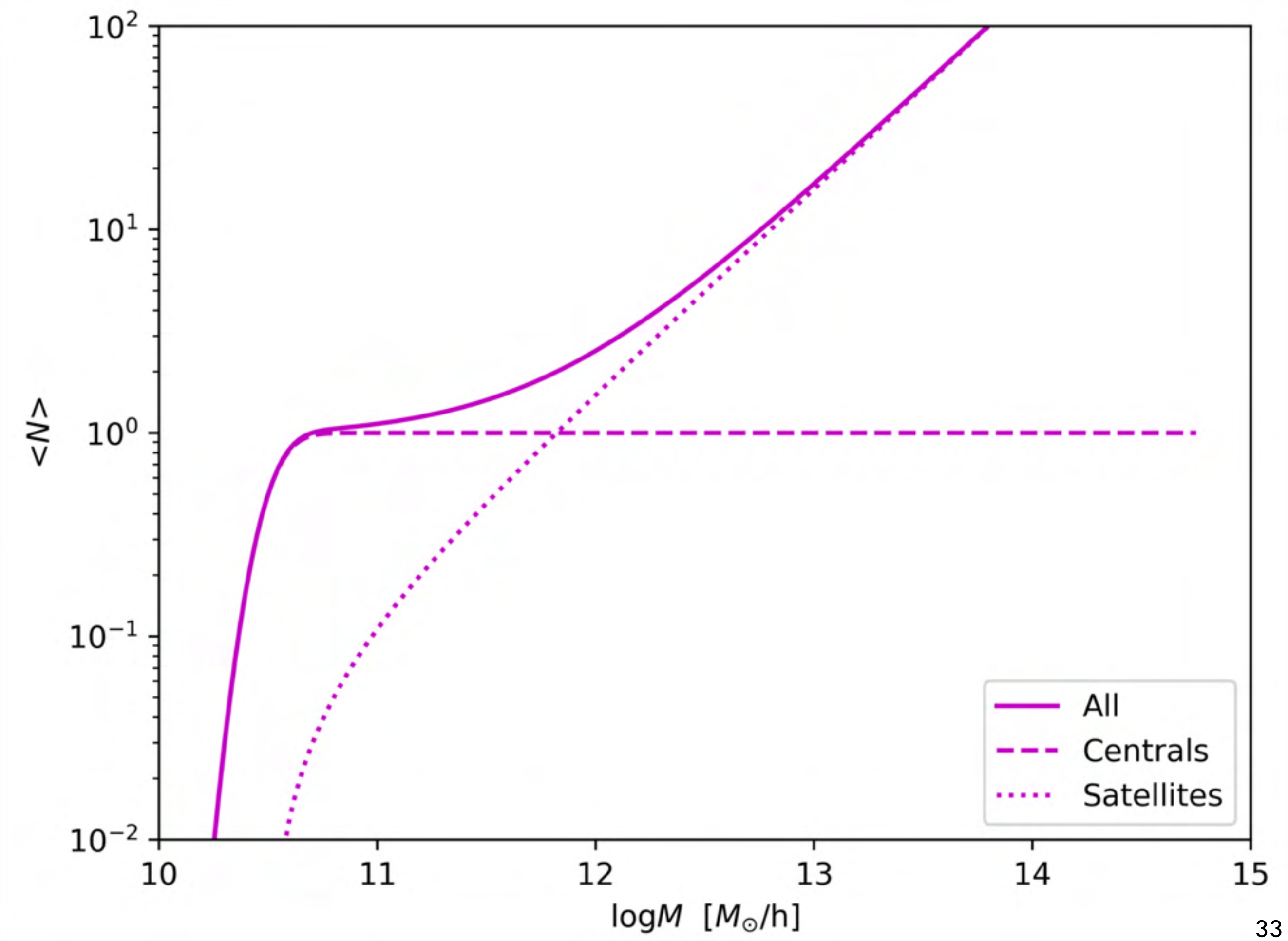

"CANONICAL" HOD SHAPE

Zehavi 2005

- Typically, a smooth step function for centrals

- And a power law for the satellites

HOD-1

$$\langle N_{\rm cen}(M)\rangle = \frac{1}{2}A_c\left(1+\mathrm{erf}\left(\frac{\log_{10}(\mathrm{M})-\mu}{\sigma}\right)\right)$$

$$\langle N_{\rm sat}(M)\rangle = A_s\left(\frac{M-M_0}{M_1}\right)^{\alpha}$$

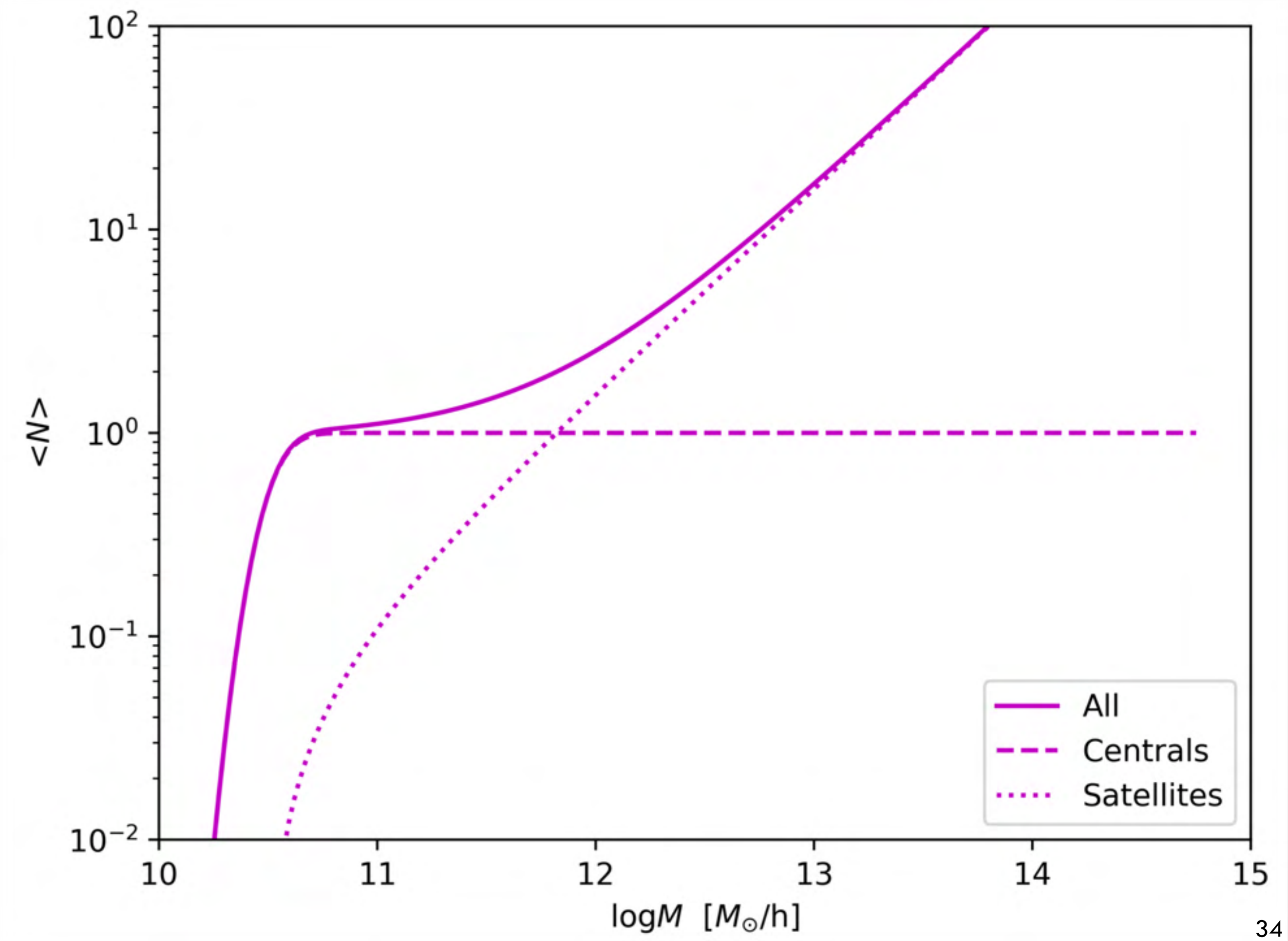

"CANONICAL" HOD SHAPE

Zehavi 2005

- Typically, a smooth step function for centrals

For "all galaxies", it would reach 1. We introduce $\mathbf{A_c}$ for the incompleteness of the ELG subsample

- And a power law for the satellites

We also introduce $\mathbf{A_s}$ to control $\mathbf{f_{sat}}$
and we fix $\log M_0 - \mu$, $\log M_1 - \mu$

HOD-1

$$\langle N_{\rm cen}(M)\rangle = \frac{1}{2} A_c \left(1 + \operatorname{erf}\left(\frac{\log_{10}(\mathrm{M}) - \mu}{\sigma}\right)\right)$$

$$\langle N_{\rm sat}(M)\rangle = A_s \left(\frac{M - M_0}{M_1}\right)^{\alpha}$$

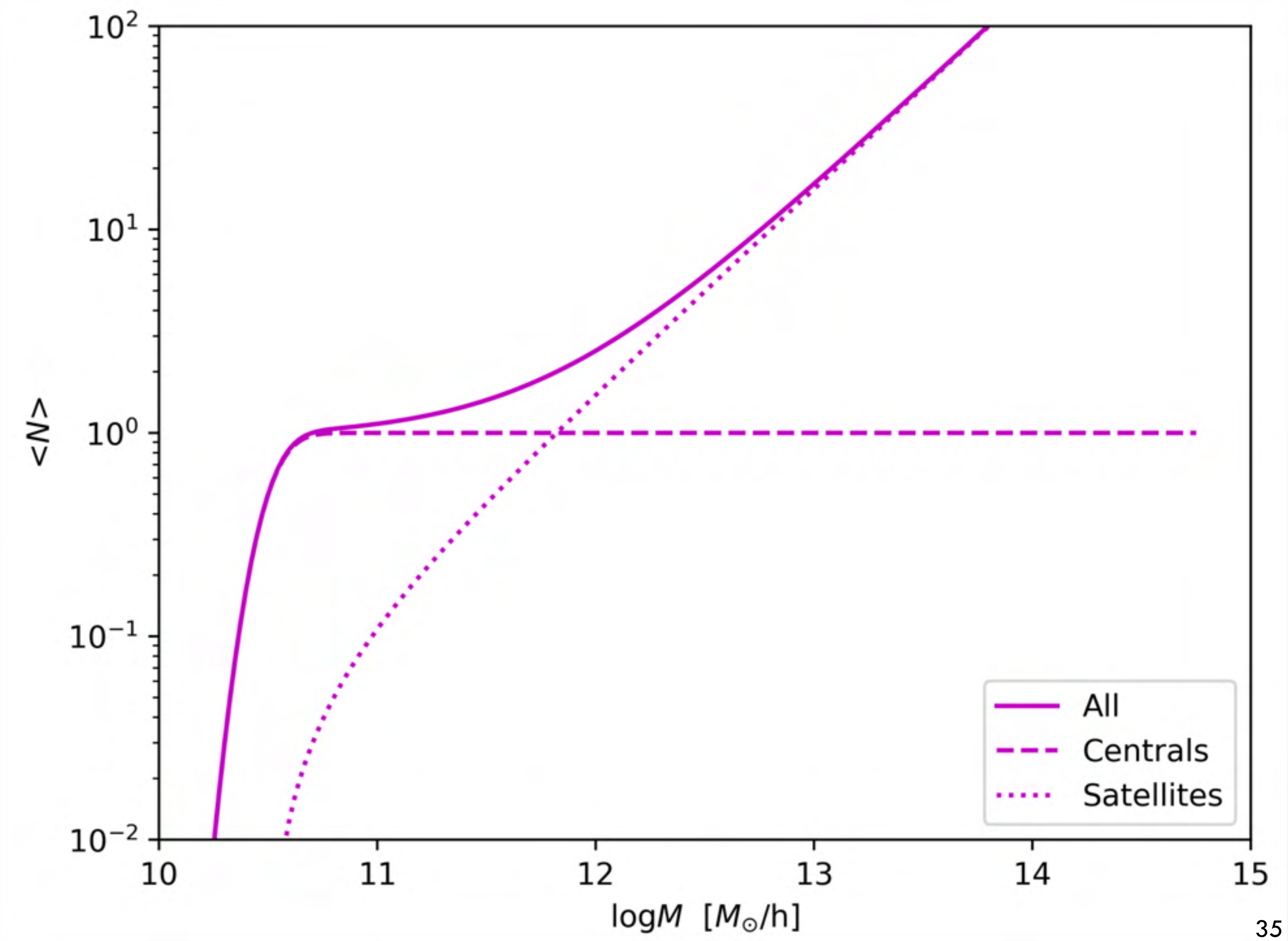

"CANONICAL" HOD SHAPE

Zehavi 2005

- Typically, a smooth step function for centrals

For "all galaxies", it would reach 1. We introduce $\mathbf{A_c}$ for the incompleteness of the ELG subsample

- And a power law for the satellites

We also introduce $\mathbf{A_s}$ to control $\mathbf{f_{sat}}$

and we fix $\log M_0 - \mu$, $\log M_1 - \mu$

HOD-1

$$\langle N_{\rm cen}(M)\rangle = \frac{1}{2}A_c\left(1+\mathrm{erf}\left(\frac{\log_{10}(\mathrm{M})-\mu}{\sigma}\right)\right)$$

$$\langle N_{\rm sat}(M)\rangle = A_s\left(\frac{M-M_0}{M_1}\right)^{\alpha}$$

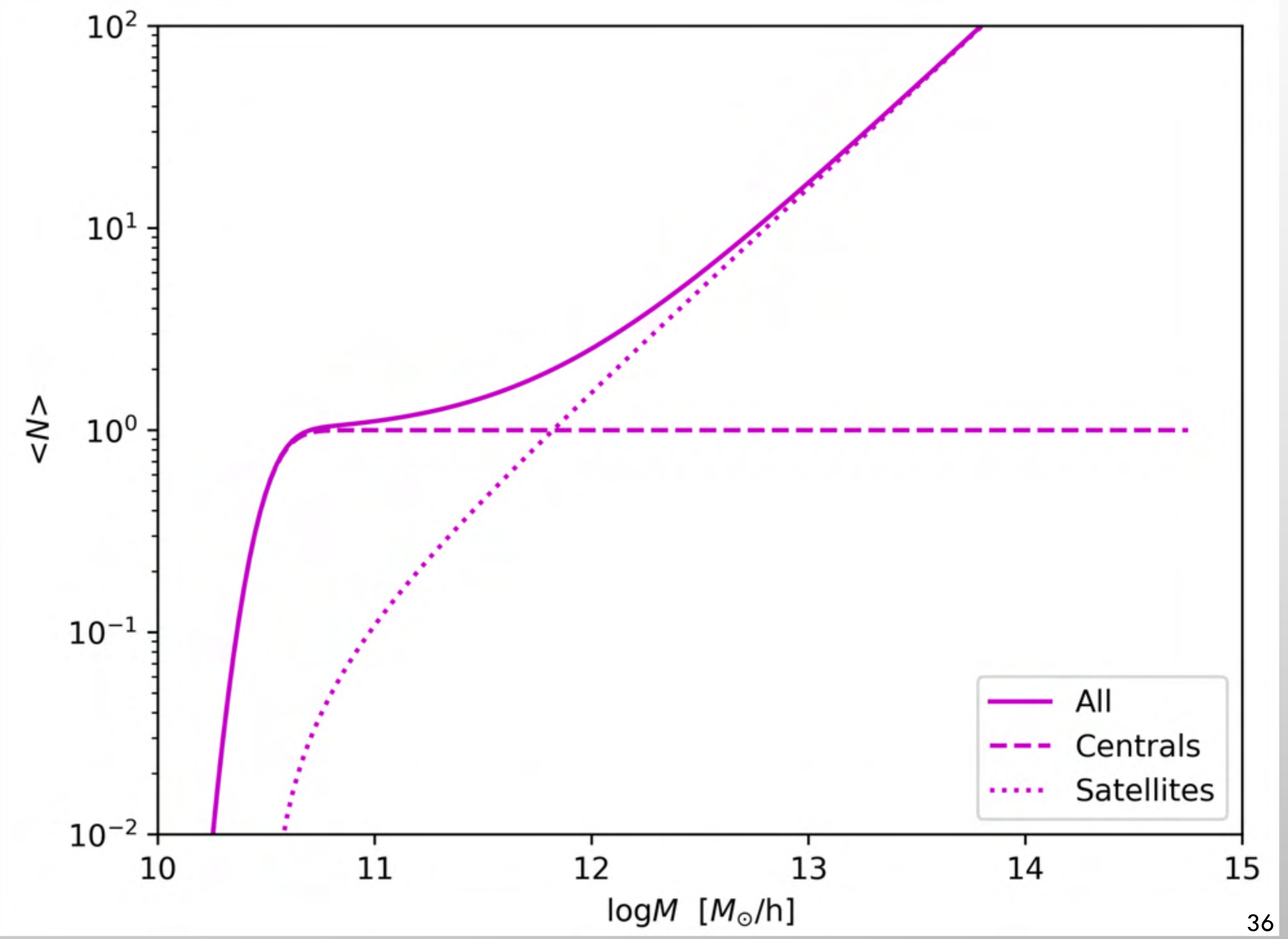

"CANONICAL" HOD SHAPE

Zehavi 2005

- Typically, a smooth step function for centrals

For "all galaxies", it would reach 1. We introduce $\mathbf{A_c}$ for the incompleteness of the ELG subsample

- And a power law for the satellites

We also introduce $\mathbf{A_s}$ to control $\mathbf{f_{sat}}$

and we **FIX $\log M_0$-μ , $\log M_1$-μ**

HOD-1

$$\langle N_{\rm cen}(M)\rangle = \frac{1}{2} A_c \left(1 + \mathrm{erf}\left(\frac{\log_{10}(M) - \mu}{\sigma}\right)\right)$$

$$\langle N_{\rm sat}(M)\rangle = A_s \left(\frac{M - M_0}{M_1}\right)^{\alpha}$$

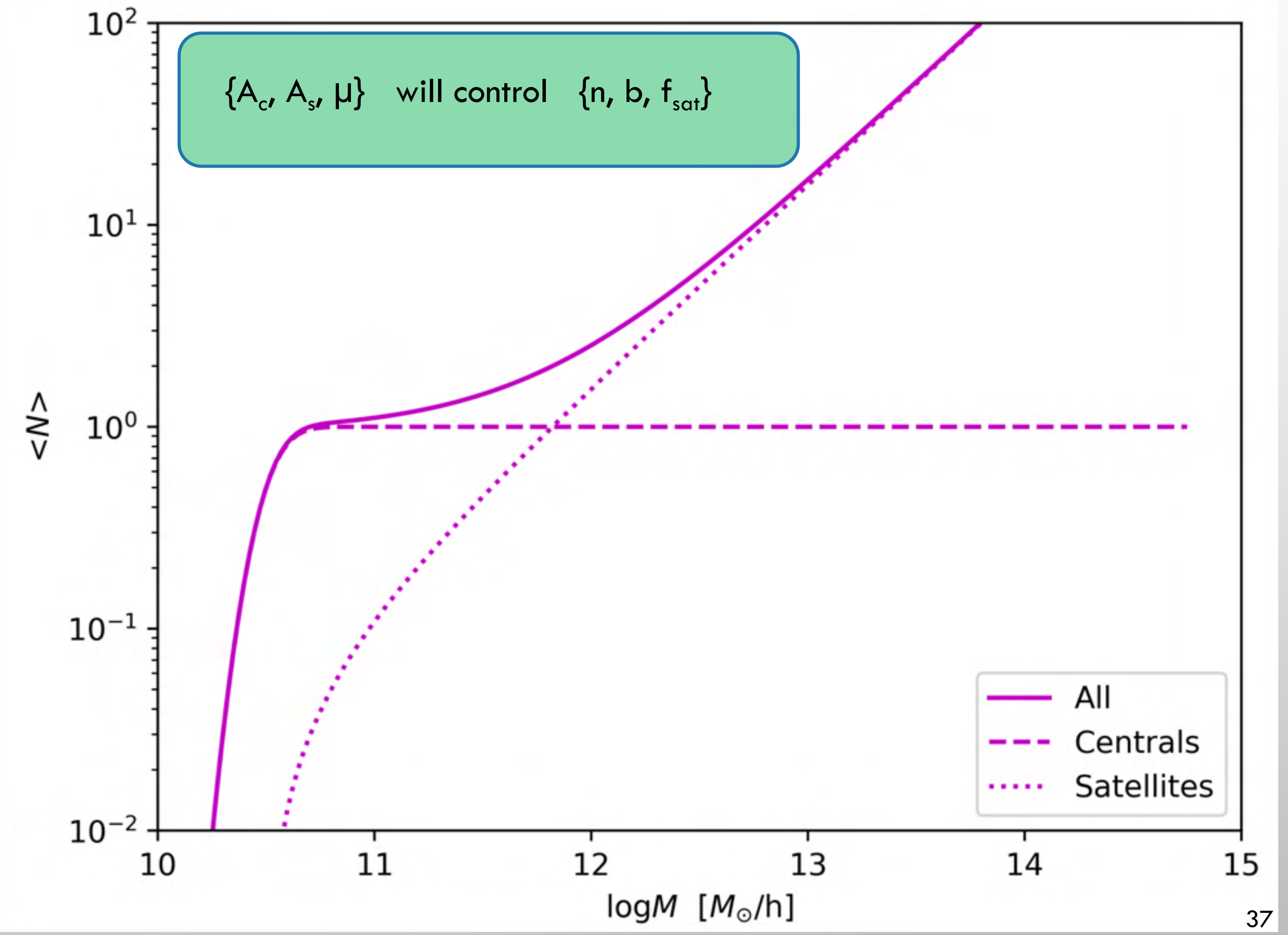

BUT NOT ALL GALAXIES ARE EMISSION LINE GALAXIES

ALTERNATIVE: LEARN HOD FROM SAMS

WE FIT A SIMPLE FORMULA TO THE RESULTS FROM GONZÁLEZ-PÉREZ ET AL. 2018 USING GALFORM

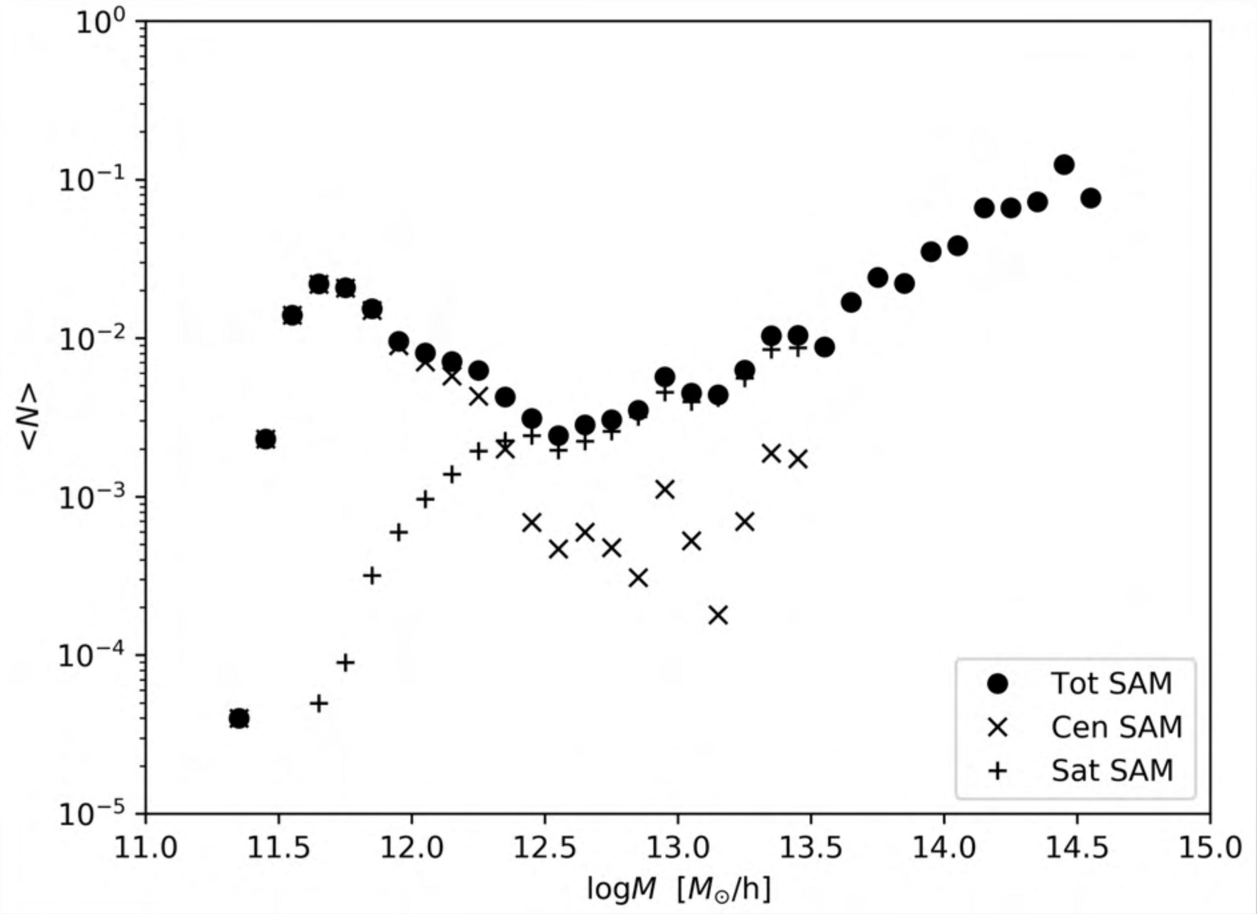

HOD: GAUSSIAN + (2) POWER LAW

WE FIT A SIMPLE FORMULA TO THE RESULTS FROM GONZÁLEZ-PÉREZ ET AL. 2018 GALFORM

HOD-2

$$< N_{cent} >= \frac{A_c}{\sqrt{2\pi\sigma^2}} \exp\{\frac{(log M_h - \mu)^2}{2\sigma^2}\}$$

$$< N_{sat} >= A_s \left(\frac{M_h - M_0}{M_1}\right)^{\alpha}$$

- FIX ALL SCALING RATIOS (M_0/M, M_1/M, $A = 0.8$, $\Sigma = 1$)

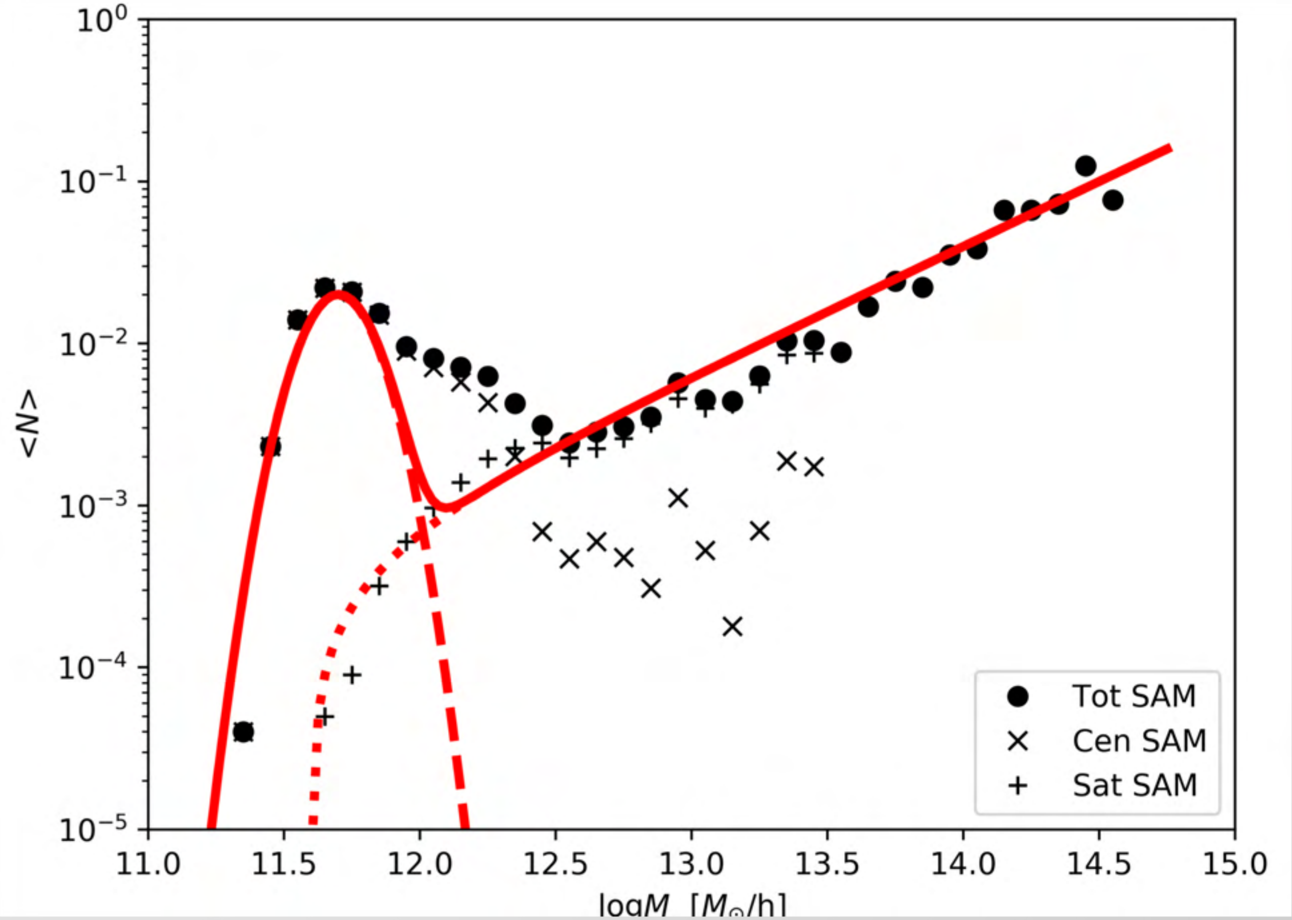

HOD: GAUSSIAN + (2) POWER LAW

WE FIT A SIMPLE FORMULA TO THE RESULTS FROM GONZÁLEZ-PÉREZ ET AL. 2018 GALFORM

HOD-2

$$< N_{cent} >= \frac{A_c}{\sqrt{2\pi\sigma^2}} \exp\{\frac{(logM_h - \mu)^2}{2\sigma^2}\}$$

$$< N_{sat} >= A_s \left(\frac{M_h - M_0}{M_1}\right)^{\alpha}$$

- FIX ALL SCALING RATIOS (M_0/M, M_1/M, $A = 0.8$, $\Sigma = 1$)
- A BETTER FIT:

HOD-3

$$\langle N_{\rm cen}(M_h)\rangle = \begin{cases} \frac{A_c}{2\pi\sigma^2} \cdot e^{-\frac{(\log M_h - \mu)^2}{2\sigma^2}} & \text{if} \quad M_h < \mu \\ A_c \left(\frac{\log M_h}{\mu}\right)^{\gamma} & \text{if} \quad M_h > \mu \end{cases}$$

$$< N_{sat} >= A_s \left(\frac{M_h - M_0}{M_1}\right)^{\alpha}$$

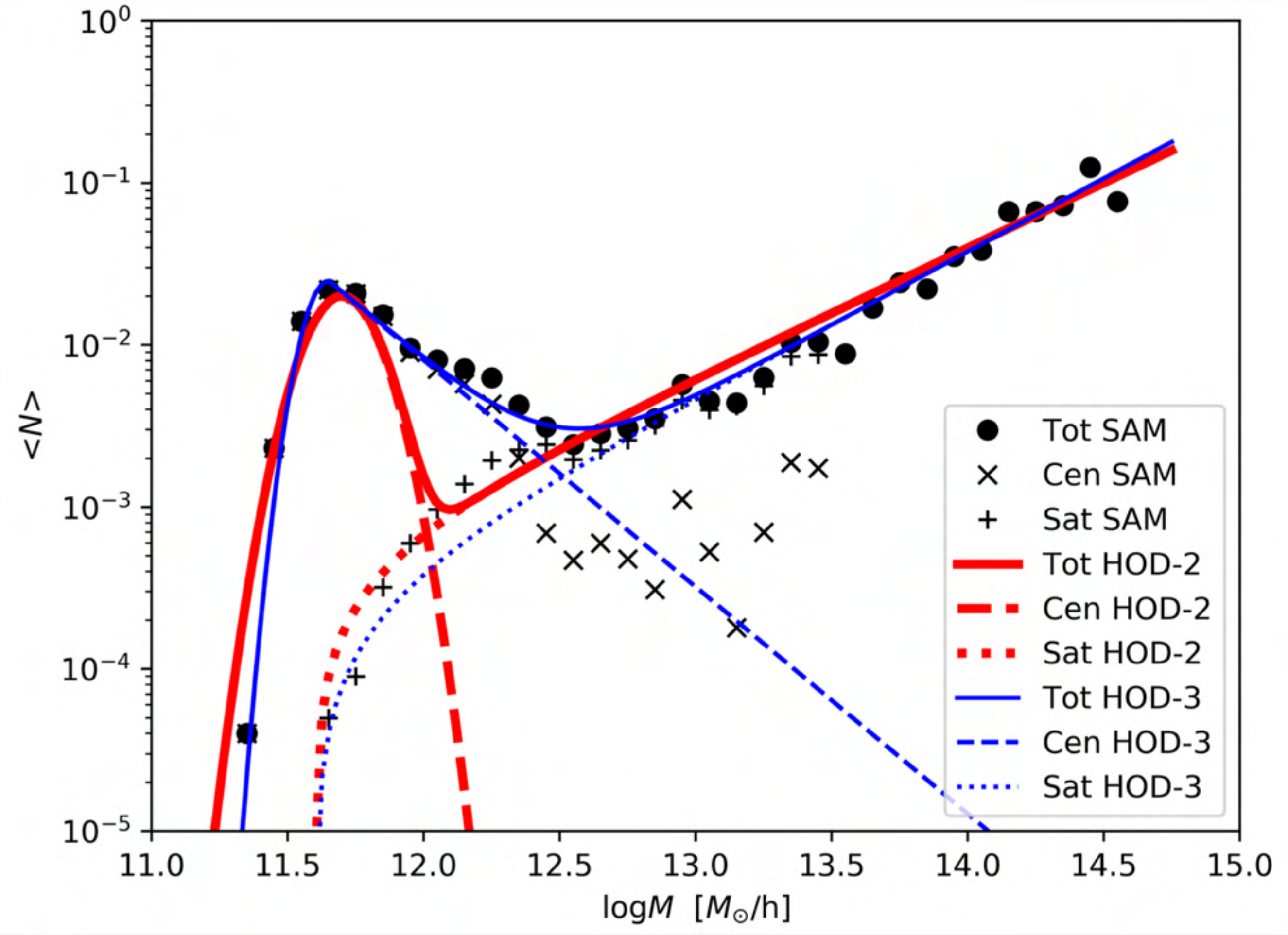

- IN THIS CASE THE RATIOS ARE: ($\gamma=-1.4$, M_0/μ, M_1/μ, $\alpha = 0.9$, $\sigma = 0.8$)

BASIC CONSTRAINS ON HOD

- WE CAN FIT THE LARGE SCALE LINEAR BIAS AND NUMBER DENSITY ANALYTICALLY:

$$\bar{n}_{\rm gal} = \int n(M_h)\left[\langle N_{\rm cen}(M_h)\rangle + \langle N_{\rm sat}(M_h)\rangle\right] {\rm d}M_h$$

$$\bar{n}_{\rm eBOSS} = 2.187 \cdot 10^{-4} ({\rm Mpc}/h)^{-3}$$

$$b_{\rm gal} = \frac{1}{\bar{n}_{\rm gal}} \int n(M_h) \cdot b(M_h)\left[\langle N\rangle_{\rm cen}(M_h) + \langle N\rangle_{\rm sat}(M_h))\right] {\rm d}M_h$$

$$b_{\rm eBOSS} = 1.320 \pm 0.014$$

BASIC CONSTRAINS ON HOD

- WE CAN FIT THE LARGE SCALE LINEAR BIAS AND NUMBER DENSITY ANALYTICALLY:

$$\bar{n}_{\rm gal} = \int n(M_h)\big[\langle N_{\rm cen}(M_h)\rangle + \langle N_{\rm sat}(M_h)\rangle\big]{\rm d}M_h$$

$$\bar{n}_{\rm eBOSS} = 2.187 \cdot 10^{-4} ({\rm Mpc}/h)^{-3}$$

$$b_{\rm gal} = \frac{1}{\bar{n}_{\rm gal}} \int n(M_h) \cdot b(M_h)\big[\langle N\rangle_{\rm cen}(M_h) + \langle N\rangle_{\rm sat}(M_h))\big]{\rm d}M_h$$

$$b_{\rm eBOSS} = 1.320 \pm 0.014$$

- WE CAN ADDITIONALLY CHOOSE F_{SAT}

$$f_{\rm sat} = \frac{1}{\bar{n}_{\rm gal}} \int n(M_h)\langle N_{\rm sat}(M_h)\rangle {\rm d}M_h$$

PART III. VARYING THE HOD MODELLING: EFFECT ON CLUSTERING

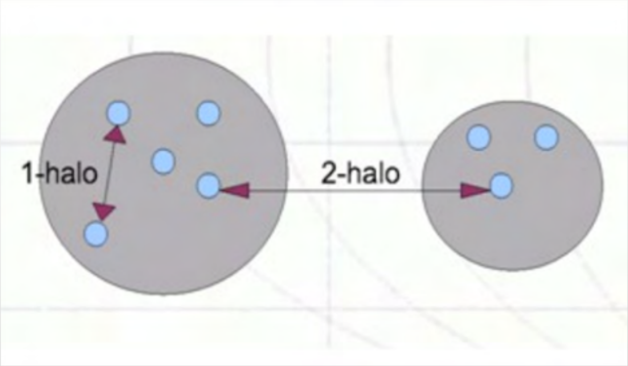

CLUSTERING STATISTICS

Isotropic 2-Point Correlation Function (2PCF)

$$\xi(r)) = \frac{\langle N_{g,\mathrm{pairs}}(r \pm dr/2)\rangle}{\langle n \rangle dV} - 1$$

$$\xi(r) = \frac{DD(r \pm dr/2)}{RR(r \pm dr/2)} - 1 \qquad \xi = \frac{DD - 2DR + RR}{RR}$$

2D 2PCF:

$$\xi(x, y) = \frac{DD(x, y) - 2DR(x, y) + RR(x, y)}{RR(x, y)}$$

2PCF multipoles:

$$\xi_\ell(s) = (2\ell + 1) \int_0^1 \xi(s, \mu) L_\ell(\mu) d\mu$$

Projected Correlation Function

$$w_p(r_p) = 2 \int_0^{\pi_{\max}} \xi(r_p, \pi) d\pi$$

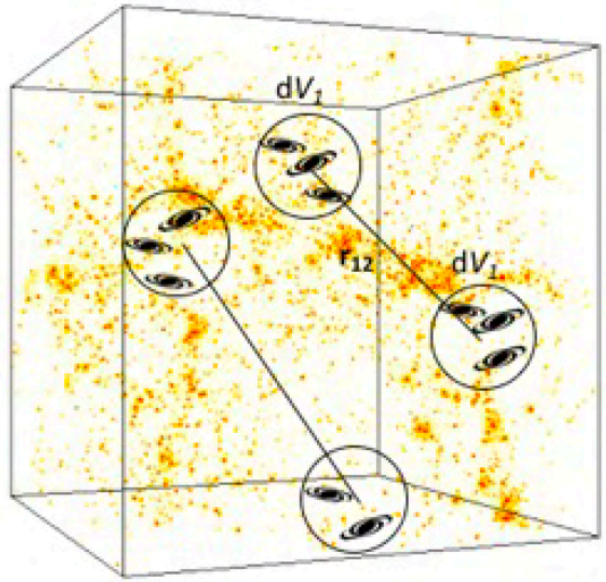

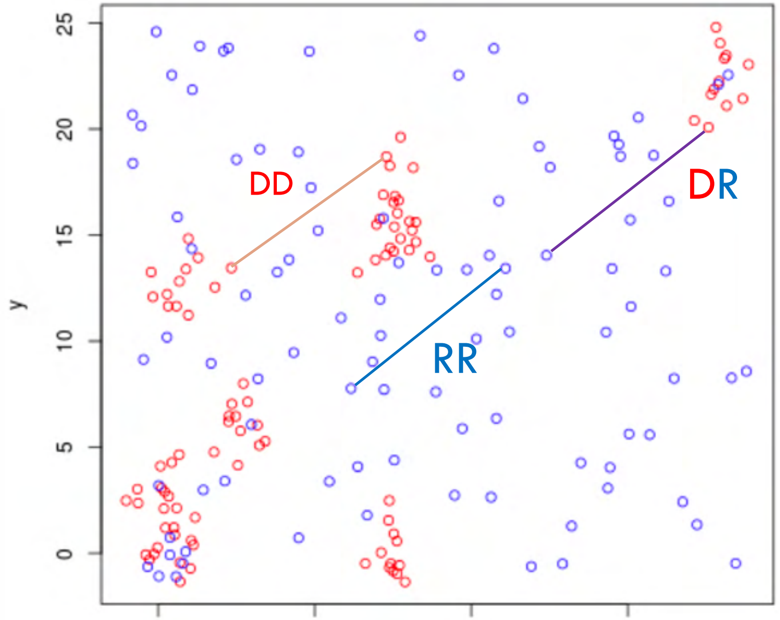

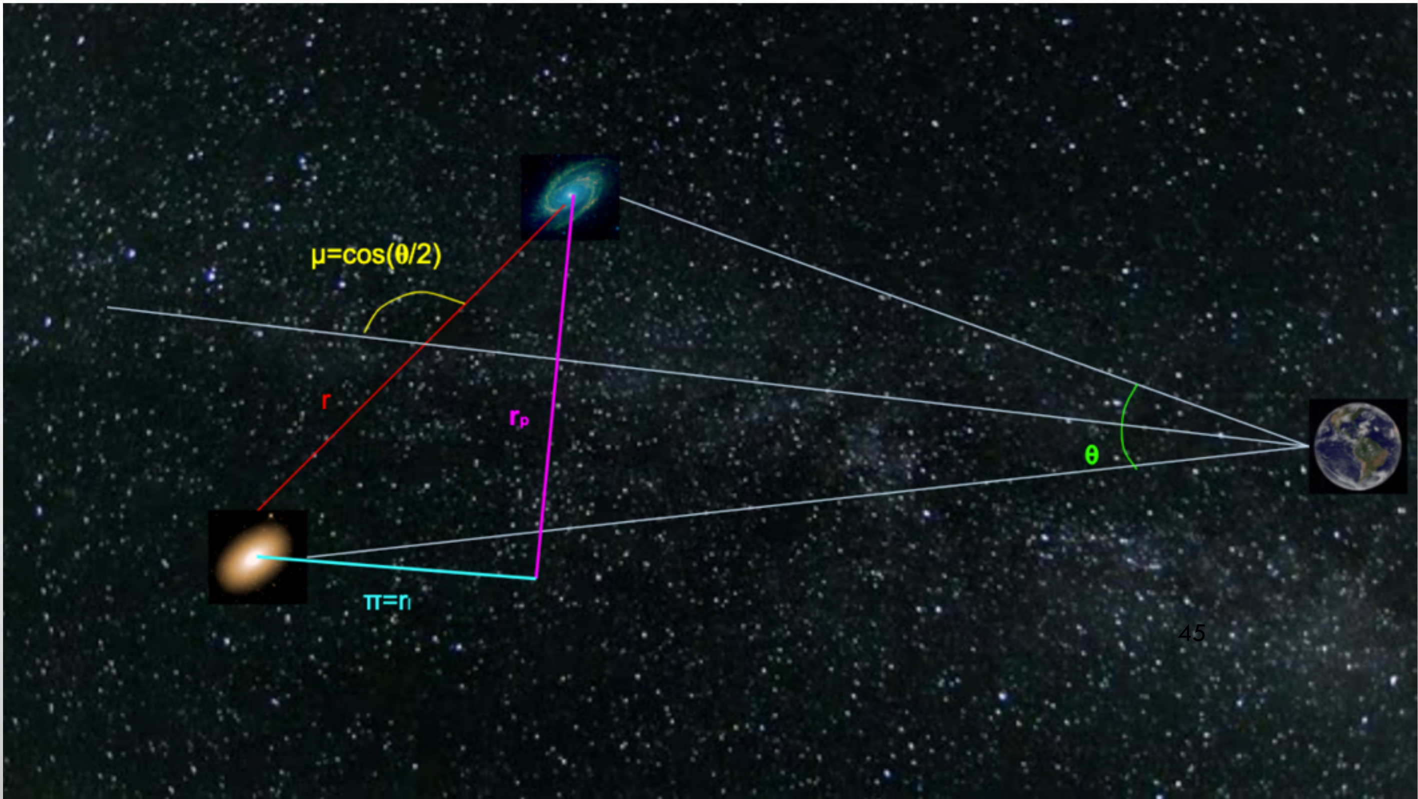

HOD VARIATIONS: CHANGING SHAPES

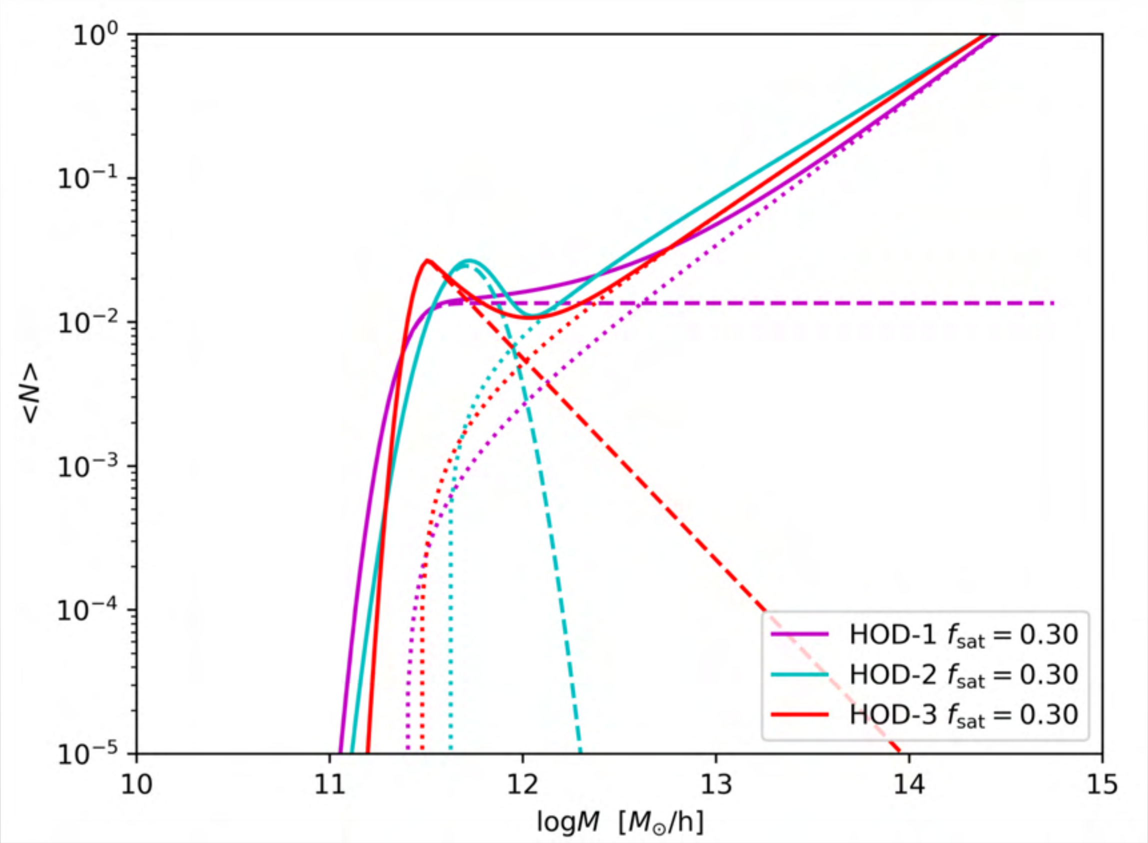

Effect on clustering ?

Same n,b f_{sat} for the 3 HODs

HOD VARIATIONS: CHANGING SHAPES

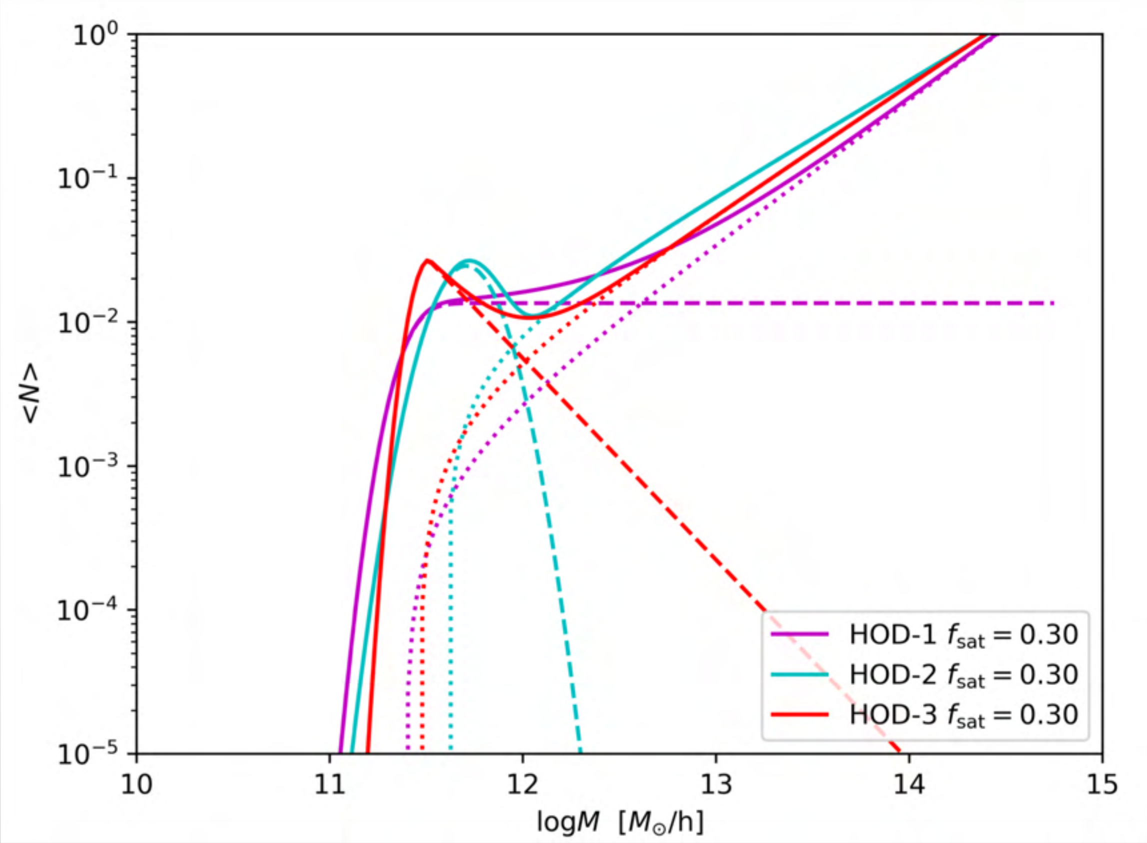

Projected correlation function

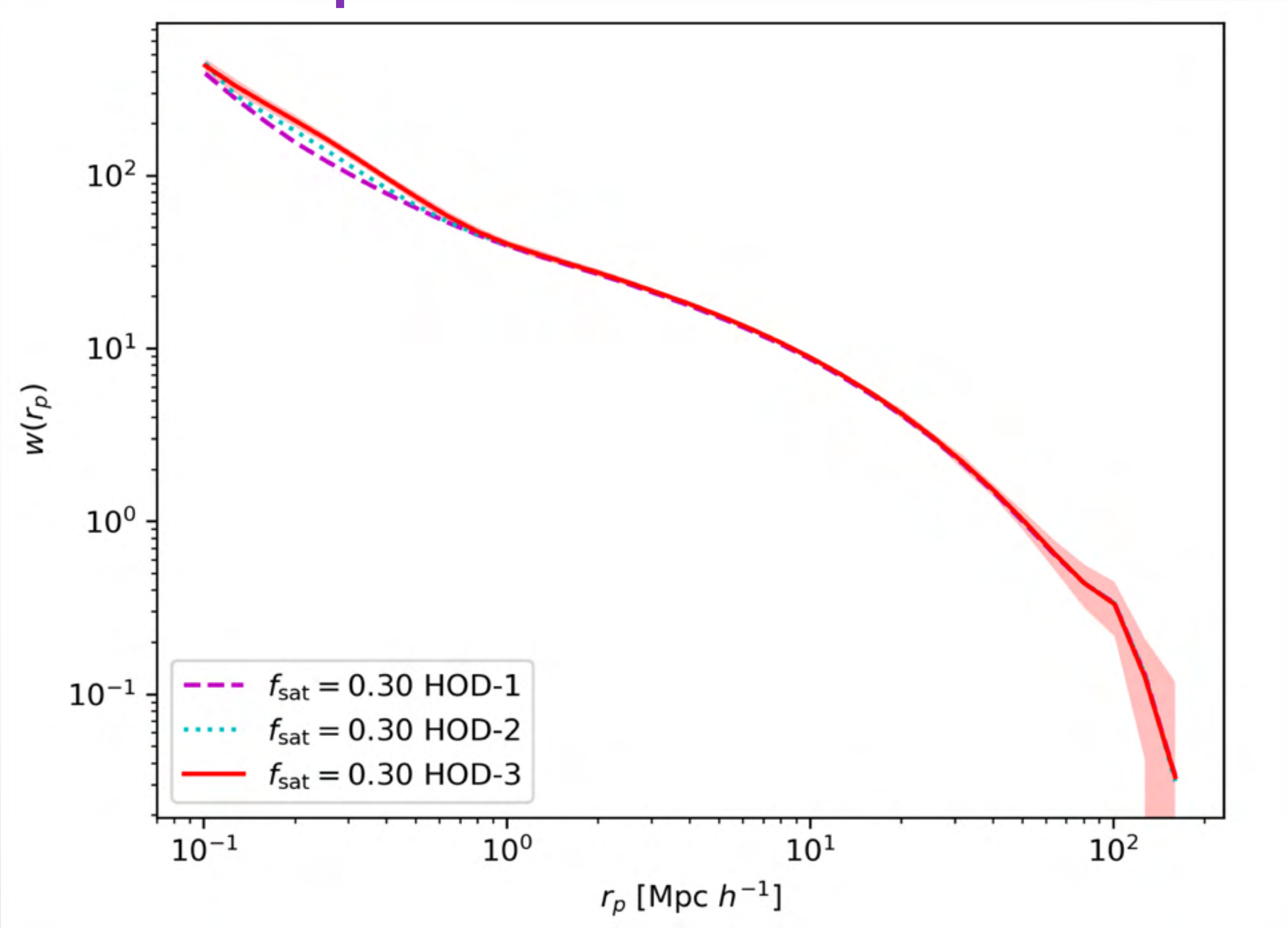

HOD VARIATIONS: CHANGING SHAPES

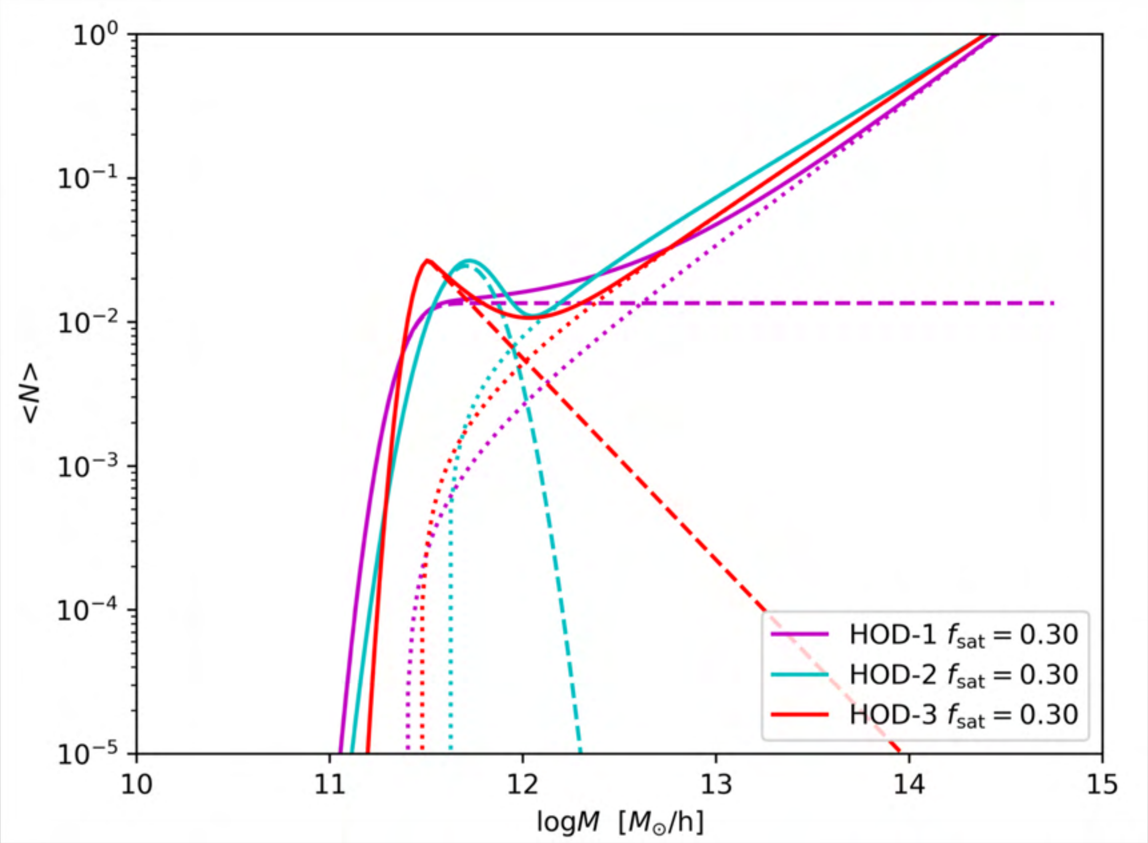

Quadrupole

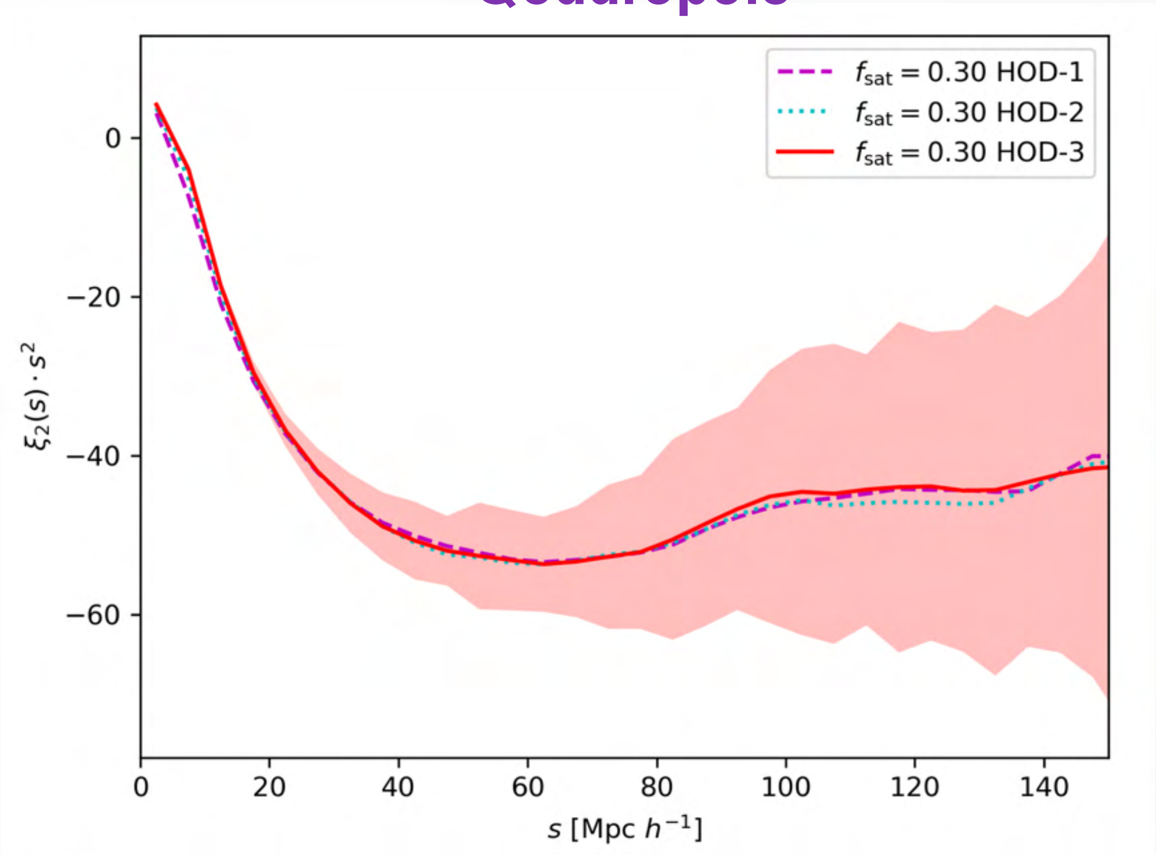

HOD: CHANGING SATELLITE FRACTION

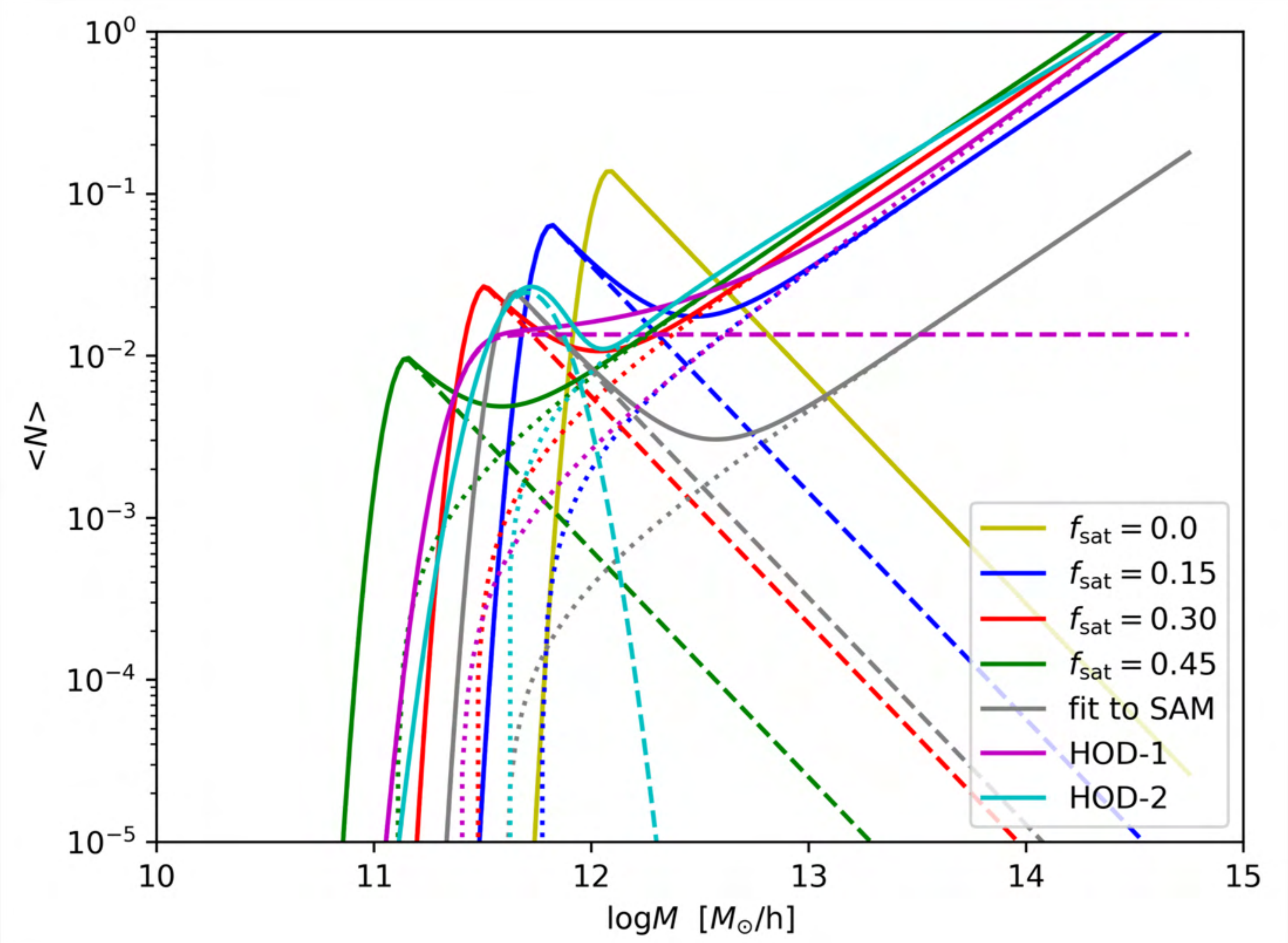

Effect on clustering ?

When not specified, we use HOD-3

Fix n & b, vary f_{sat}

HOD: CHANGING SATELLITE FRACTION

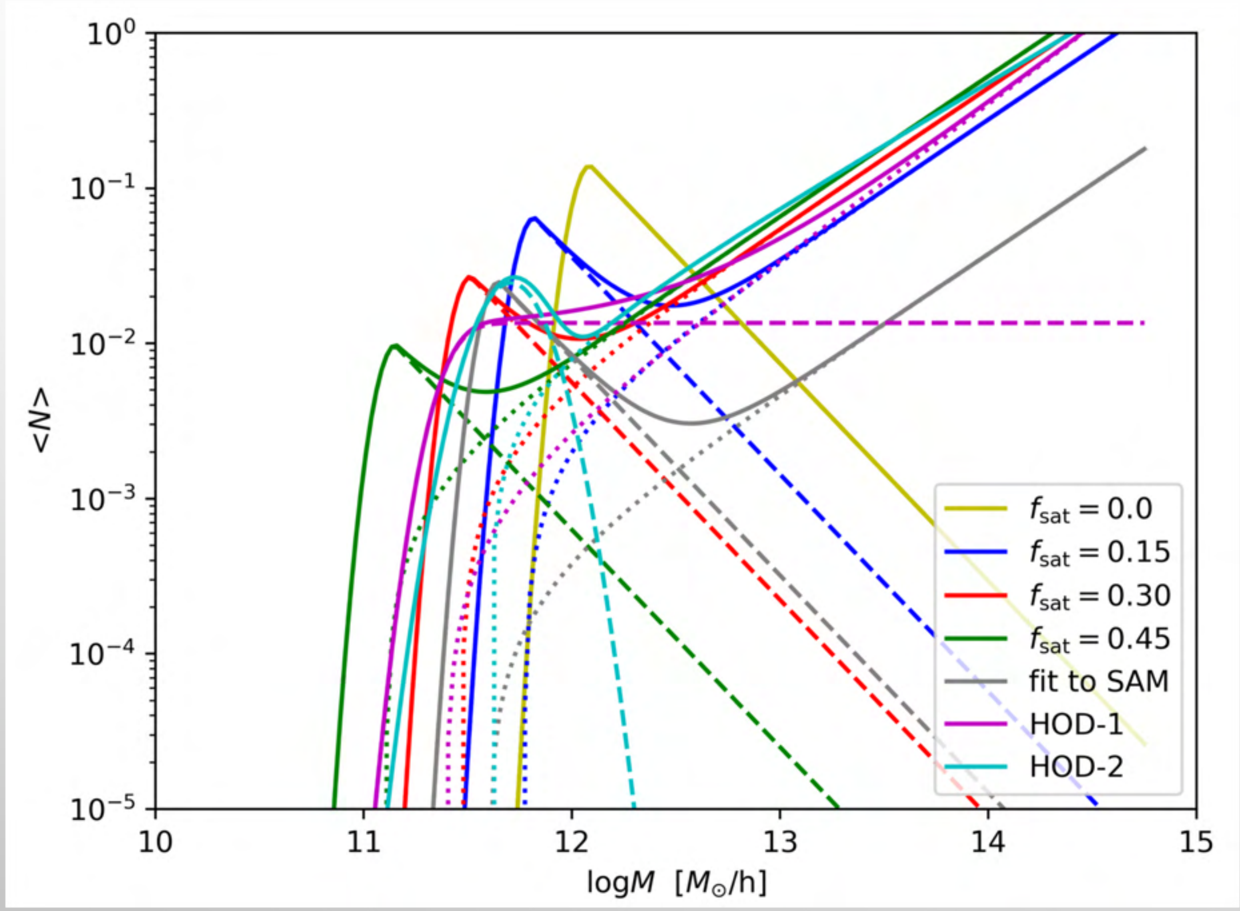

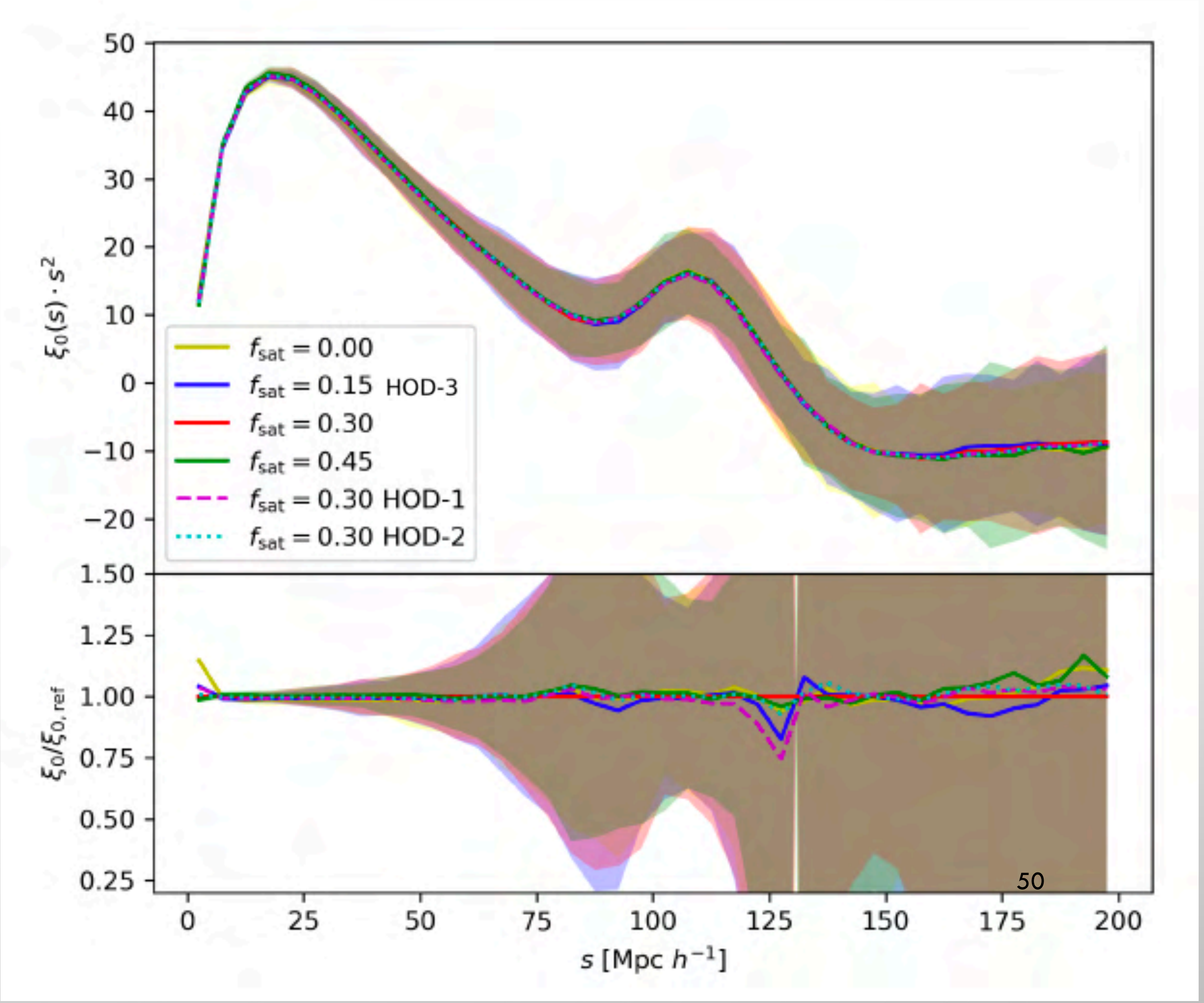

HOD: CHANGING SATELLITE FRACTION

- CHANGING HOD SHAPE AND SATELLITE FRACTION: <N_{CEN}>, <N_{SAT}>

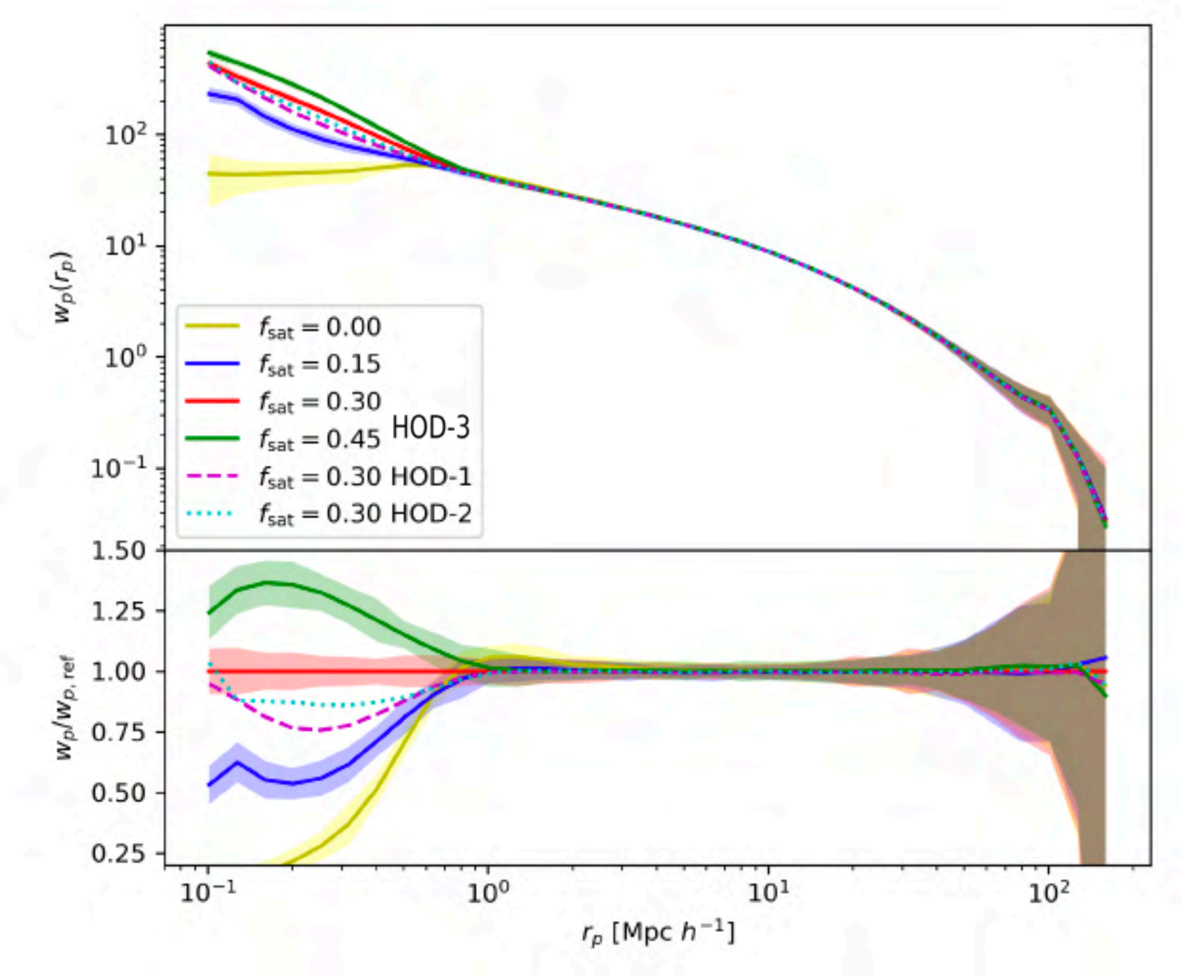

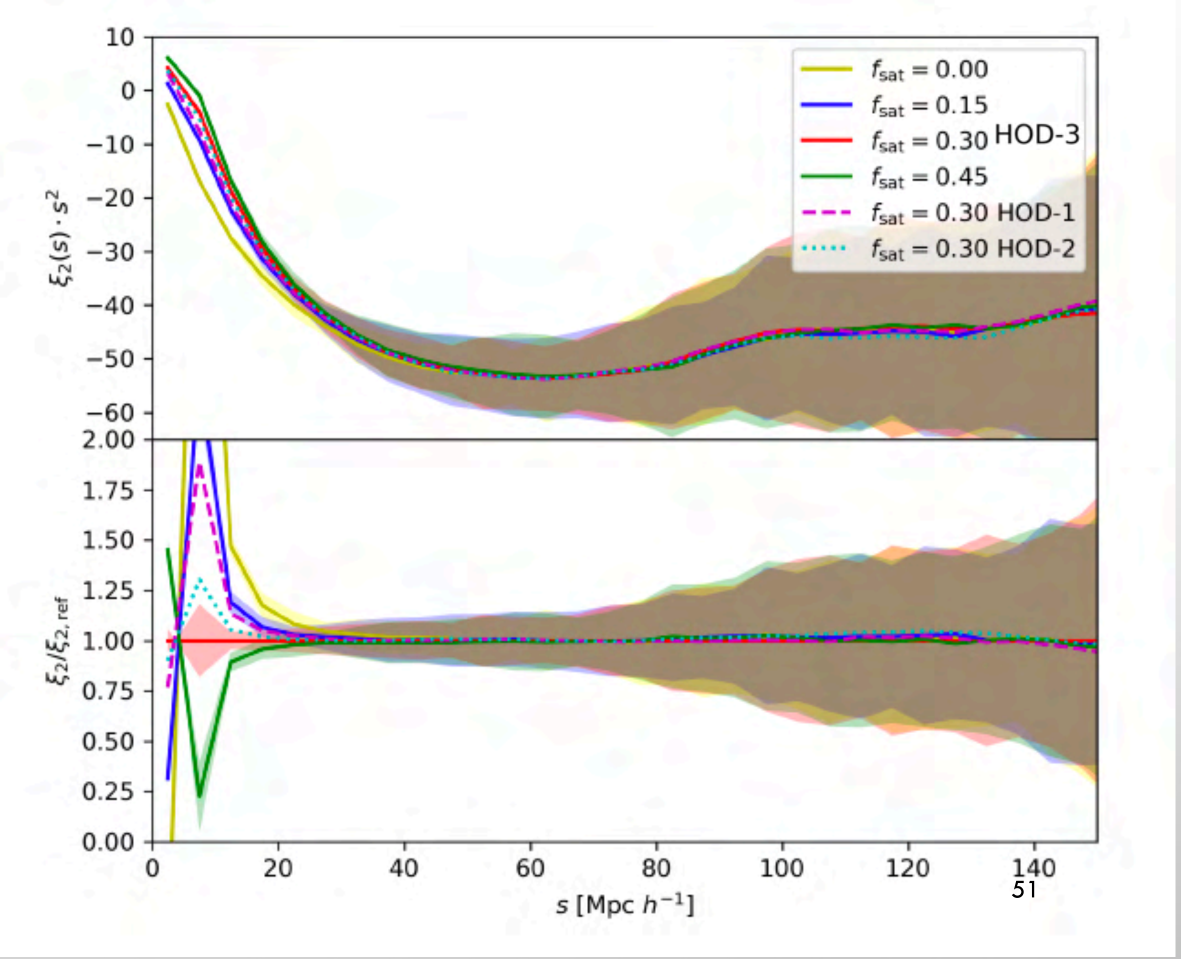

PROBABILITY DISTRIBUTION FUNCTION FOR SATELLITES

- Once we fix $\langle N_{cen} \rangle$ and $\langle N_{sat} \rangle$, we need to define the probability distribution function (PDF): $P(N|\langle N \rangle)$
- For satellite, what it is typically assumed is the **Poisson** distribution:

$$P(N|\lambda) = \frac{e^{-N}\lambda^N}{N!}$$

Where $\lambda \equiv \langle N \rangle$, and obtaining $\sigma = \sqrt{\langle N \rangle}$

PROBABILITY DISTRIBUTION FUNCTION FOR SATELLITES

- Once we fix <N_{cen}> and <N_{sat}>, we need to define the probability distribution function (PDF): P(N|<N>)

- For satellite, what it is typically assumed is the **Poisson** distribution:

$$P(N|\lambda) = \frac{e^{-N}\lambda^N}{N!}$$

Where $\lambda \equiv \langle N \rangle$, and obtaining $\sigma = \sqrt{\langle N \rangle}$

- Alternatively, we could use a **Negative Binomial** distribution, which has a (1+**β**) larger scatter (jimemez+19):

$$P(N|r,p) = \frac{\Gamma(N+r)}{\Gamma(r)\Gamma(N+1)} p^r (1-p)^N \text{ with}$$
$$p = \frac{1}{(1+\beta)^2},\ r = \frac{\lambda}{\beta(1+2\beta)}$$

$$\sigma = \lambda(1+\beta)$$

PROBABILITY DISTRIBUTION FUNCTION FOR SATELLITES

- Once we fix <N_{cen}> and <N_{sat}>, we need to define the probability distribution function (PDF): P(N|<N>)
- For satellites, what it is typically assumed is the **Poisson** distribution:

$$P(N|\lambda) = \frac{e^{-N}\lambda^N}{N!}$$

Where $\lambda \equiv \langle N \rangle$, and obtaining $\sigma = \sqrt{\langle N \rangle}$

- Alternatively, we could use a **Negative Binomial** distribution, which has a (1+**β**) larger scatter (jimemez+19):

$$P(N|r,p) = \frac{\Gamma(N+r)}{\Gamma(r)\Gamma(N+1)} p^r (1-p)^N \quad \text{with}$$

$$p = \frac{1}{(1+\beta)^2}, \quad r = \frac{\lambda}{\beta(1+2\beta)}$$

$$\sigma = \lambda(1+\beta)$$

- Or with lower scatter, the **Nearest Integer** (always the case for centrals):

$$P(N|\lambda) = \begin{cases} 1-(\lambda - \textsc{int}(\lambda)) & N = \textsc{int}(\lambda) \\ \lambda - \textsc{int}(\lambda) & N = \textsc{int}(\lambda)+1 \\ 0 & \text{else} \end{cases}$$

HOD: PDF VARIATIONS

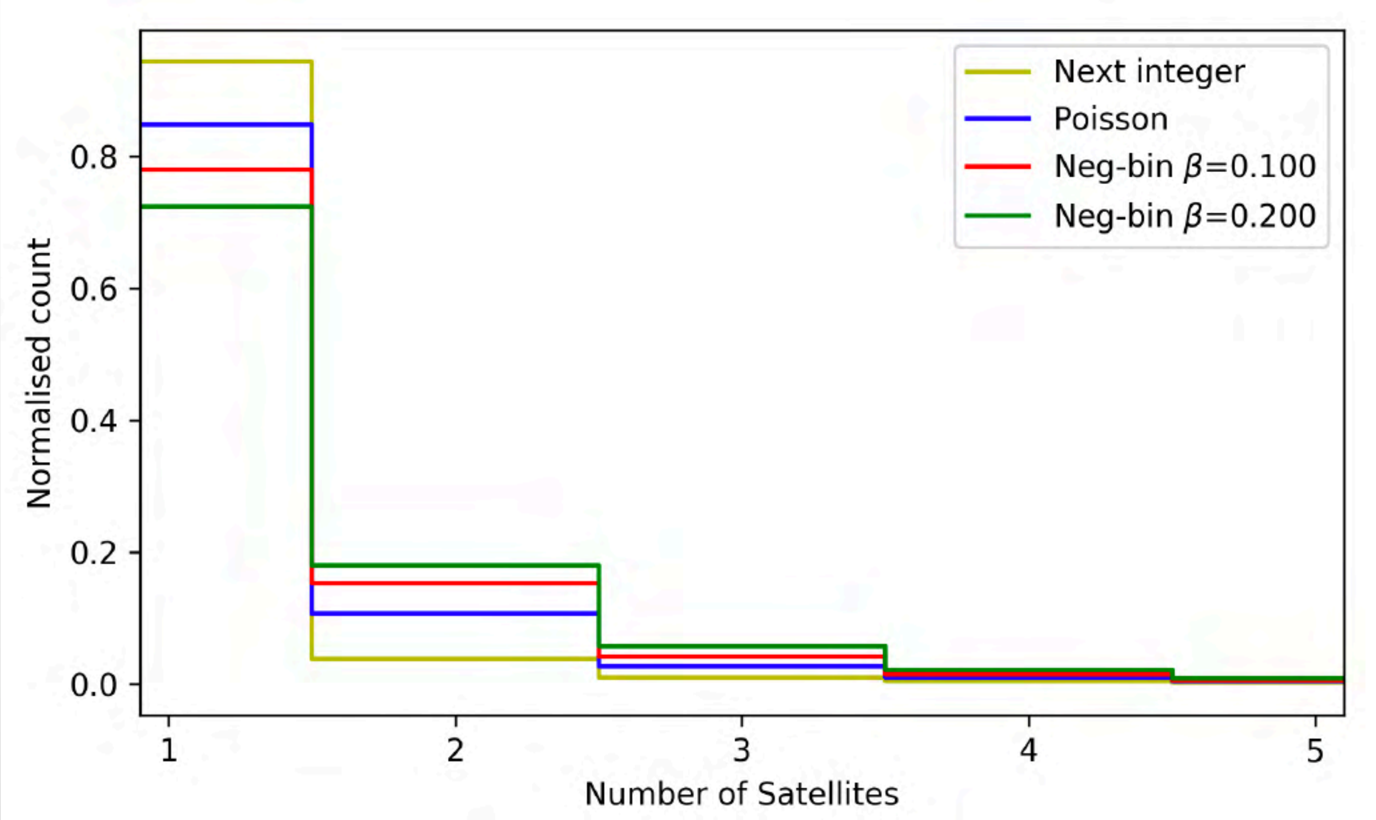

Fixed f_{sat}= 0.30
HOD-3

HOD: PDF VARIATIONS

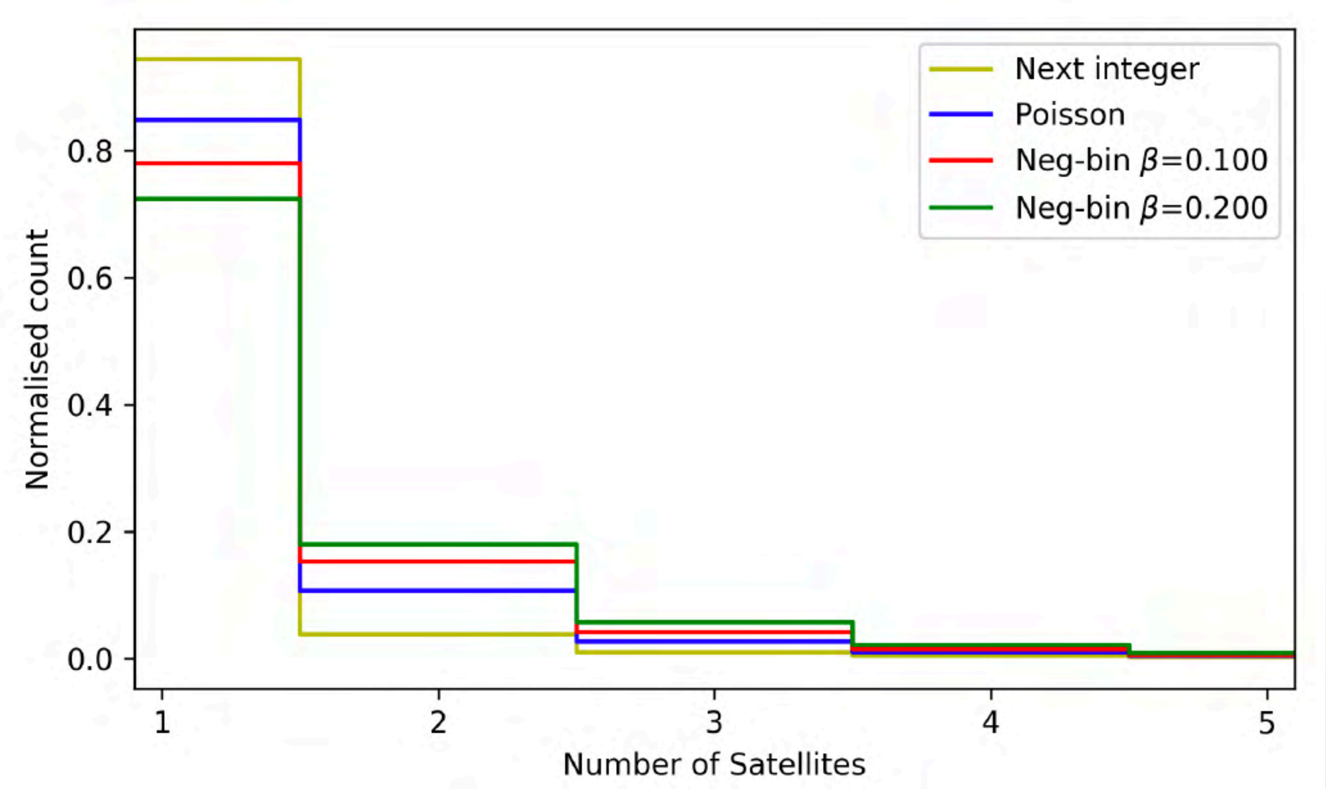

- POISSON

$$P(N|\lambda) = \frac{e^{-N}\lambda^N}{N!}$$

- NEGATIVE BINOMIAL

$$P(N|r,p) = \frac{\Gamma(N+r)}{\Gamma(r)\Gamma(N+1)} p^r (1-p)^N \text{ with}$$
$$p = \frac{1}{(1+\beta)^2}, \quad r = \frac{\lambda}{\beta(1+2\beta)}$$

- NEAREST INTEGER

$$P(N|\lambda) = \begin{cases} 1-(\lambda - \textsc{int}(\lambda)) & N = \textsc{int}(\lambda) \\ \lambda - \textsc{int}(\lambda) & N = \textsc{int}(\lambda)+1 \\ 0 & \text{else} \end{cases}$$

HOD, PDF VARIATIONS: P(N|<N>)

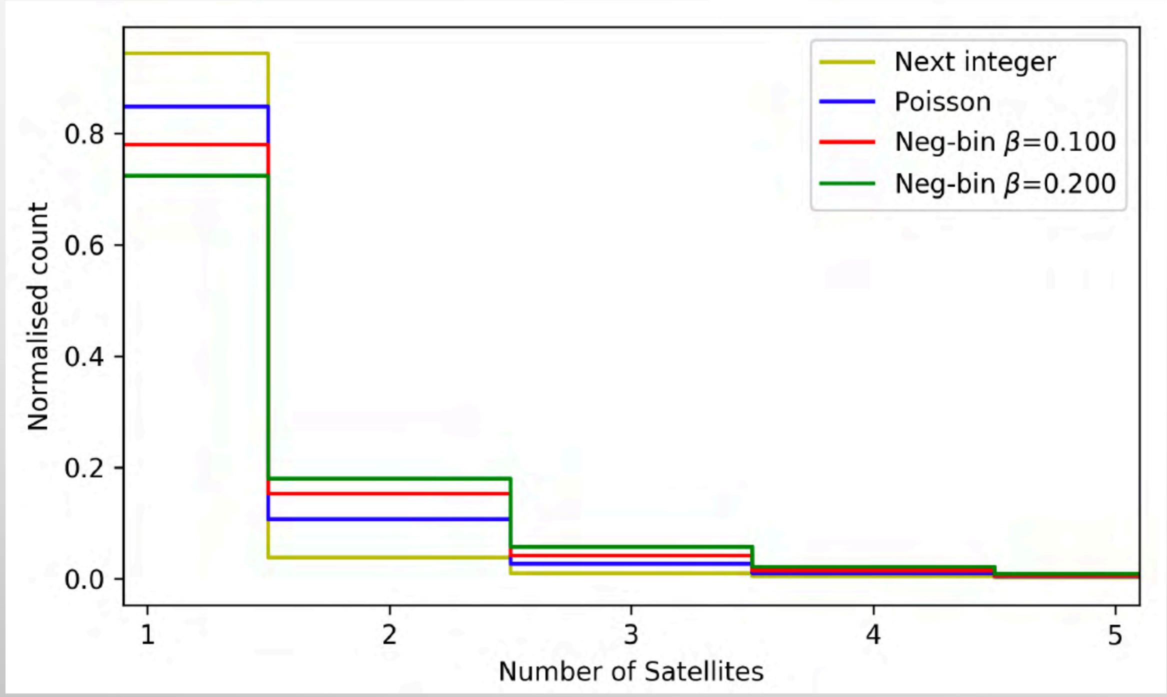

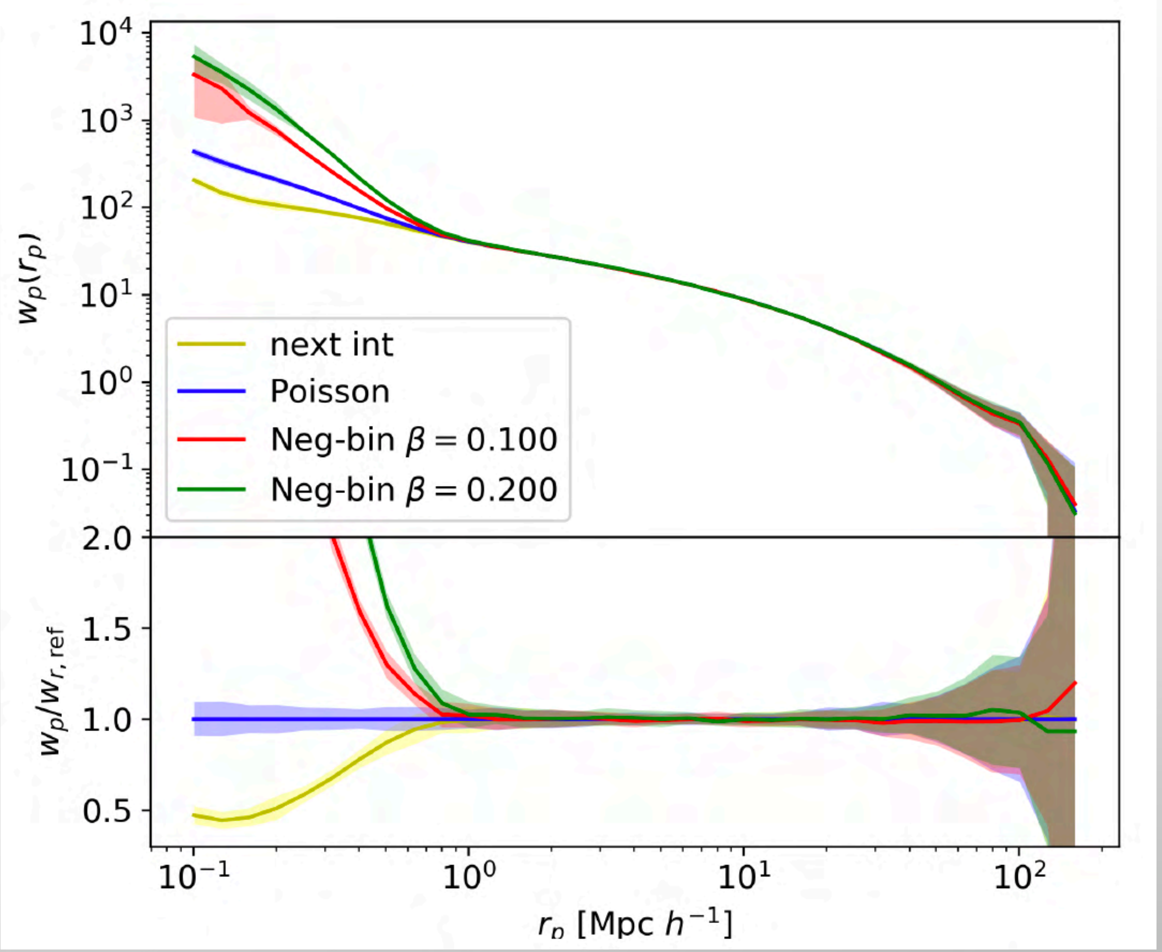

HOD, PDF VARIATIONS: P(N|<N>)

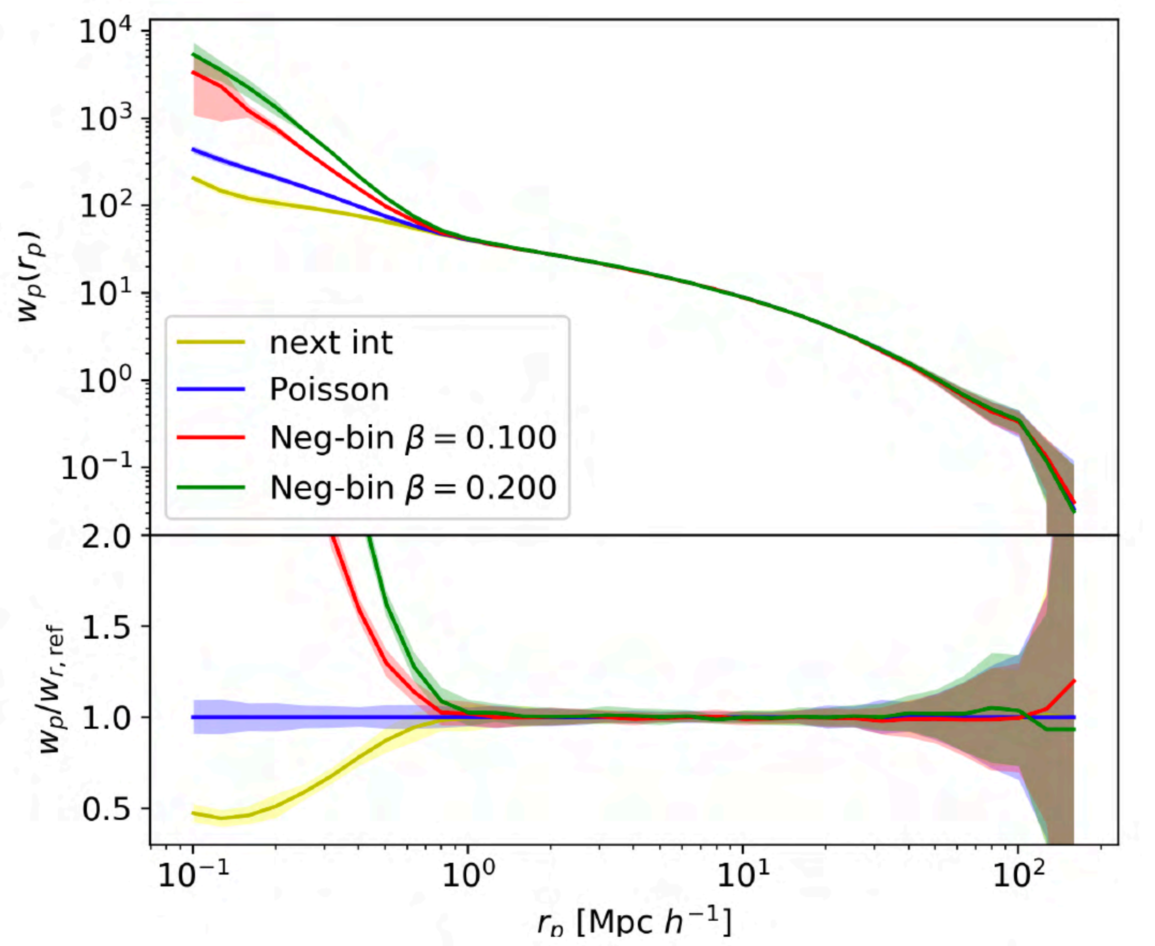

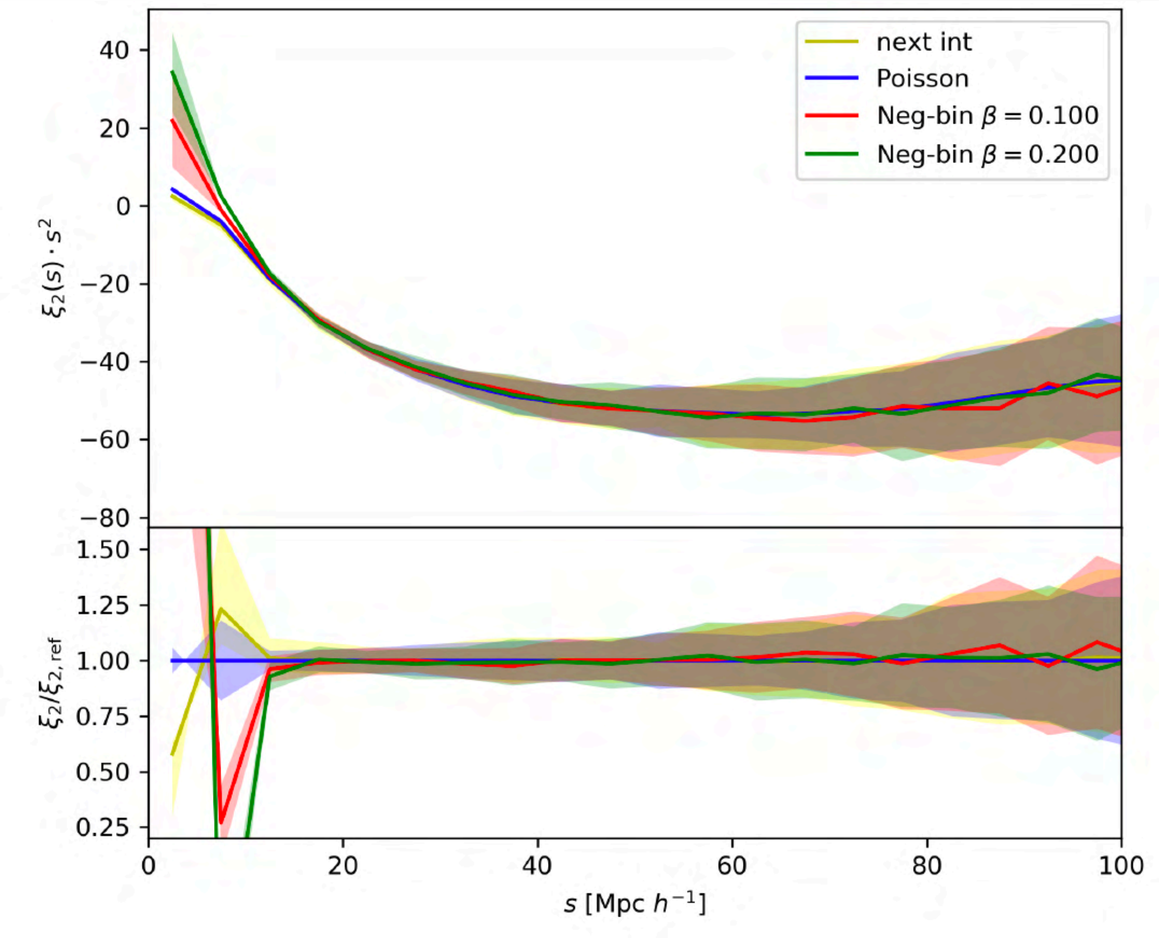

HOD: SATELLITE DENSITY PROFILES

- **NFW.** By default we are assuming a Navarro-Frenk-White (1996) distribution with concentrations from Klypin (2016). **Default**

$$\rho(x) \propto \frac{1}{x \cdot (1+x)^2}$$
$$\text{with} x = c \frac{r}{r_{\text{vir}}}$$

HOD: SATELLITE DENSITY PROFILES

- **NFW**. By default we are assuming a Navarro-Frenk-White (1996) distribution with concentrations from Klypin (2016). **Default**

$$\rho(x) \propto \frac{1}{x \cdot (1+x)^2}$$
$$\text{with} x = c \frac{r}{r_{\text{vir}}}$$

- **Modified NFW.** As in the literature there are indications of ELG prefering the outskirts of the halos (Alpaslan16, Araljic18, Orsi&Angulo18), we allow for a modification of concentrations by a free factor *K*:

$$c = K \cdot c_{\text{kly}}$$

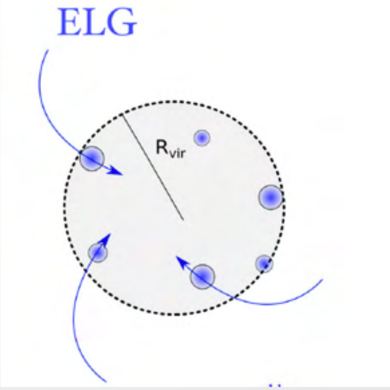

HOD: SATELLITE DENSITY PROFILES

- **NFW.** By default we are assuming a Navarro-Frenk-White (1996) distribution with concentrations from Klypin (2016). **Default**

$$\rho(x) \propto \frac{1}{x \cdot (1+x)^2}$$
$$\text{with}\, x = c\frac{r}{r_{\text{vir}}}$$

- **Modified NFW.** As in the literature there are indications of ELG prefering the outskirts of the halos (Alpaslan16, Araljic18, Orsi&Angulo18), we allow for a modification of concentrations by a free factor *K*:

$$c = K \cdot c_{\text{kly}}$$

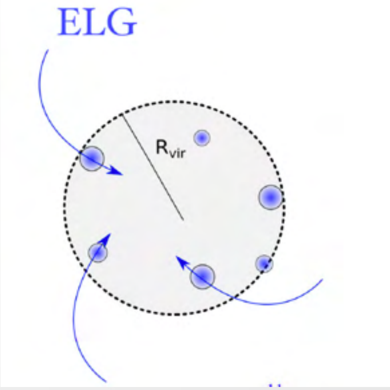

- **Particles.** We put galaxies in satellite dark matter particle locations.

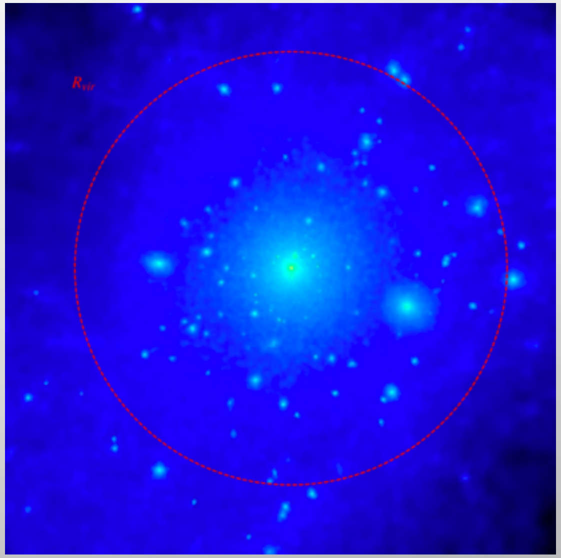

HOD: SATELLITE DENSITY PROFILES

- **NFW.** By default we are assuming a Navarro-Frenk-White (1996) distribution with concentrations from Klypin (2016). **Default**

$$\rho(x) \propto \frac{1}{x \cdot (1+x)^2}$$
$$\text{with} x = c\frac{r}{r_{\mathrm{vir}}}$$

- **Modified NFW.** As in the literature there are indications of ELG prefering the outskirts of the halos (Alpaslan16, Araljic18, Orsi&Angulo18), we allow for a modification of concentrations by a free factor *K*:

$$c = K \cdot c_{\mathrm{kly}}$$

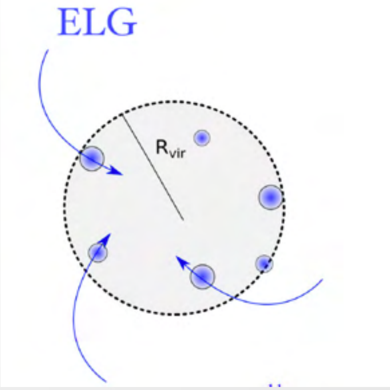

- **Particles.** We put galaxies in satellite dark matter particle locations.

- **Modified particles.**
  We modify the intrinsic concentration by moving the satellite location:

$$\vec{r}_{\mathrm{sat}} = \vec{r}_{\mathrm{h}} + \frac{1}{K}(\vec{r}_{\mathrm{DM}} - \vec{r}_{\mathrm{h}})$$

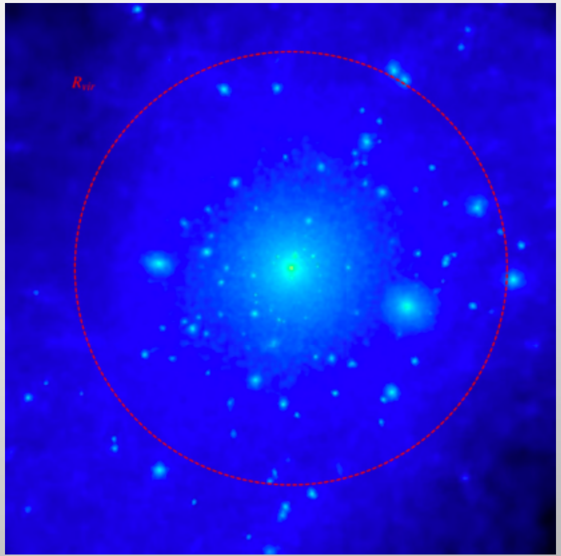

HOD: SATELLITE DENSITY PROFILES

- **NFW.**

$$\rho(x) \propto \frac{1}{x \cdot (1+x)^2}$$
$$\text{with} x = c\frac{r}{r_{\rm vir}}$$

- **MODIFIED NFW.**

$$c = K \cdot c_{\rm kly}$$

- **PARTICLES.**

- **MODIFIED PARTICLES.**

$$\vec{r}_{\rm sat} = \vec{r}_{\rm h} + \frac{1}{K}(\vec{r}_{\rm DM} - \vec{r}_{\rm h})$$

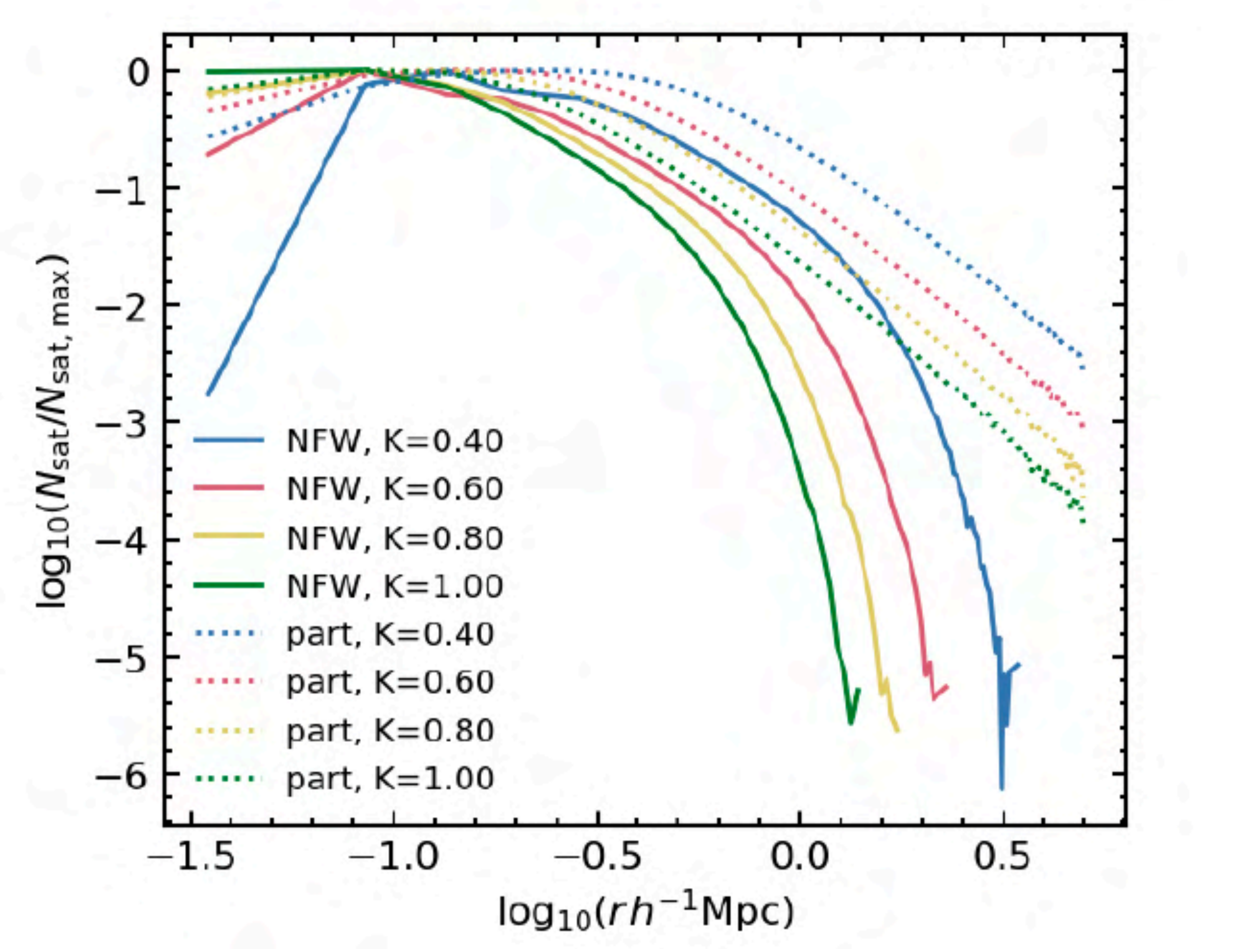

HOD: SATELLITE DENSITY PROFILES

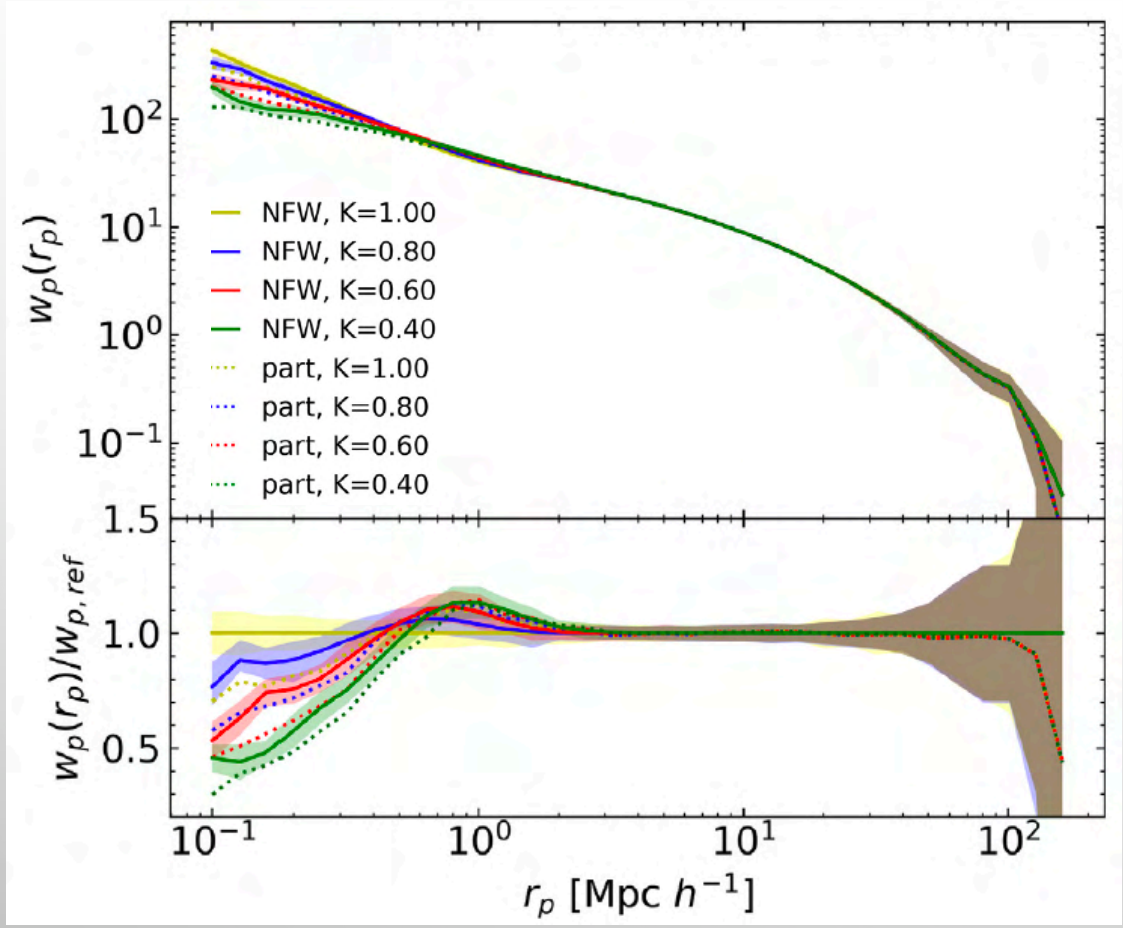

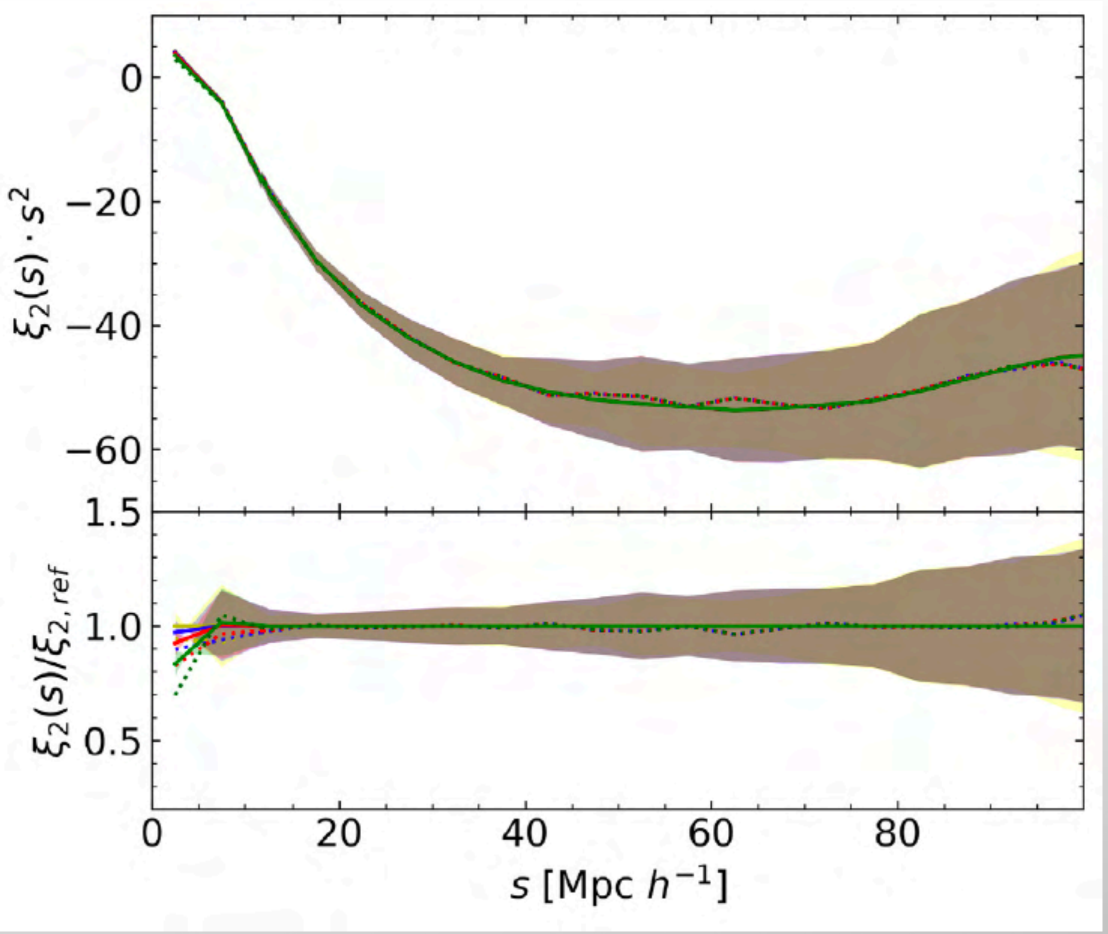

HOD: SATELLITE VELOCITY PROFILES

- VIRAL THEOREM.
  BRYAN & NORMAN (1998)

$$v_i^{\mathrm{gal}} \curvearrowleft \mathcal{N}(v_i^{\mathrm{h}}, \sigma_v) \quad \text{for } i = x, y, z$$

$$\sigma_v = 476 \cdot 0.9[\Delta_{\mathrm{vir}} E^2(z)]^{1/6} \left(\frac{M}{10^{15} M_\odot h^{-1}}\right)^{1/3} km/s$$

- VIRAL THEOREM + VELOCITY BIAS

$$v_i^{\mathrm{gal}} \curvearrowleft \mathcal{N}(v_i^{\mathrm{h}}, \alpha_v \cdot \sigma_v)$$

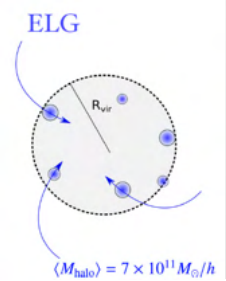

- PARTICLES (WITH VELOCITY BIAS)

$$\vec{v}_{\mathrm{sat}} = \vec{v}_{\mathrm{h}} + \alpha_v (\vec{v}_{\mathrm{DM}} - \vec{v}_{\mathrm{h}})$$

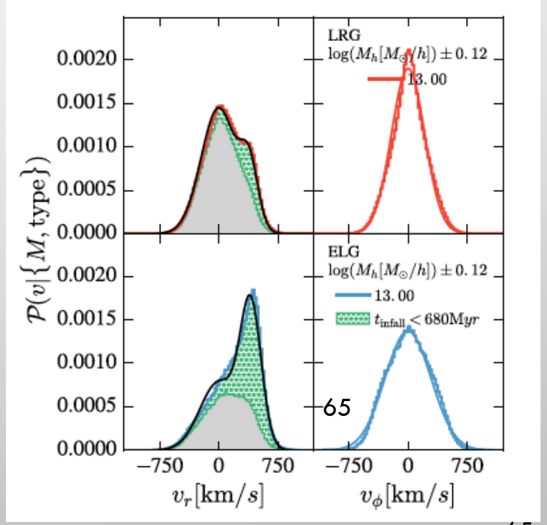

- NET **INFALL** VELOCITY
  MOTIVATED BY
  ORSI & ANGULO 2018

$$v_t^{\mathrm{infall}} \curvearrowleft \mathcal{N}(-500 km/s, 200 km/s)$$

$$\vec{v}_{\mathrm{tot}}^{\,\mathrm{gal}} = \vec{v}^{\,\mathrm{gal}} + v_r^{\mathrm{infall}} \cdot \vec{u}_r$$

$$\vec{u}_r = \frac{\vec{r}_{\mathrm{sat}} - \vec{r}_{\mathrm{h}}}{|\vec{r}_{\mathrm{sat}} - \vec{r}_{\mathrm{h}}|}$$

HOD: SATELLITE VELOCITY PROFILES

- VIRAL THEOREM.
  BRYAN & NORMAN (1998)

- VIRAL THEOREM + VELOCITY BIAS

- PARTICLES (WITH VELOCITY BIAS)

- NET INFALL VELOCITY
  MOTIVATED BY ORSI & ANGULO 2018

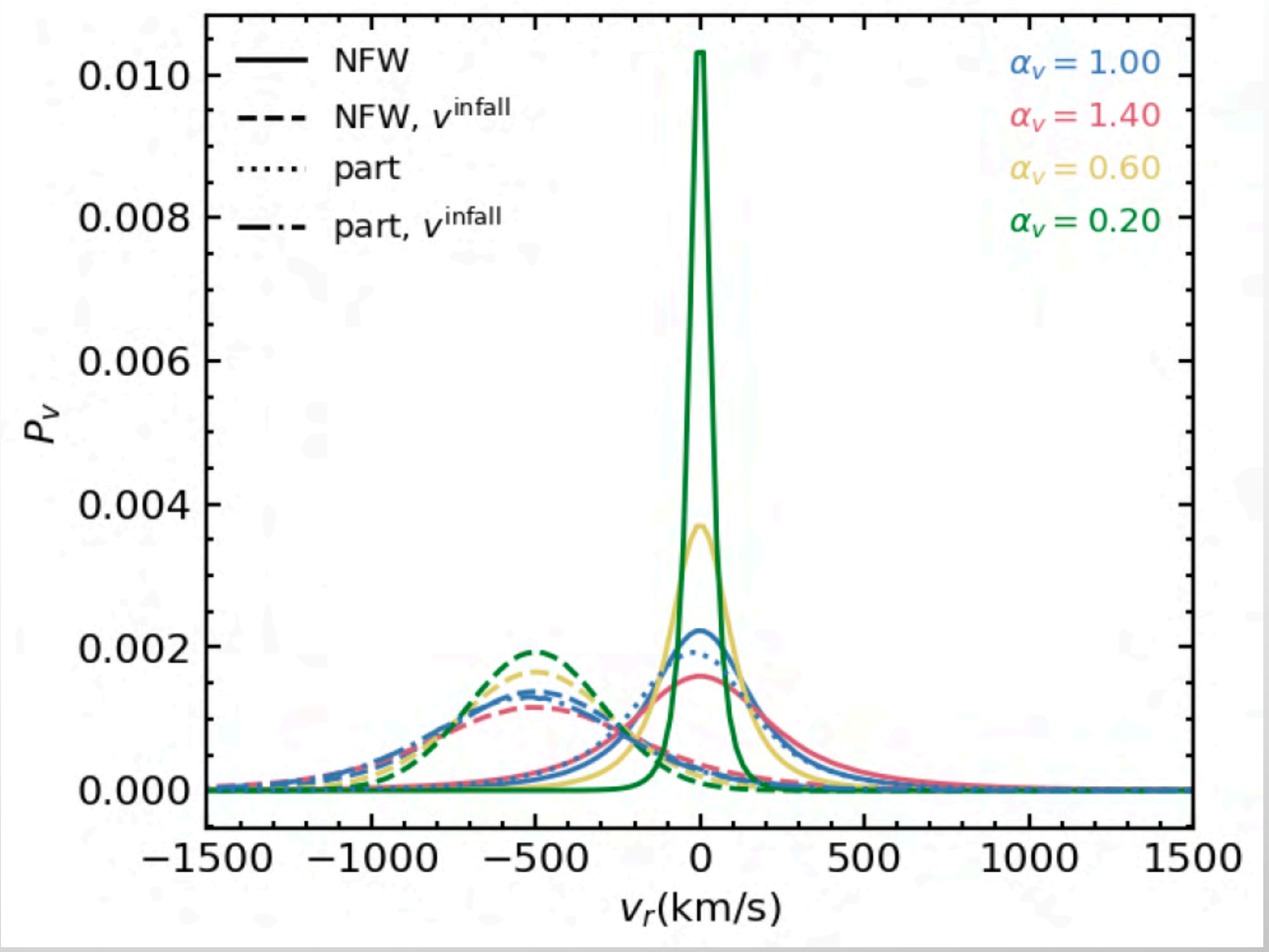

HOD: SATELLITE VELOCITY PROFILES

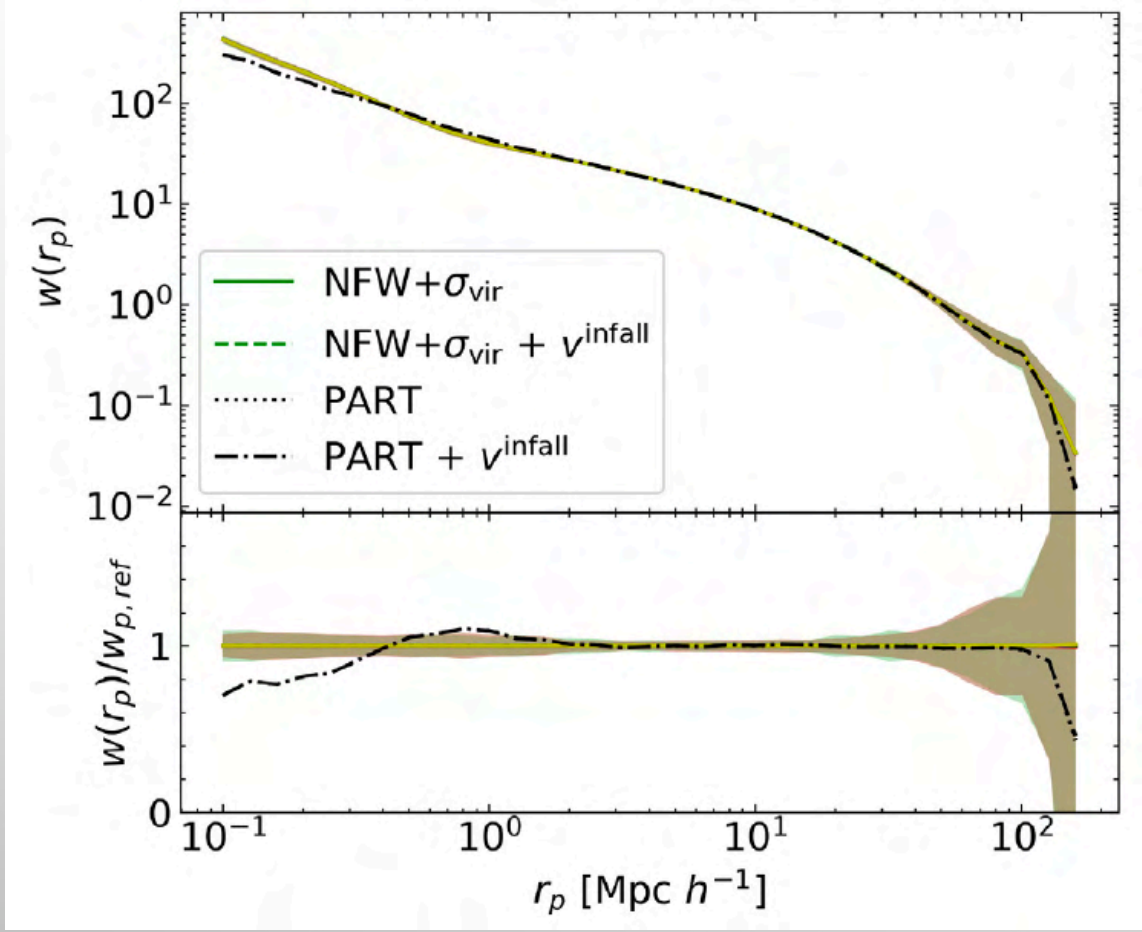

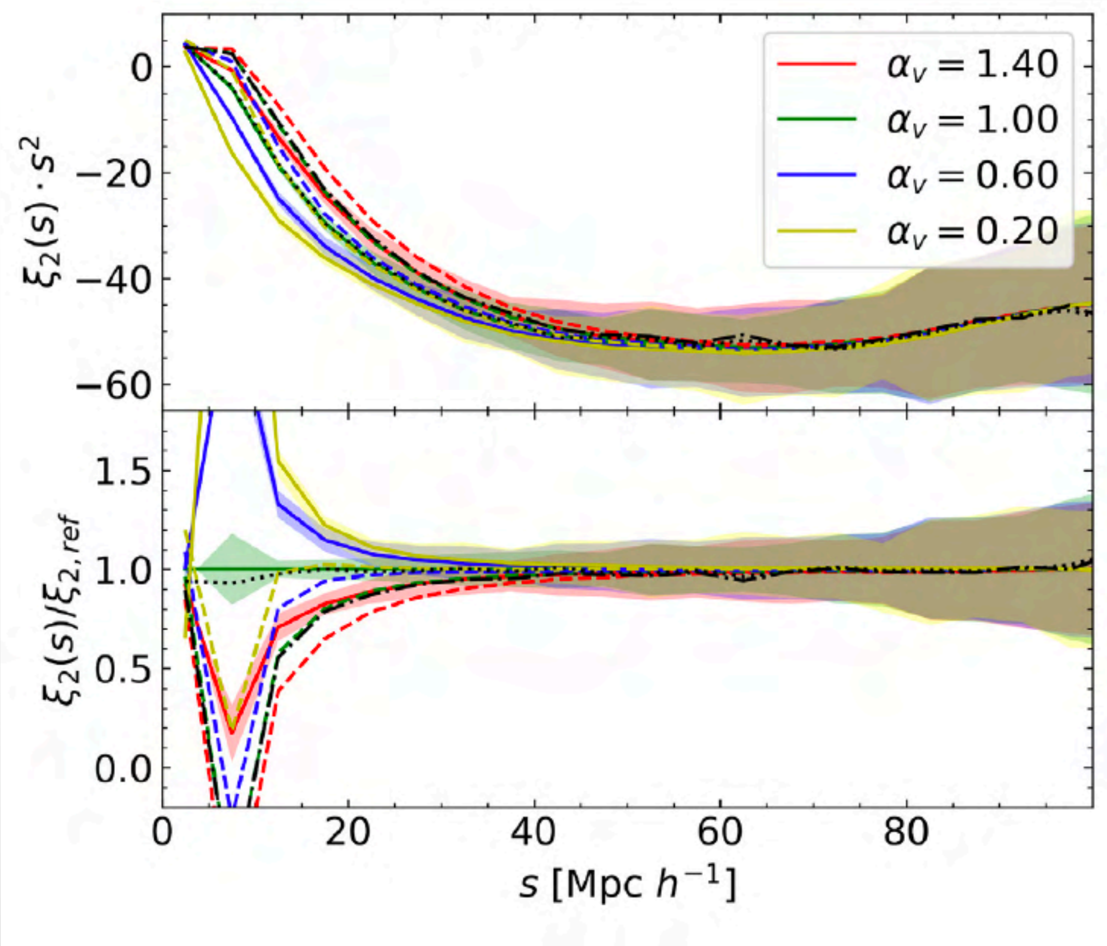

PART IV. CONSTRAINING THE MODEL WITH DATA.

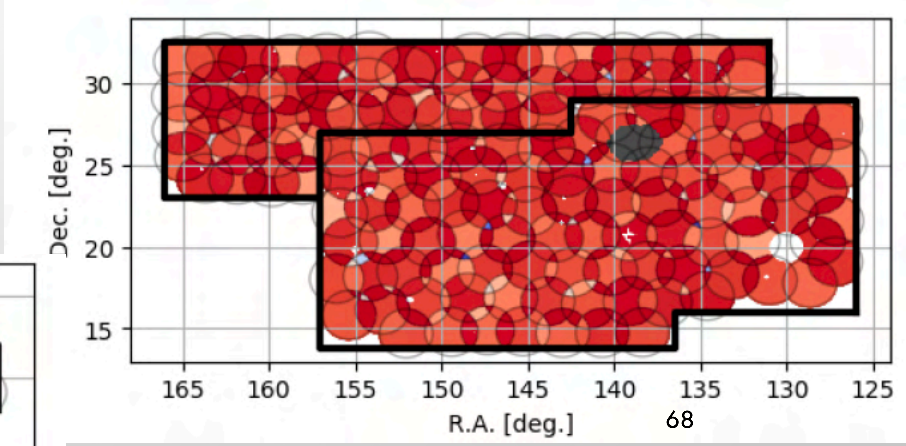

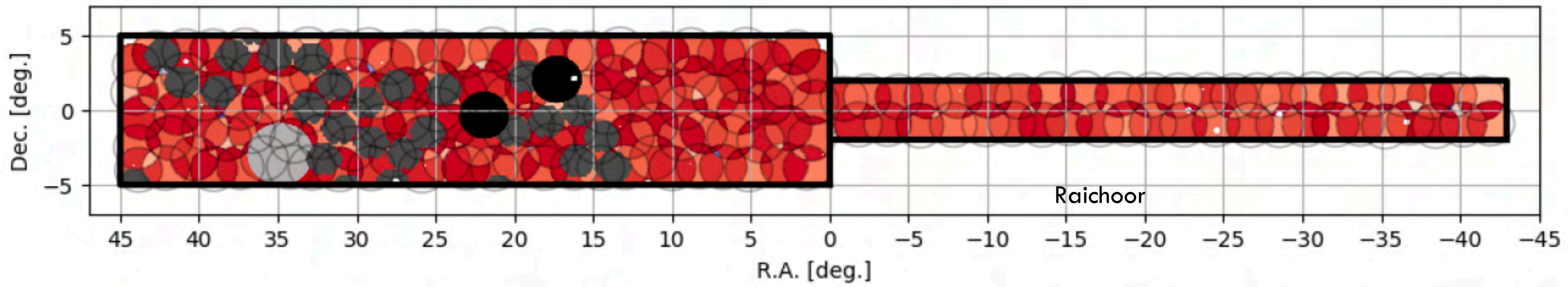

Raichoor

FITTING EBOSS DATA

$$\theta_{0,2,r_p} = \{\xi_0(r_0), \xi_2(r_2)\, wp(r_p), \} \qquad \forall\ \{15 < r_0 < 40;\ 10 < r_2 < 25;\ 0.02 \leq r_p \leq 10\}\ [\mathrm{Mpc}/h]$$

$$\chi^2 = \vec{\theta}^T C^{-1} \vec{\theta}$$

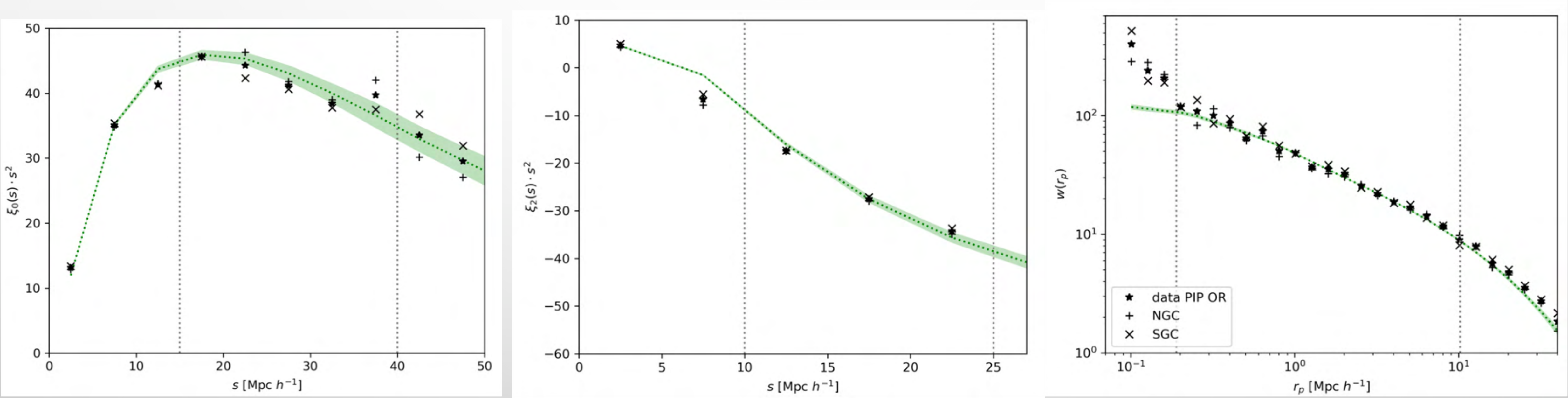

The PIP weights (Bianchi 2017) are able to correct for fibre collisions (see Mohammad et. al 2020)

FITTING PARAMETER {f_{SAT}, K}

Varying fraction of satellites and concentration rescaling (K)

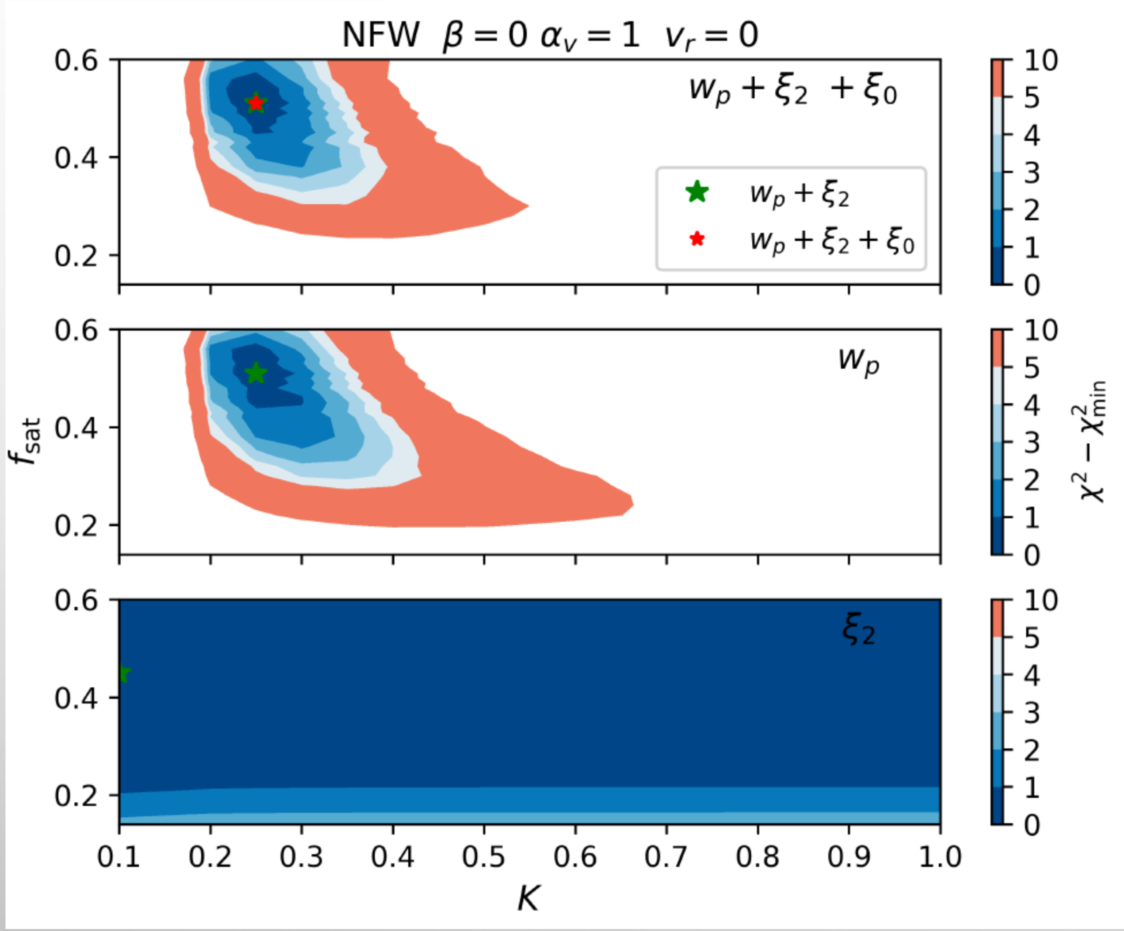

Modified NFW profile:
- NFW profiles with concentrations c rescaled by **K**

$$c = K \cdot c_{\rm kly}$$

Default: HOD-3, Poisson, **NFW**, viral th, no infall vel.

FITTING PARAMETER {f_{SAT}, K}

Varying fraction of satellites and concentration rescaling (K)

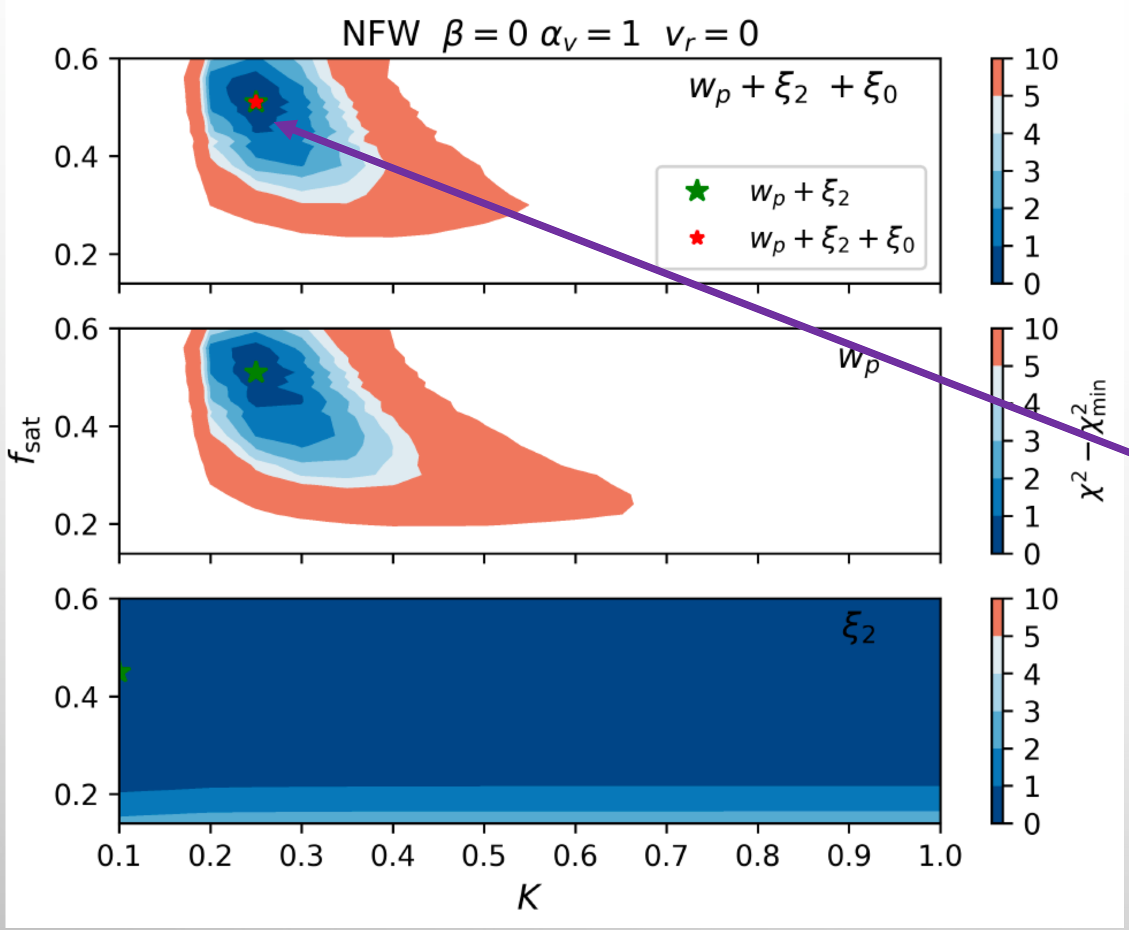

Modified NFW profile:

- NFW profiles with concentrations c rescaled by **K**

$$c = K \cdot c_{\rm kly}$$

Evidence in favour of under-concentrated profiles for ELG!

Default: HOD-3, Poisson, **NFW**, viral th, no infall vel.

FITTING PARAMETER $\{f_{SAT}, \beta\}$

Varying fraction of satellites and PDF scatter

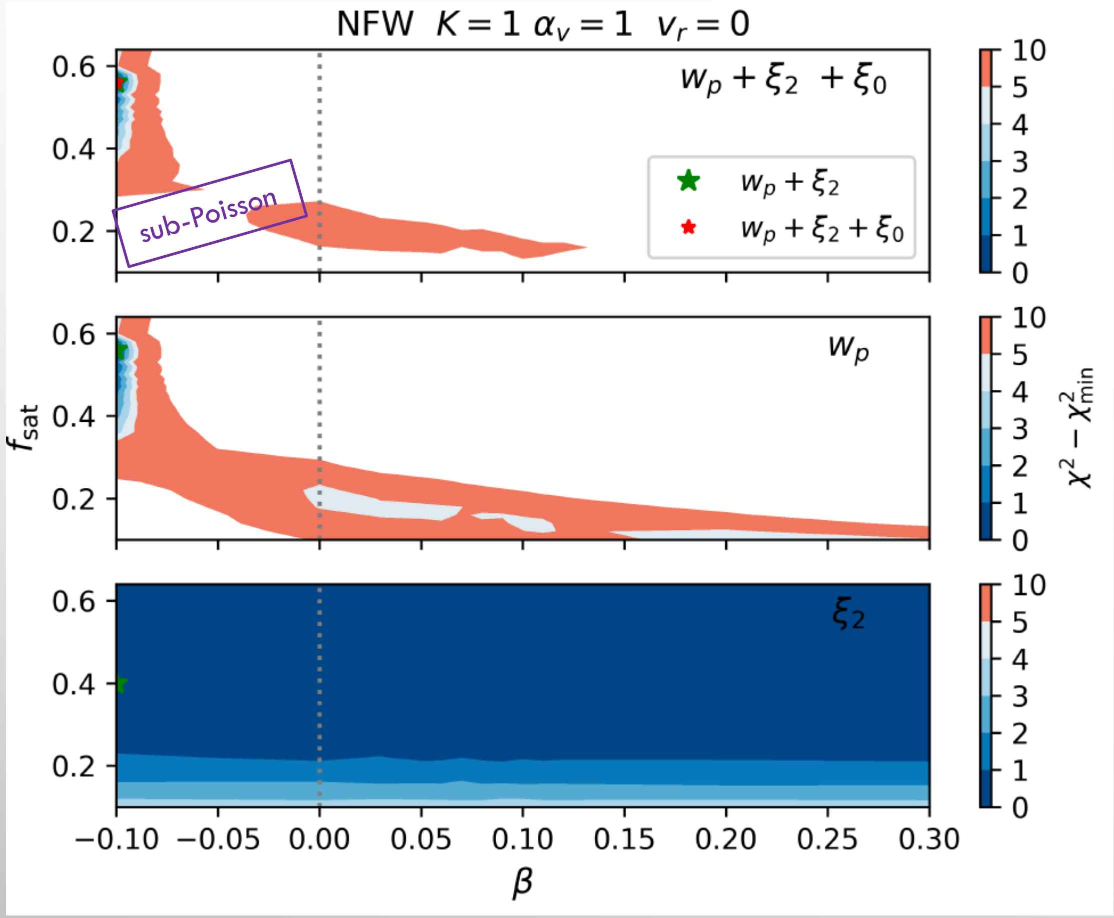

$$\sigma = (1+\beta)\cdot\sqrt{N}$$

Default: HOD-3, Poisson, **NFW**, viral th, no infall vel.

FITTING PARAMETER $\{f_{SAT}, \alpha_v\}$

Varying f_{sat} and velocity bias (assumed v_r=0)

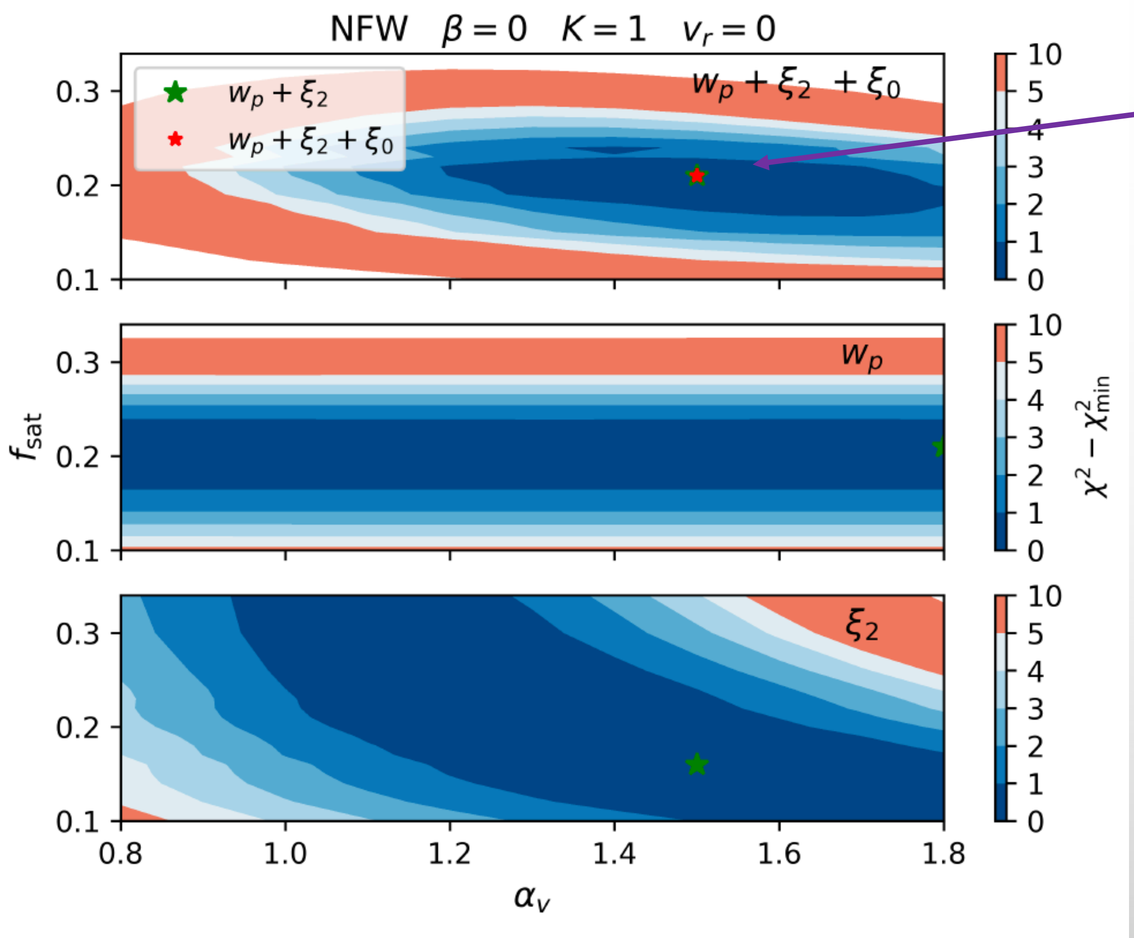

Evidence for a velocity bias

$$v_i^{gal} \curvearrowleft N(v_i^h, \alpha_v \cdot \sigma_v)$$

Default: HOD-3, Poisson, **NFW**, viral th

WHAT ABOUT THE INFALL VELOCITY?

FITTING PARAMETER $\{f_{SAT}, \alpha_v\}$ w V_{INFALL}=0 OR V_{INFALL}=500

Varying f_{sat} and velocity bias (assumed vt=0)

In the pressence of v_{infall}, the evidence for a velocity bias goes away

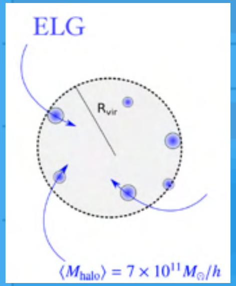

$$v_t^{\mathrm{infall}} \curvearrowleft \mathcal{N}(-500km/s, 200km/s)$$

$$\vec{v}^{\mathrm{gal}}_{\mathrm{tot}} = \vec{v}^{\mathrm{gal}} + v_r^{\mathrm{infall}} \cdot \vec{u}_r$$

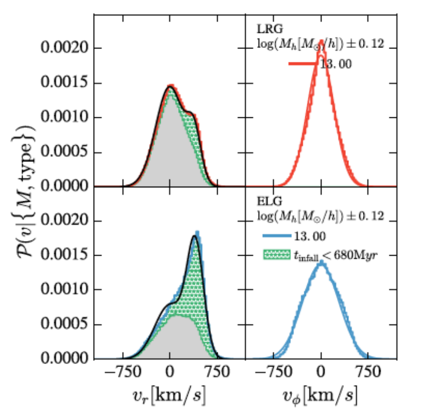

Varying f_{sat} and velocity bias, but with net infall vel.

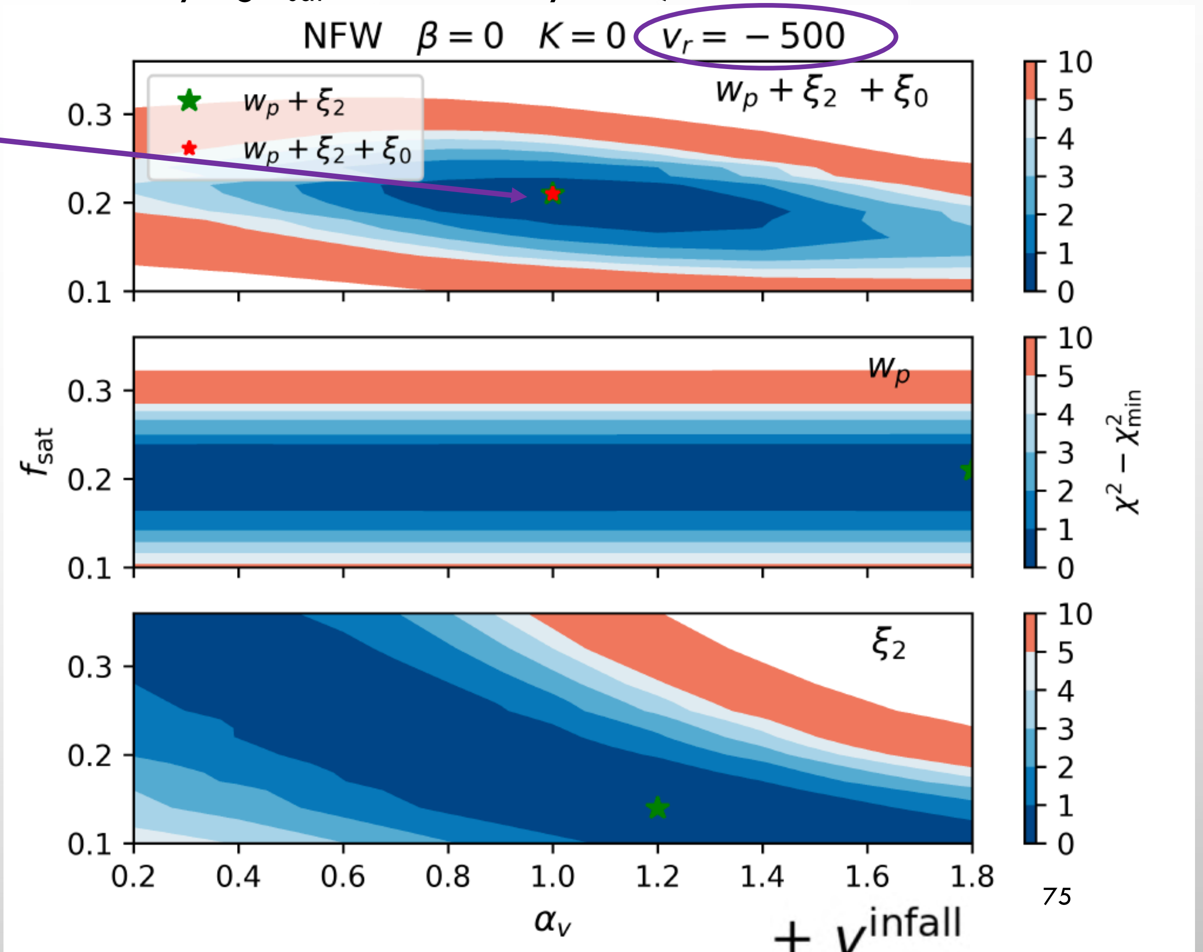

$+\ v^{\mathrm{infall}}$

Default: HOD-3, Poisson, NFW, viral th

FITTING PARAMETER $\{f_{sat}, \alpha_v\}$ w V_{INFALL}=0 OR V_{INFALL}=500

Varying f_{sat} and velocity bias (assumed vt=0)

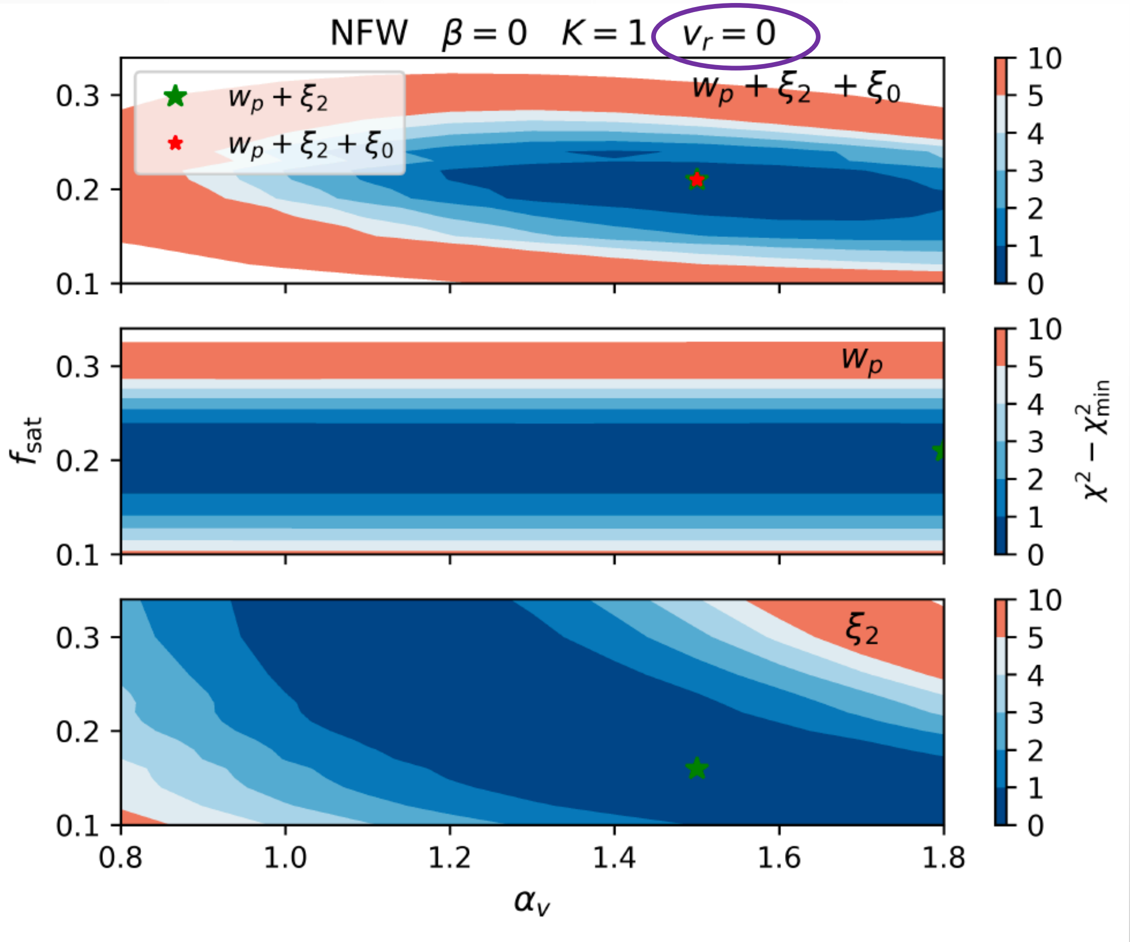

Varying f_{sat} and velocity bias, but with net infall vel.

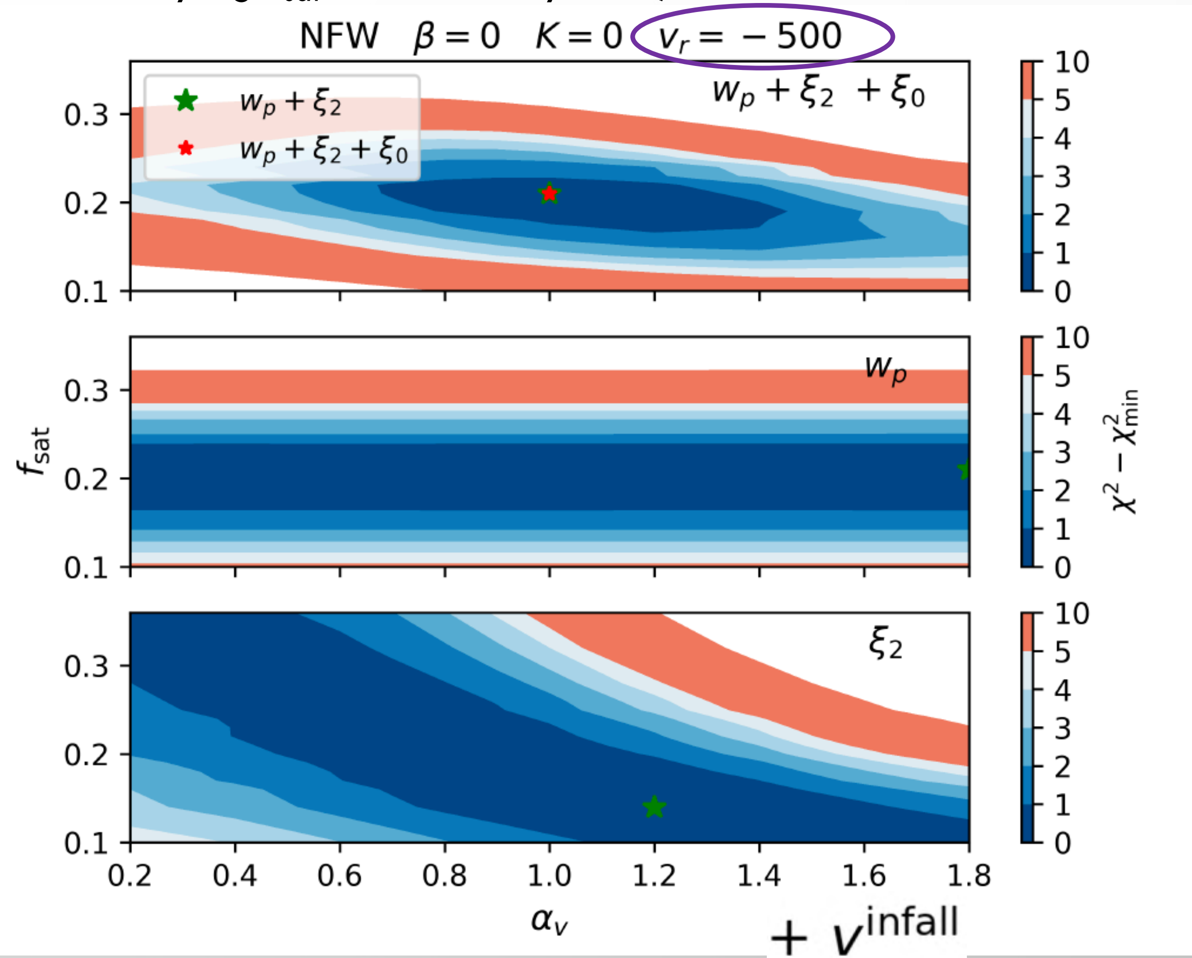

$+ v^{infall}$

Default: HOD-3, Poisson, NFW, viral th

WHAT IF WE USE THE PARTICLE PROFILES FOR THE SATELLITES, INSTEAD OF THE ANALYTIC NFW?

Same fits as above, but with **Particles** profiles

Evidence for sub-Poissonian PDF goes away

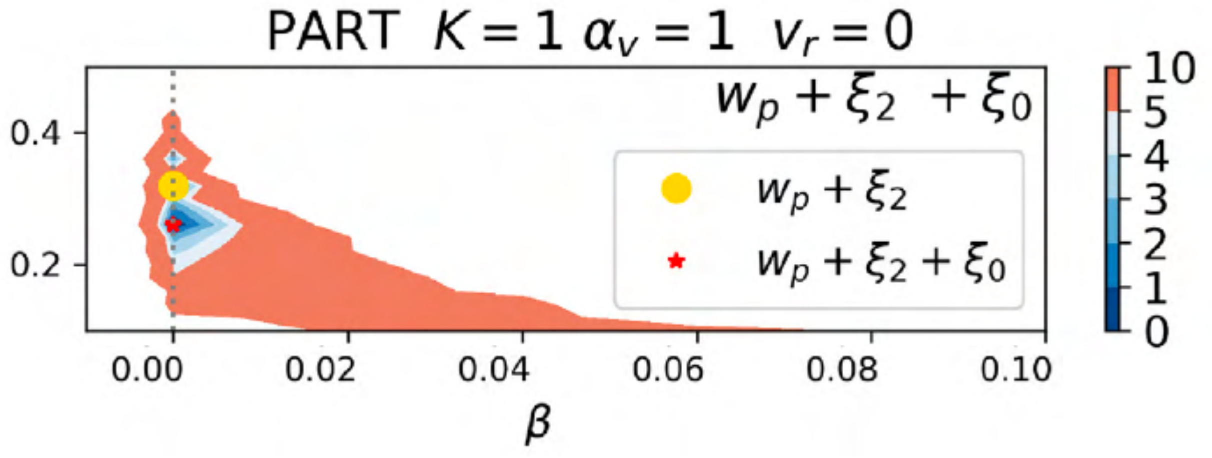

Default: HOD-3, Poisson, **Part**, no infall vel.

Same fits as above, but with **Particles** profiles

Evidence for sub-Poissonian PDF goes away

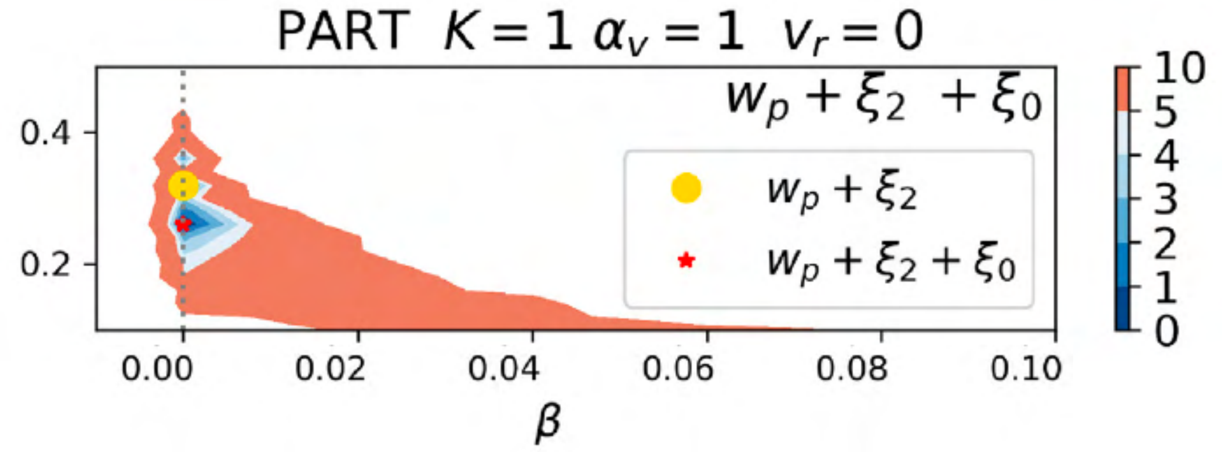

Evidence for under-concentrated profiles remains (although slightly larger K)

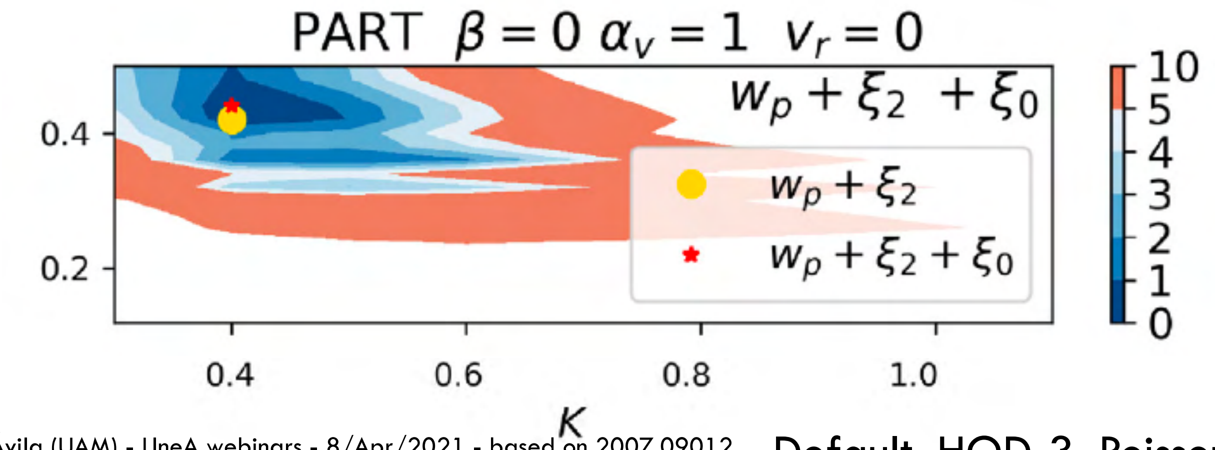

Default: HOD-3, Poisson, **Part**, no infall vel.

Same fits as above, but with **Particles** profiles

Evidence for sub-Poissonian PDF goes away

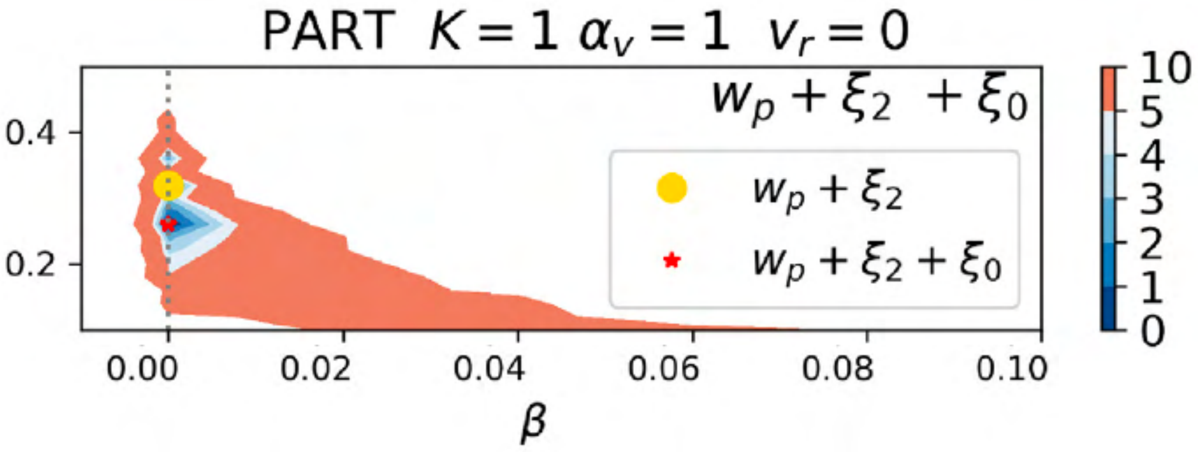

Evidence for velocity bias remains (although slightly lower)

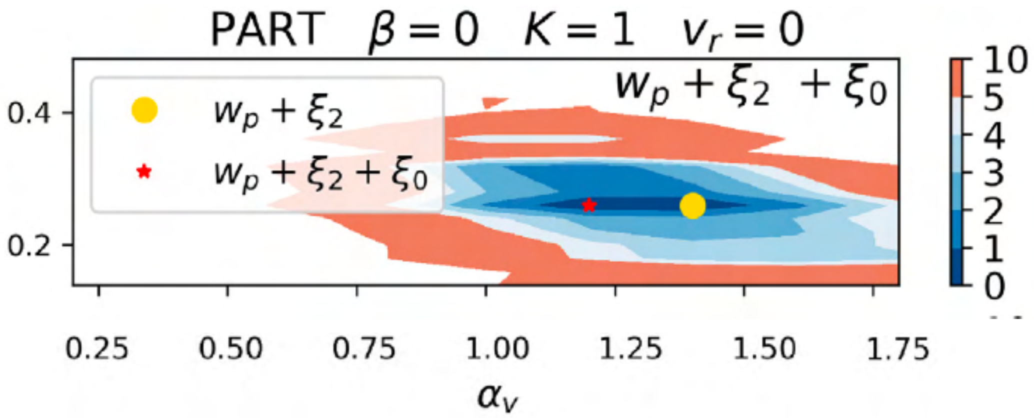

Evidence for under-concentrated profiles remains (although slightly larger K)

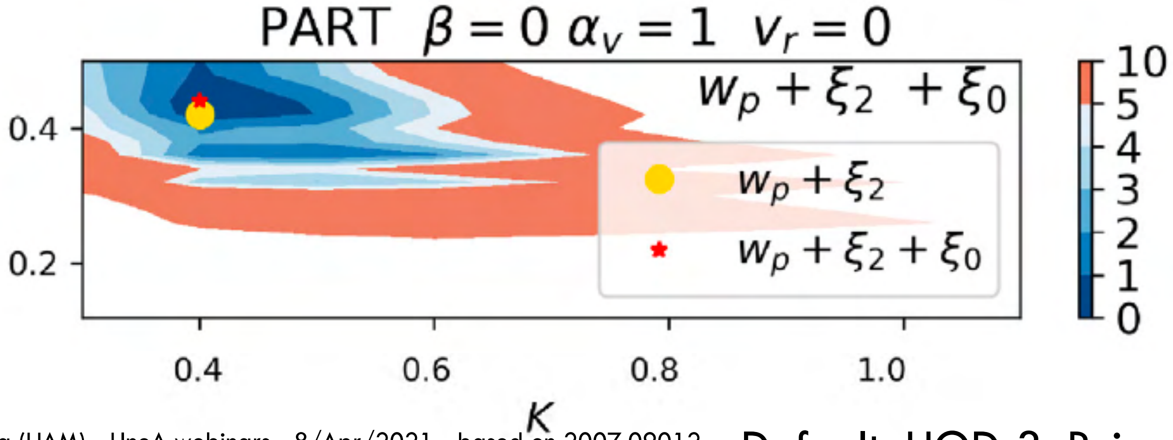

Default: HOD-3, Poisson, **Part**, no infall vel.

WAIT,
SO WHAT HAPPENS IF YOU CHANGE THE SHAPE OF THE MEAN **HOD?**
THAT'S WHAT EVERYBODY ALWAYS LOOKS AT

SAME AS ABOVE BUT CHANGING MEAN HOD

- ALL THE CHANGES ARE ABSORBED BY A CHANGE IN THE FRACTION OF SATELLITES $\mathbf{f_{SAT}}$
- THE REST OF VARIABLES REMAIN UNCHANGED

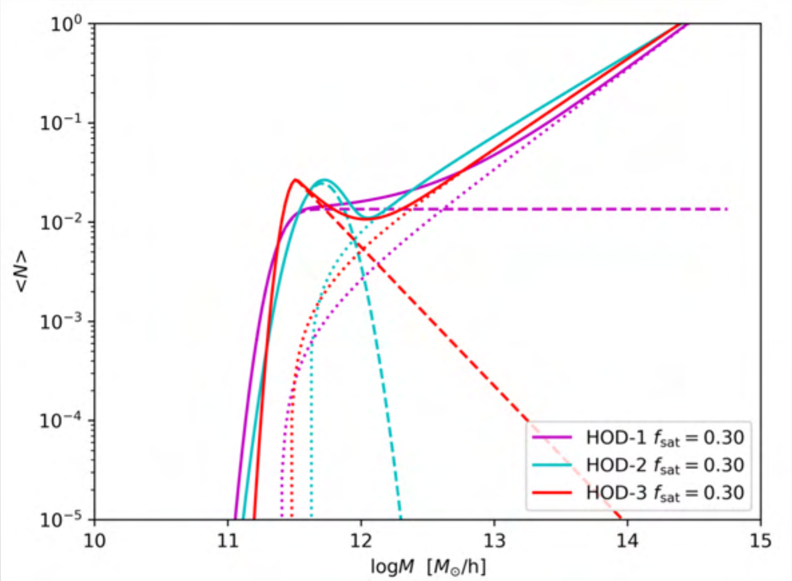

Default: HOD-3, Poisson, NFW, viral th

SAME AS ABOVE BUT CHANGING MEAN HOD

- ALL THE CHANGES ARE ABSORBED BY A CHANGE IN THE FRACTION OF SATELLITES $\mathbf{f_{SAT}}$
- THE REST OF VARIABLES REMAIN UNCHANGED

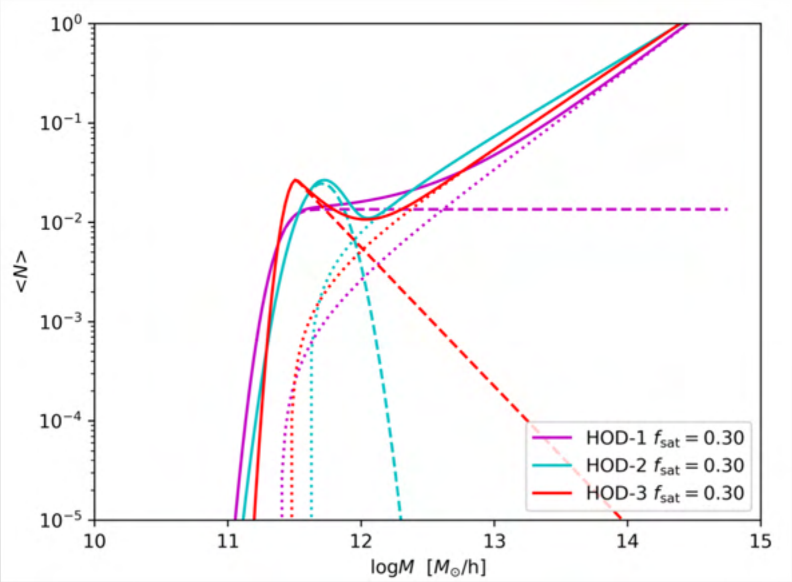

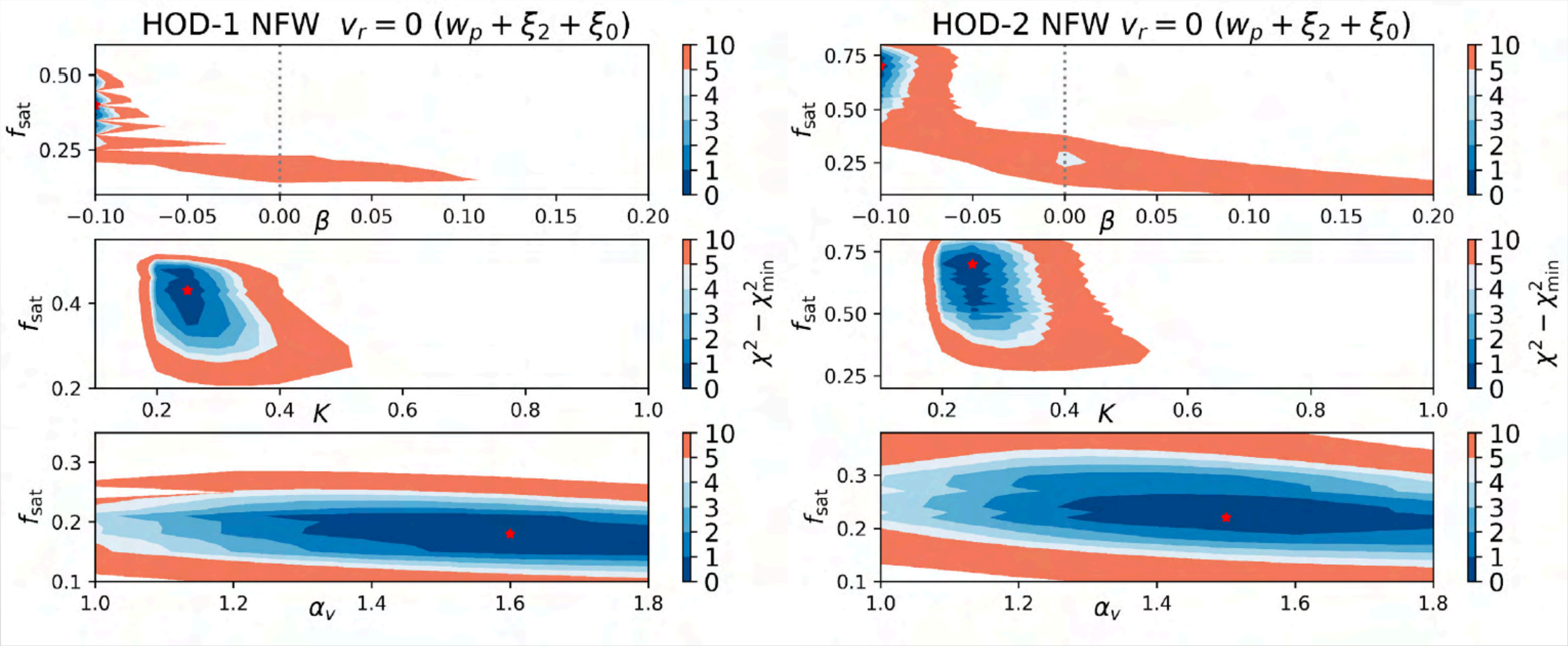

Default: HOD-3, Poisson, NFW, viral th

OKAY,
BUT ALL THOSE VARIABLES MUST BE DEGENERATED ONE TO ANOTHER

FIT SIMULTANEOUSLY PDF & CONCENTRATIONS

$\{f_{SAT}, \beta, K\}$

- THIS GIVES THE BEST OF ALL FITS
- DATA STILL PREFERS (VERY) UNDER-CONCENTRATED PROFILES
- Now, super-poissonian PDF is preferred (**β>0**)

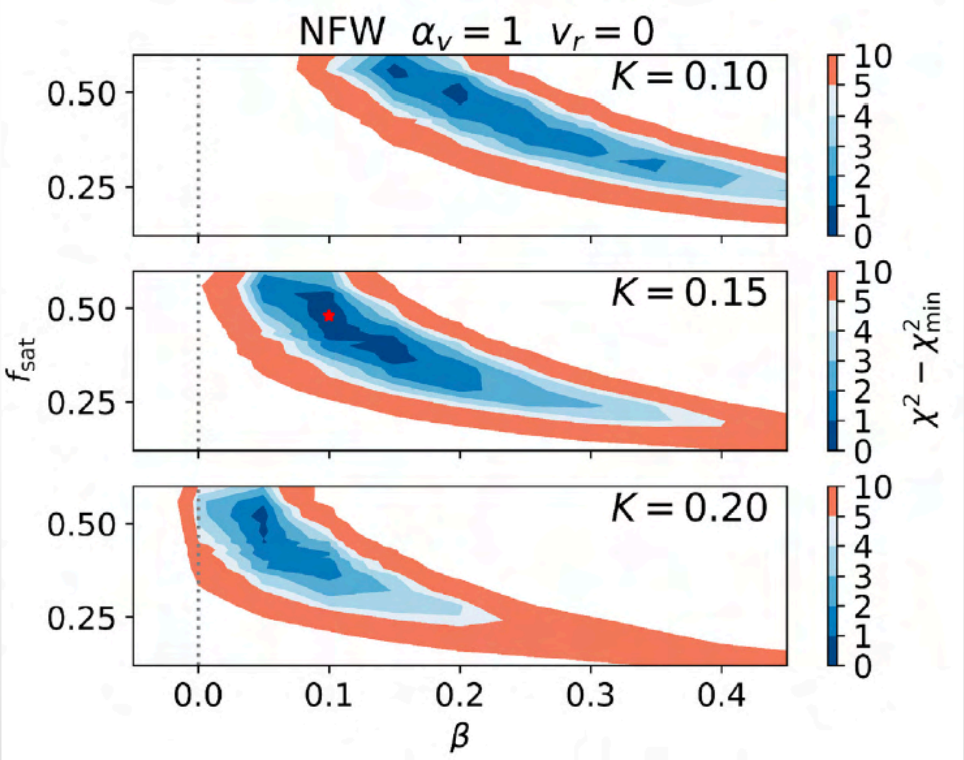

FIT SIMULTANEOUSLY PDF & VELOCITY BIAS
$\{f_{SAT}, \beta, \alpha_v\}$

- FIT REMAINS AT α_v=1.5
- However, PDF prefers to go Poissonian (**β=0**)

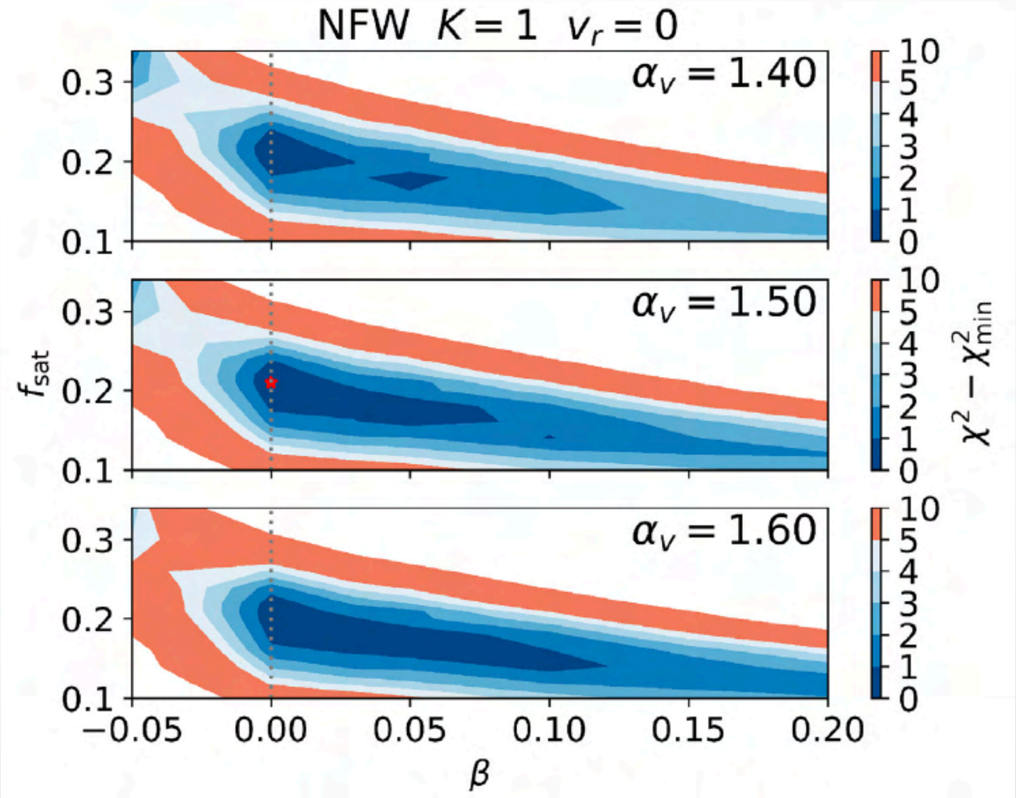

FIT SIMULTANEOUSLY VELOCITY BIAS & CONCENTRATIONS $\{f_{SAT}, \alpha_v, K\}$

- VELOCITY BIAS DISAPPEARS (α_v=1.0)
- CONCENTRATIONS REMAIN AT SIMILAR VALUES K~0.25

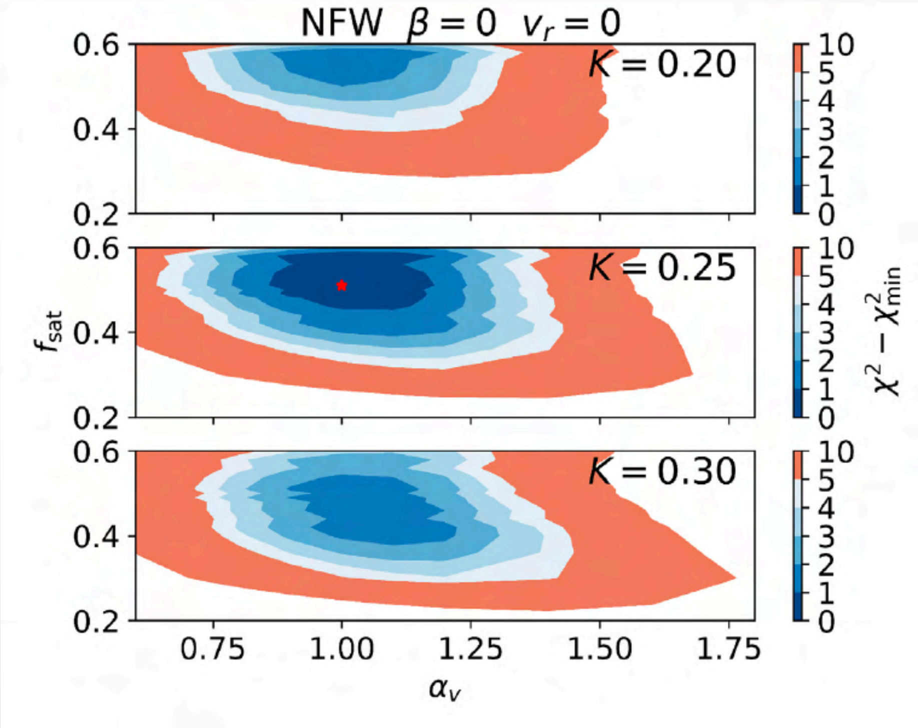

ALRIGHT,
WHAT SHOULD WE CONCLUDE ABOUT ALL THOSE CONTOUR PLOTS?

SUMMARY OF THE FITS

- Clear and consistent preference for under-concentrated profiles K ~ 0.15-0.4. $c \rightarrow K \cdot c$
- This factor (K) is key to obtain a good fit
- Mean HOD shape sub-dominant (re-absorbed by f_{sat})
- Slight evidence for high velocity bias (or infall velocity)
- Slight preference for Particle profiles
- The fraction of satellites is very susceptible to model assumptions (HOD-shape, profiles…) varying from 22% to 70% (but most models around 50%)
- No clear preference for the PDF type, very sensitive to the rest of assumptions

Mock	HOD	f_{sat}	β	K	α_v	Profile	v^{infall}	χ^2_{tot} (bins: 14+3+5)
0	HOD-3	**0.22**	0	1	1	NFW	0	31.3
1	HOD-3	**0.56**	**N-I**	1	1	NFW	0	24
2	HOD-3	**0.51**	0	**0.25**	1	NFW	0	12.7
3	HOD-3	**0.21**	0	1	**1.5**	NFW	0	28.3
4	HOD-3	**0.21**	0	1	**1.0**	NFW	−500	28
5	HOD-3	**0.36**	**0.0**	1	1	PART	0	23
6	HOD-3	**0.44**	0	**0.4**	1	PART	0	13.5
7	HOD-3	**0.26**	0	1	**1.2**	PART	0	21.4
8	HOD-3	**0.26**	0	1	**0.8**	PART	−500	21.2
9	HOD-3	**0.48**	**0.10**	**0.15**	1	NFW	0	10.9
10	HOD-3	**0.21**	**0.0**	1	**1.5**	NFW	0	28.3
11	HOD-3	**0.51**	0	**0.25**	**1.0**	NFW	0	12.7
12	HOD-1	**0.40**	**N-I**	1	1	NFW	0	25
13	HOD-1	**0.43**	0	**0.25**	1	NFW	0	12.4
14	HOD-1	**0.18**	0	1	**1.6**	NFW	0	28.6
15	HOD-2	**0.70**	**N-I**	1	1	NFW	0	28.4
16	HOD-2	**0.70**	0	**0.25**	1	NFW	0	13.8
17	HOD-2	**0.22**	0	1	**1.5**	NFW	0	29.1

PART V. COSMOLOGY

SO... IS THIS ALL REALLY RELEVANT FOR COSMOLOGY?

TESTING RSD ANALYSIS PIPELINE

Finger-of-God

Kaiser

$$P_g(k,\mu) = \left(1+\frac{(k\mu\sigma_v)^2}{2}\right)^{-2}\left[P_{g,\delta\delta}(k) + 2f\mu^2 P_{g,\delta\theta}(k) + f^2\mu^4 P_{\theta\theta}(k) + b_1^3 A(k,\mu,\beta) + b_1^4 B(k,\mu,\beta)\right]$$

RSD correction terms

WE RUN THE EBOSS FITTING PIPELINE TO OUR MOCKS

USING EXTENDED TNS MODEL

DETAILS OF THE MODEL CHOICES IN: DE MATTIA+2021, ALAM+2021

$$P_{g,\delta\delta}(k) = b_1^2 P_{\delta\delta}(k) + 2b_1 b_2 P_{b2,\delta}(k) + 2b_{s2} b_1 P_{bs2,\delta}(k) + 2b_{3nl} b_1 \sigma_3^2(k) P_m^{\rm lin}(k) + b_2^2 P_{b22}(k) + 2b_2 b_{s2} P_{b2s2}(k) + b_{s2}^2 P_{bs22}(k) + N$$

$$P_{g,\delta\theta}(k) = b_1 P_{\delta\theta}(k) + b_2 P_{b2,\theta}(k) + b_{s2} P_{bs2,\theta}(k) + b_{3nl}\sigma_3^2(k) P_m^{\rm lin}(k)$$

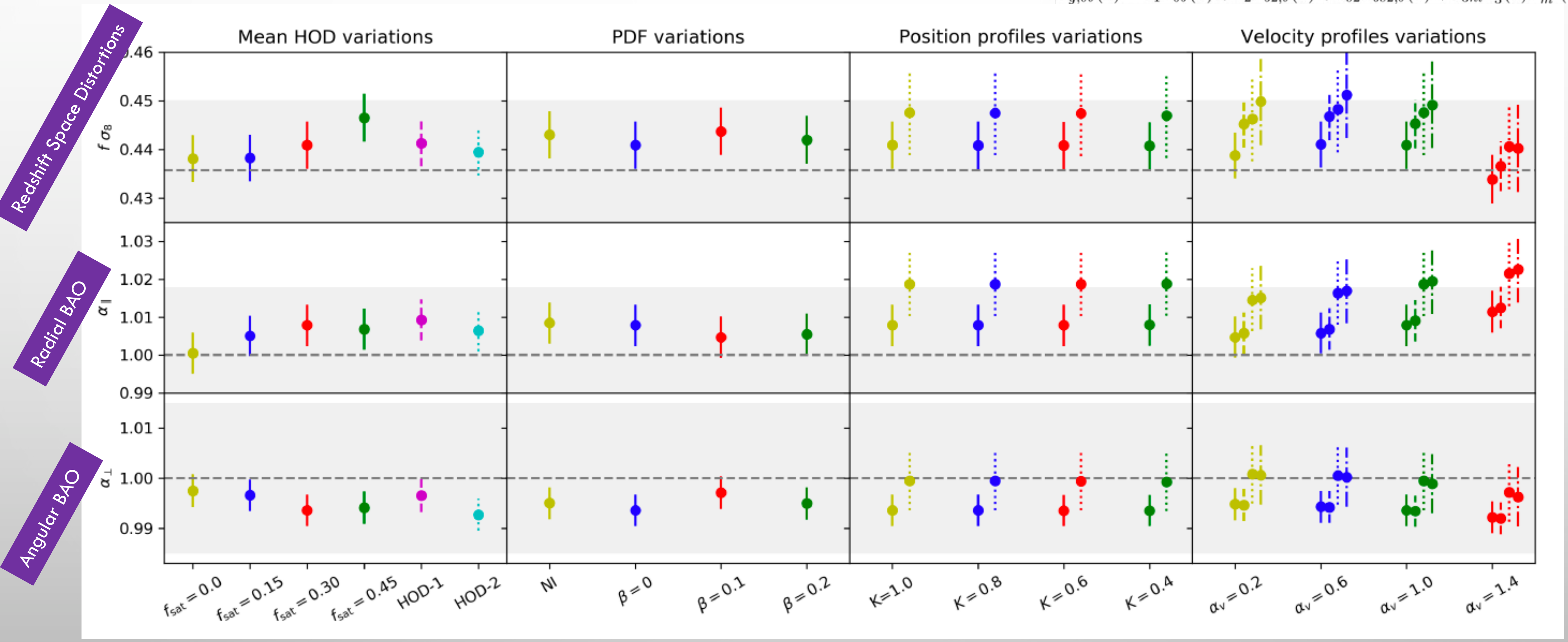

TESTING RSD ANALYSIS PIPELINE

Finger-of-God

Kaiser

$$P_g(k,\mu) = \left(1+\frac{(k\mu\sigma_v)^2}{2}\right)^{-2}\left[P_{g,\delta\delta}(k) + 2f\mu^2 P_{g,\delta\theta}(k) + f^2\mu^4 P_{\theta\theta}(k)\right.$$
$$\left. + b_1^3 A(k,\mu,\beta) + b_1^4 B(k,\mu,\beta)\right]$$

RSD correction terms

$P_0(k) + P_2(k)$
$0.02<k<0.2$
$+ P_4(k)$
$0.02<k<0.15$

[h/Mpc]

WE RUN THE EBOSS FITTING PIPELINE TO OUR MOCKS

USING EXTENDED TNS MODEL

DETAILS OF THE MODEL CHOICES IN: DE MATTIA+2021, ALAM+2021

$$P_{g,\delta\delta}(k) = b_1^2 P_{\delta\delta}(k) + 2b_1 b_2 P_{b2,\delta}(k) + 2b_{s2} b_1 P_{bs2,\delta}(k) + 2b_{3nl} b_1 \sigma_3^2(k) P_m^{\text{lin}}(k) + b_2^2 P_{b22}(k) + 2b_2 b_{s2} P_{b2s2}(k) + b_{s2}^2 P_{bs22}(k) + N$$

$$P_{g,\delta\theta}(k) = b_1 P_{\delta\theta}(k) + b_2 P_{b2,\theta}(k) + b_{s2} P_{bs2,\theta}(k) + b_{3nl}\sigma_3^2(k) P_m^{\text{lin}}(k)$$

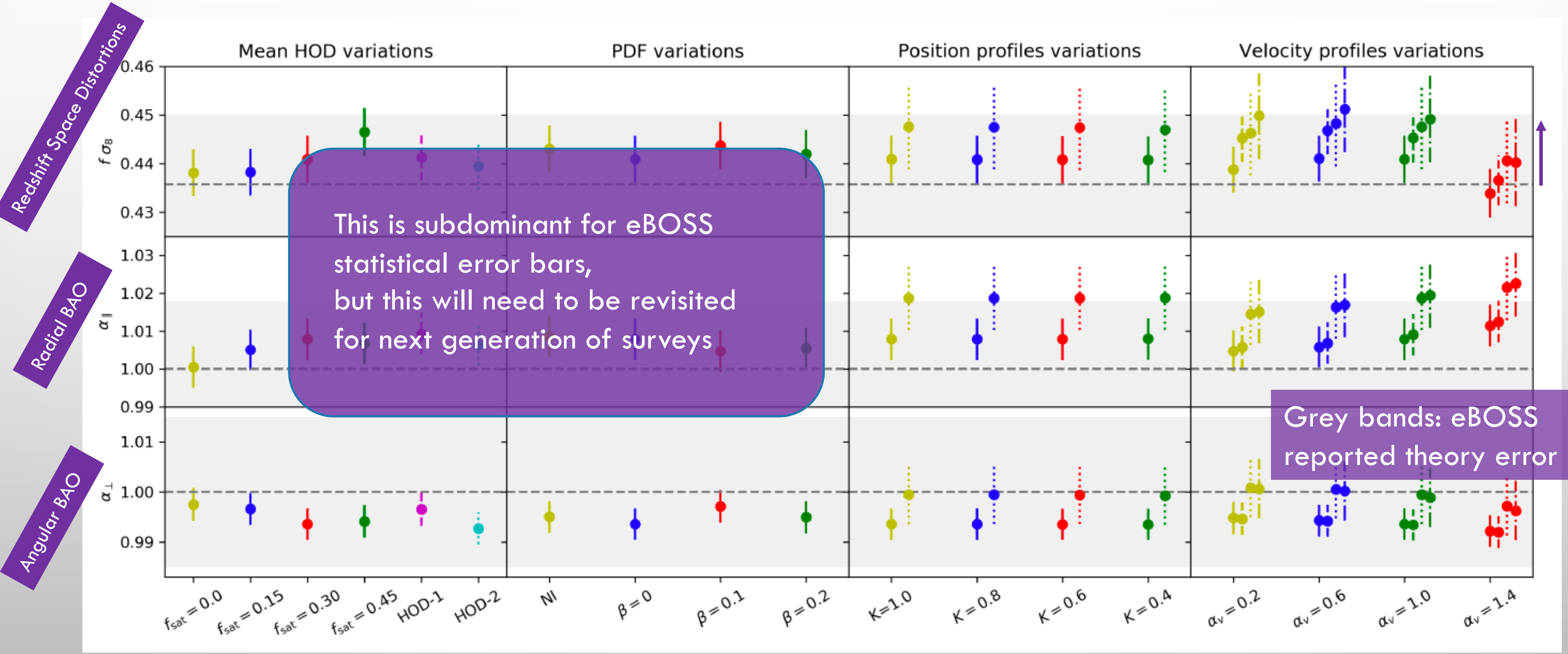

This is subdominant for eBOSS statistical error bars,
but this will need to be revisited for next generation of surveys

Grey bands: eBOSS reported theory error bars

HOW CAN THE 1-HALO TERM REALLY AFFECT OUR COSMOLOGICAL FITS?

REMEMBER, THE QUADRUPOLE IS AFFECTED

- UP TO ~50 Mpc/h

- But also, in Fourier space, things are more mixed up…

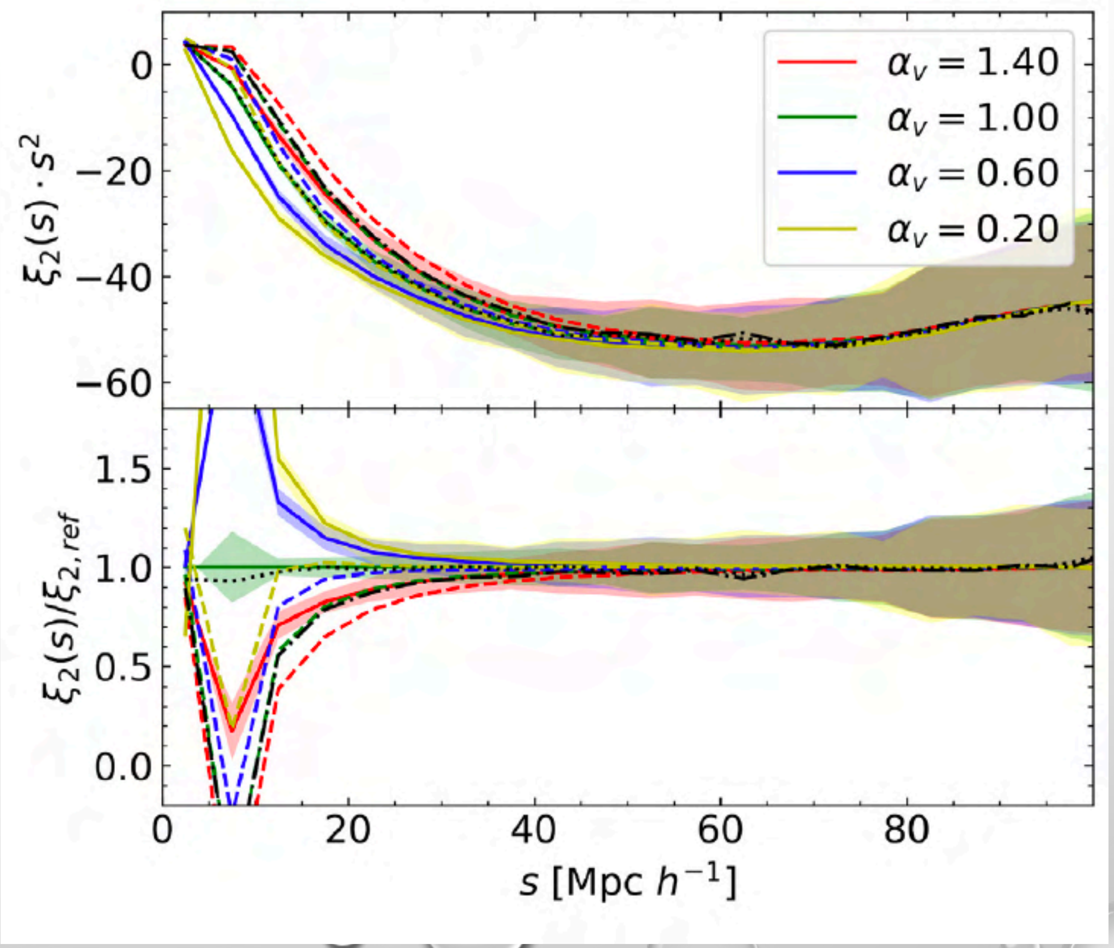

CLUSTERING IN FOURIER SPACE

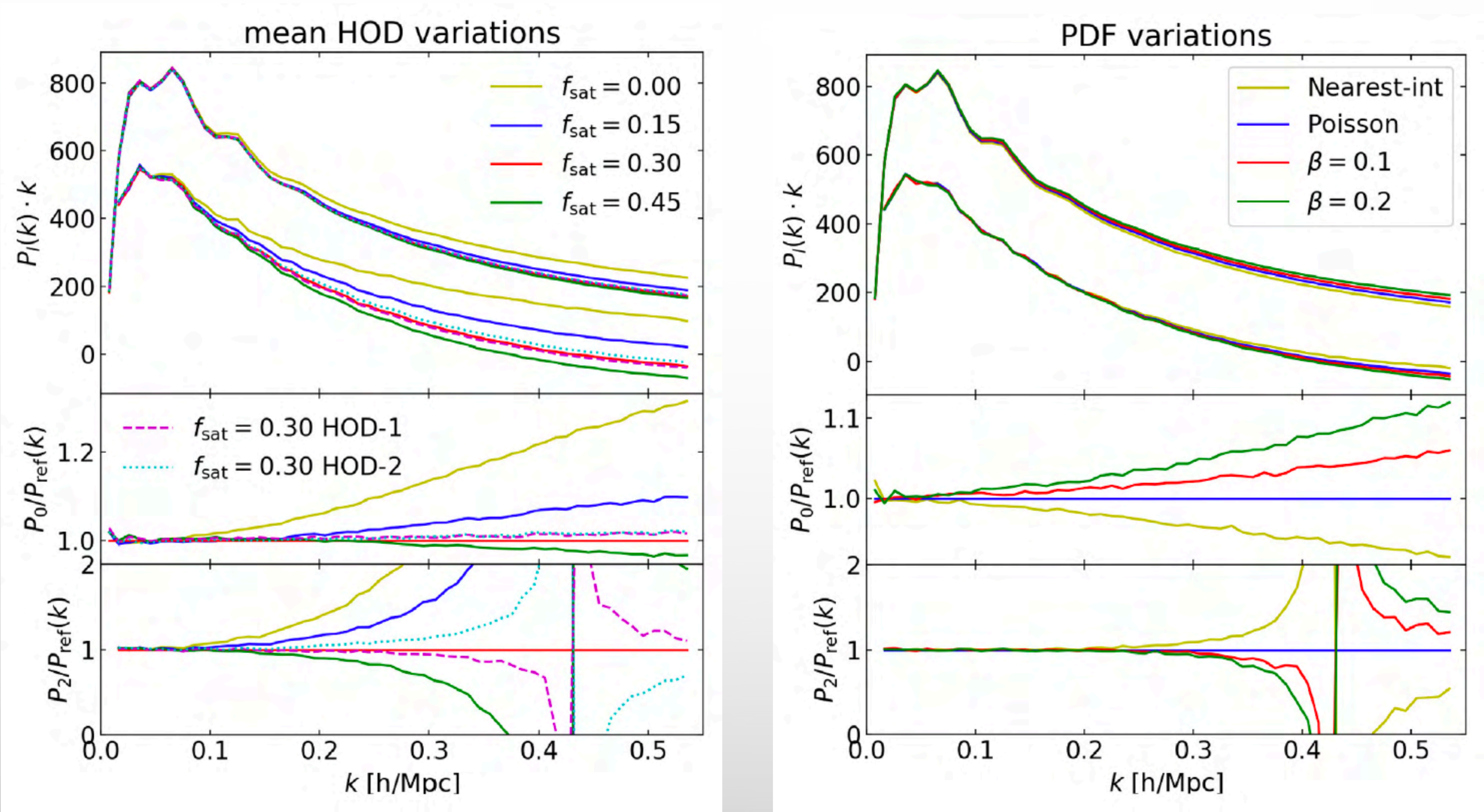

CLUSTERING IN FOURIER SPACE

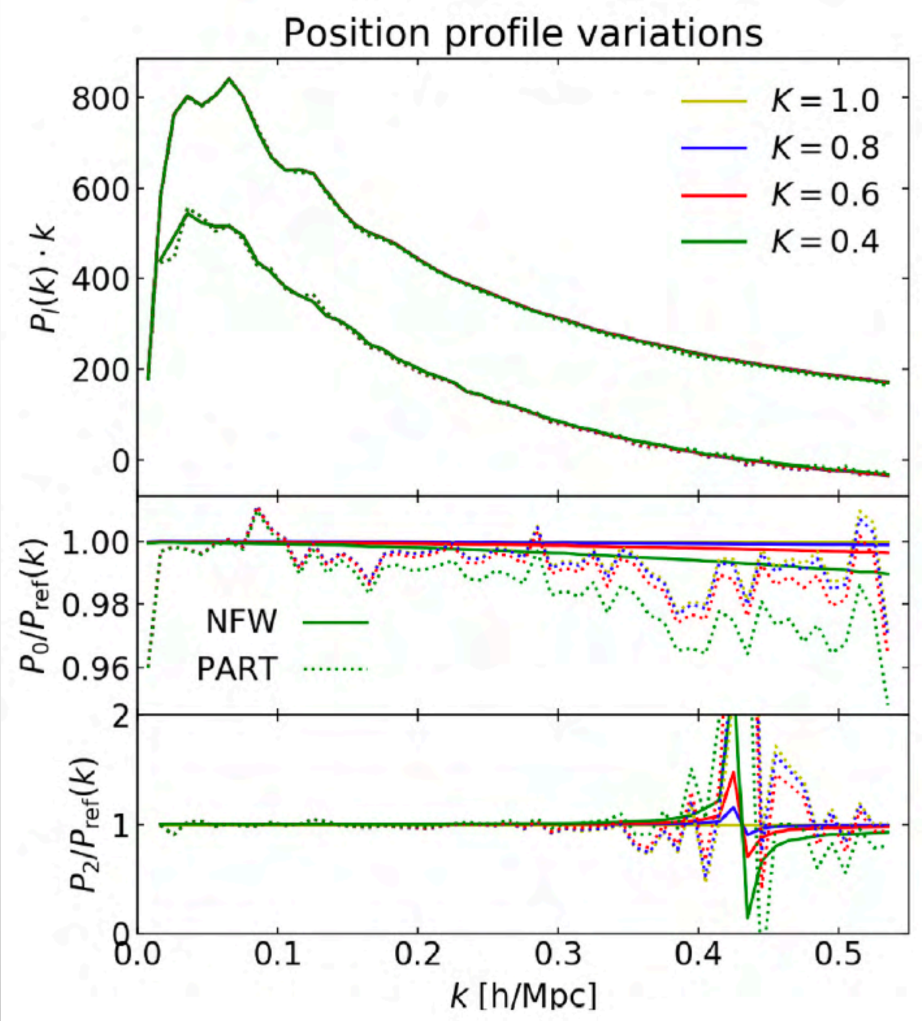

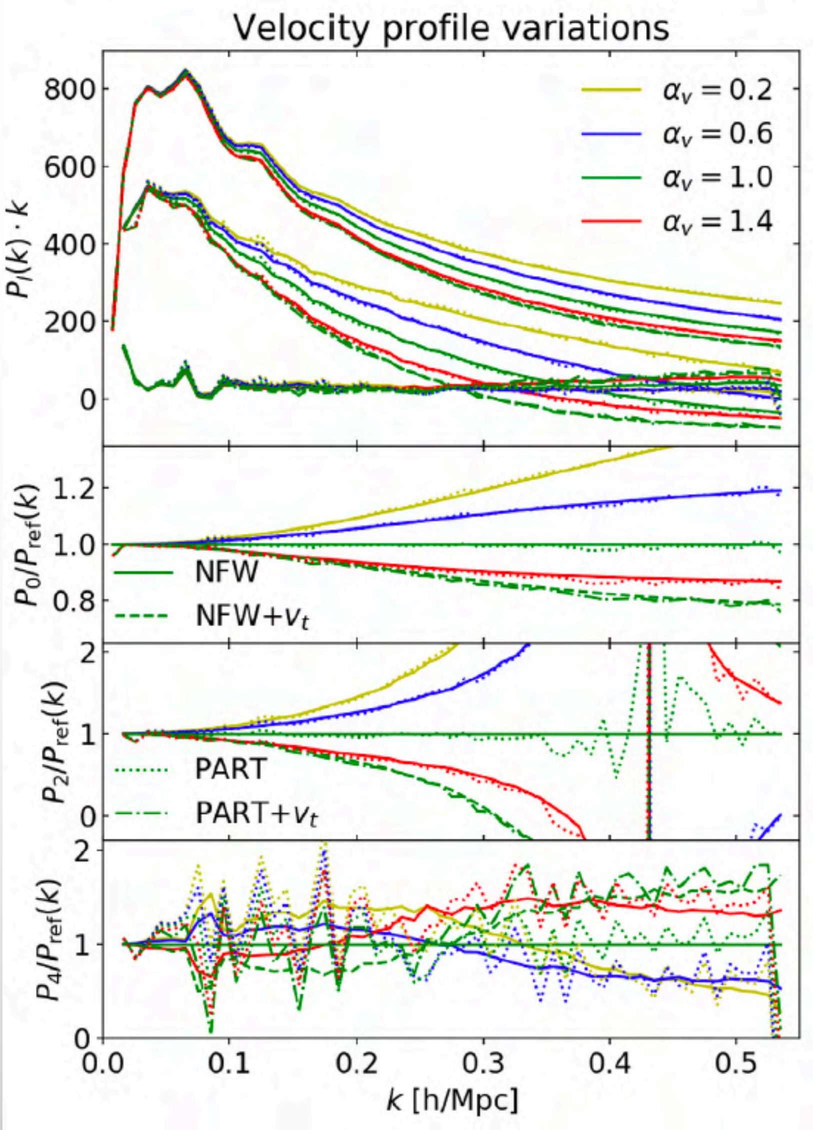

PART V. OUTLOOK

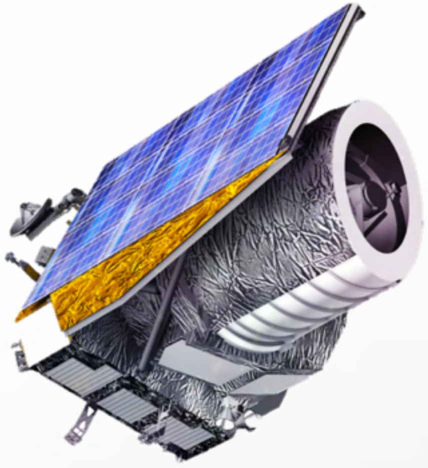

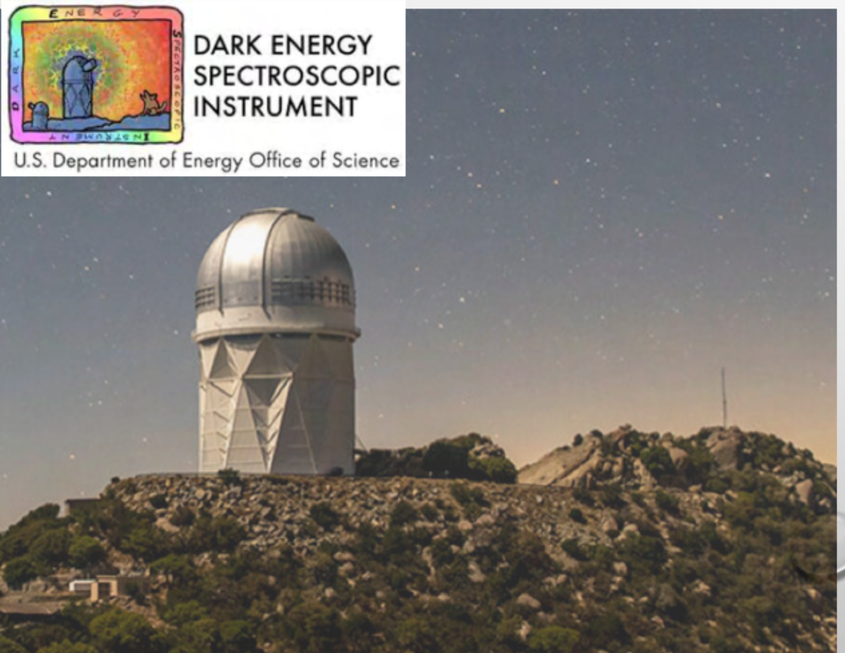

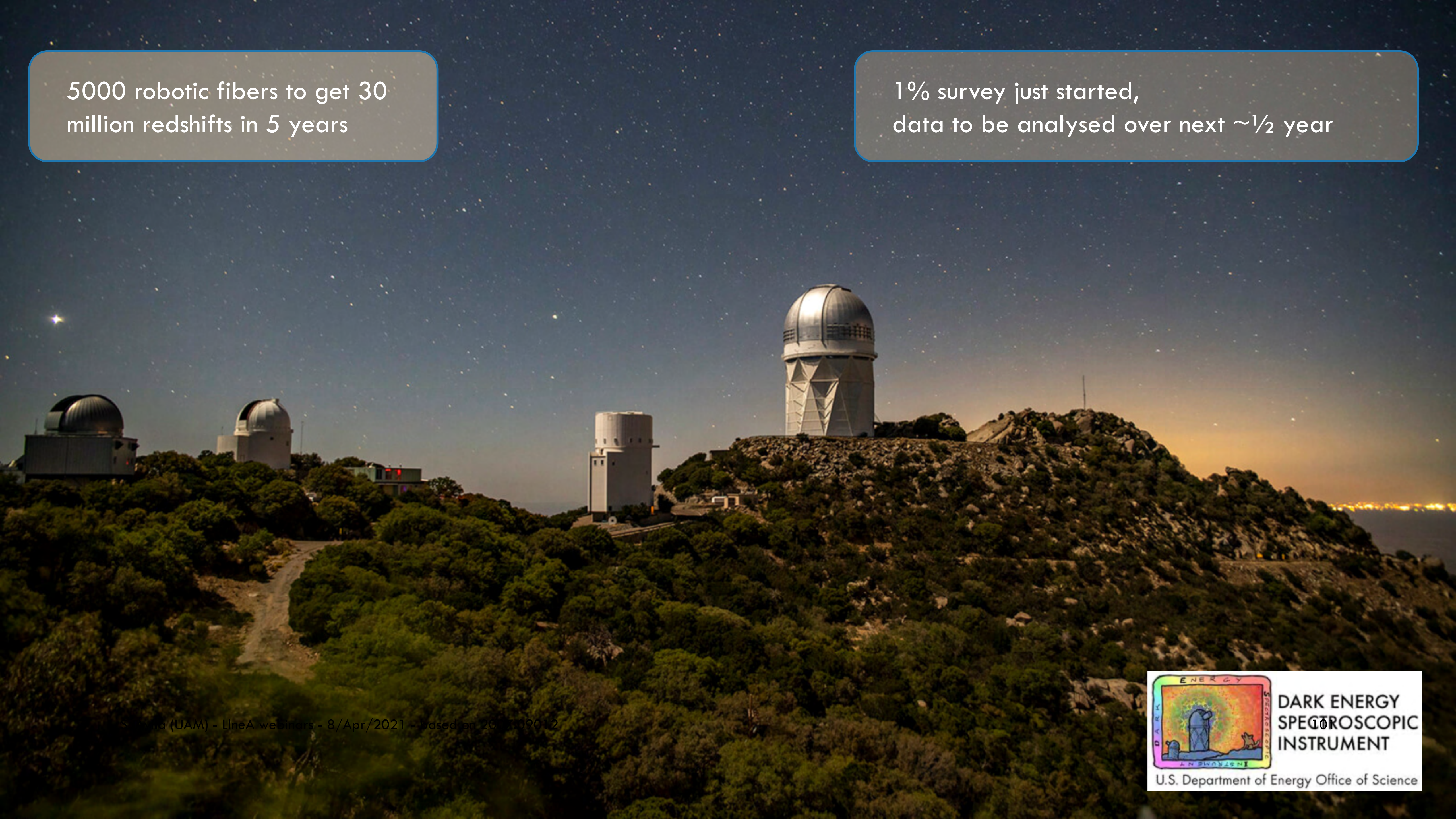

5000 robotic fibers to get 30 million redshifts in 5 years

1% survey just started,
data to be analysed over next ~½ year

DARK ENERGY SPECTROSCOPIC INSTRUMENT
U.S. Department of Energy Office of Science

5000 robotic fibers to get 30 million redshifts in 5 years

1% survey just started,
data to be analysed over next ~½ year

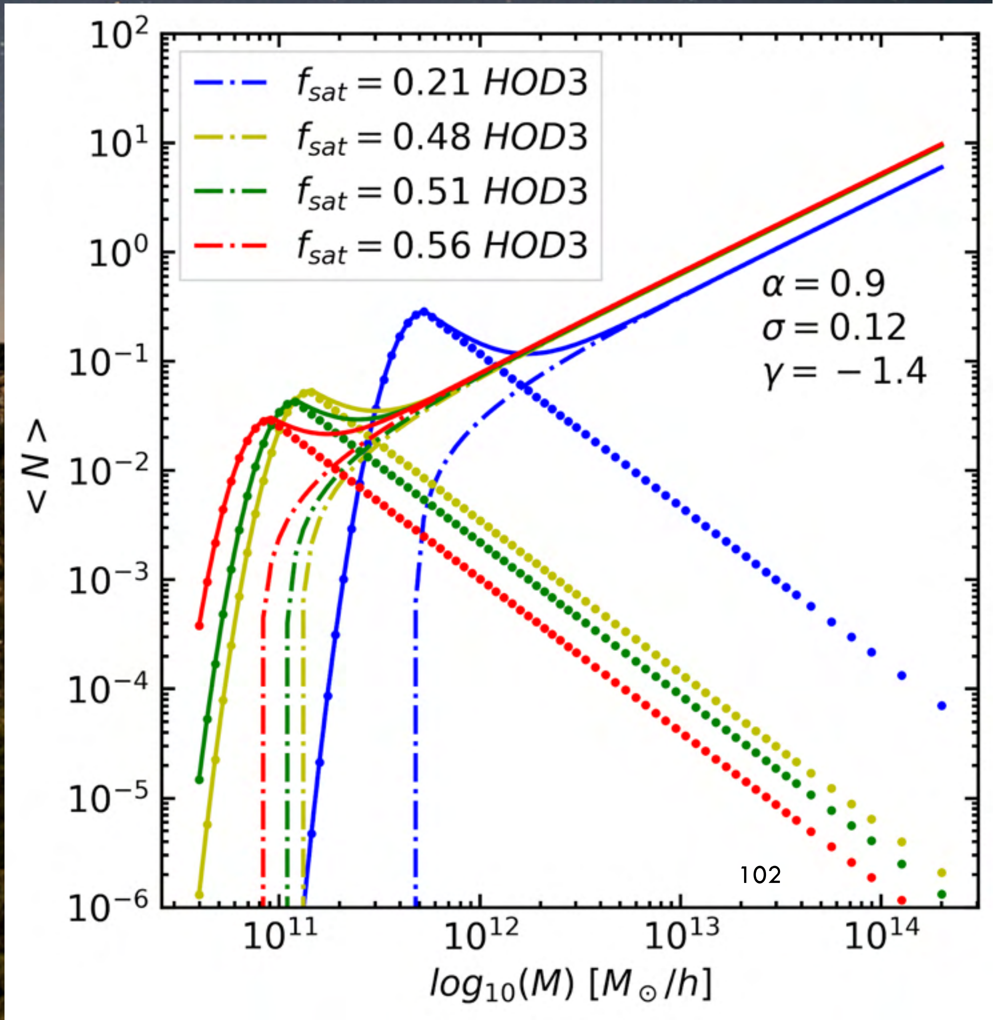

We have adapted the pipeline to implement what we learnt from Avila+2020 and eBOSS to DESI.
(B. Vos-Ginés, V. González-Pérez, Ávila+ DESI)

within HOD mock challenge key project.

DARK ENERGY SPECTROSCOPIC INSTRUMENT
U.S. Department of Energy Office of Science

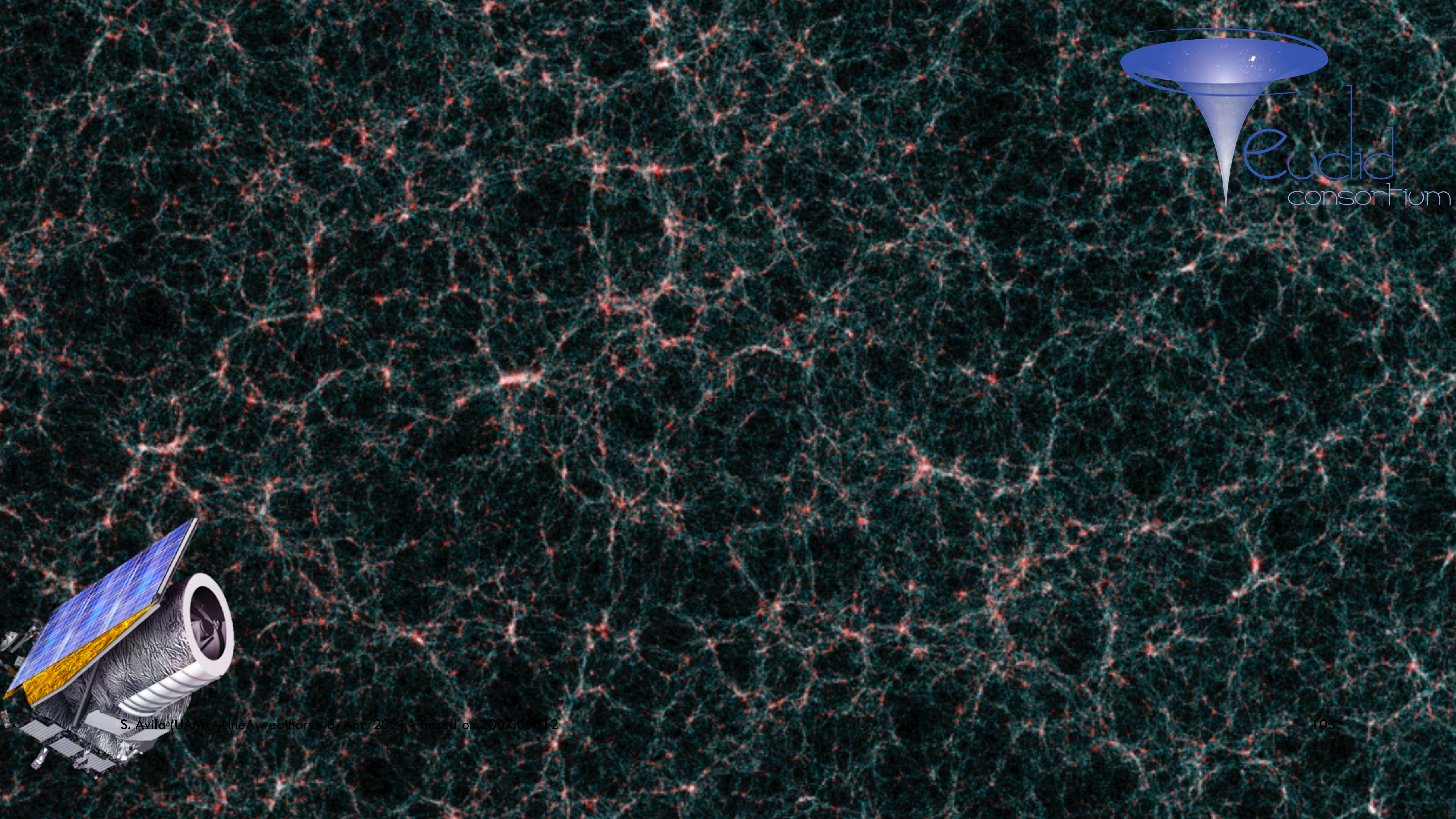
euclid
consortium

Euclid, 2 experiments in 1

Area ~ 15,000 deg^2

Spectroscopic H-alpha emission line survey in

$0.9<z<1.8$

~30 million galaxies

Photometric survey

30 gal/$arcmin^2$

$0<z<2.5$

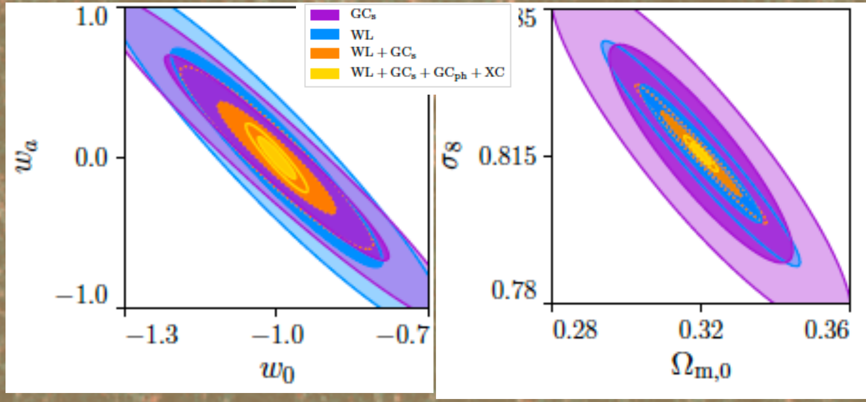

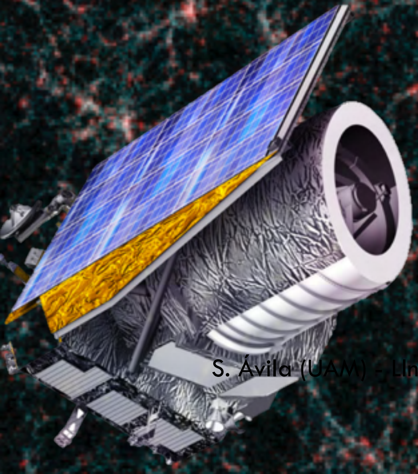

https://arxiv.org/abs/1910.09273

European Space Agency
Agence spatiale européenne

Euclid, 2 experiments in 1

Area ~ 15,000 deg^2

Spectroscopic H-alpha emission line survey in

$0.9<z<1.8$

~30 million galaxies

Photometric survey

30 gal/arcmin^2

$0<z<2.5$

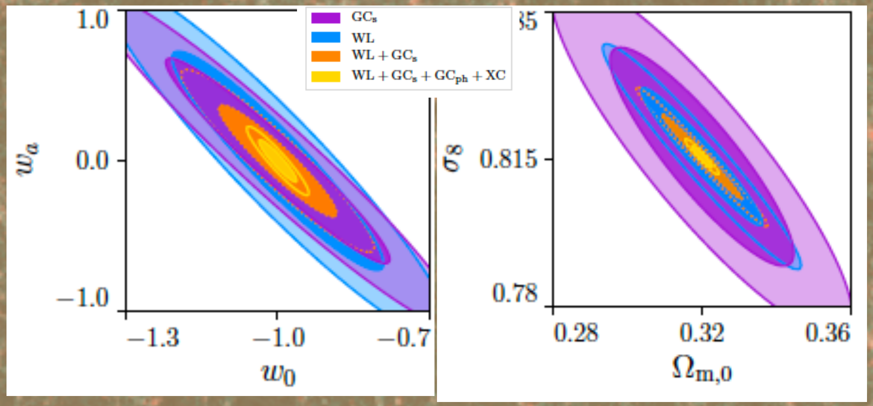

Planning to also adapt the same pipeline to Euclid and run a HOD mock challenge

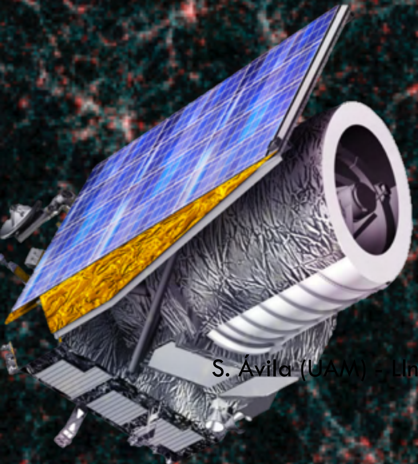

https://arxiv.org/abs/1910.09273

European Space Agency
Agence spatiale européenne

MOVING FORWARD WITH NEW SIMULATIONS

Unique suite with galactic physics and an effective volume ~7 times larger than Euclid/DESI

Ideal to test clustering models

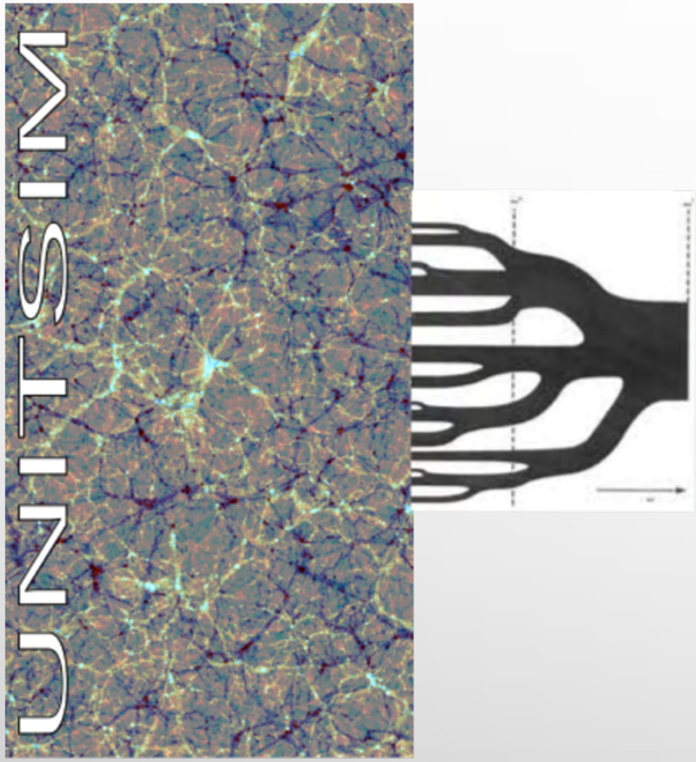

SAGE

get_emlines

Euclid H-alpha Galaxies

Study halo-galaxy connection

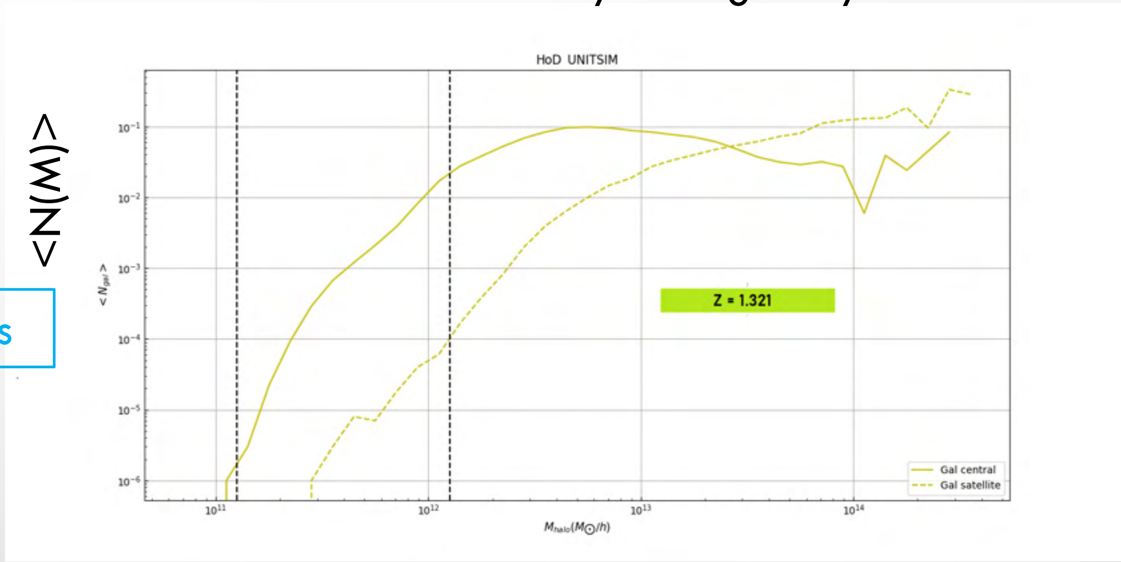

Reyes, Avila, Gonzalez-Perez, Knebe in prep.

Knebe, Lopez-Cano, Avila, …
arXiv:2103.13088
Deriving abundance and clustering of H-alpha ELGs (Euclid targets). Catalogues available.

Square Kilometer Array

The phase-I SKA HI intensity mapping program will survey 20,000 deg^2 in the $0.3<z<3$ range.

Very large scales!!

Square Kilometer Array

Vos-Ginés, Ávila, Cunnington, in prep.: is BAO still visible after observational effects?

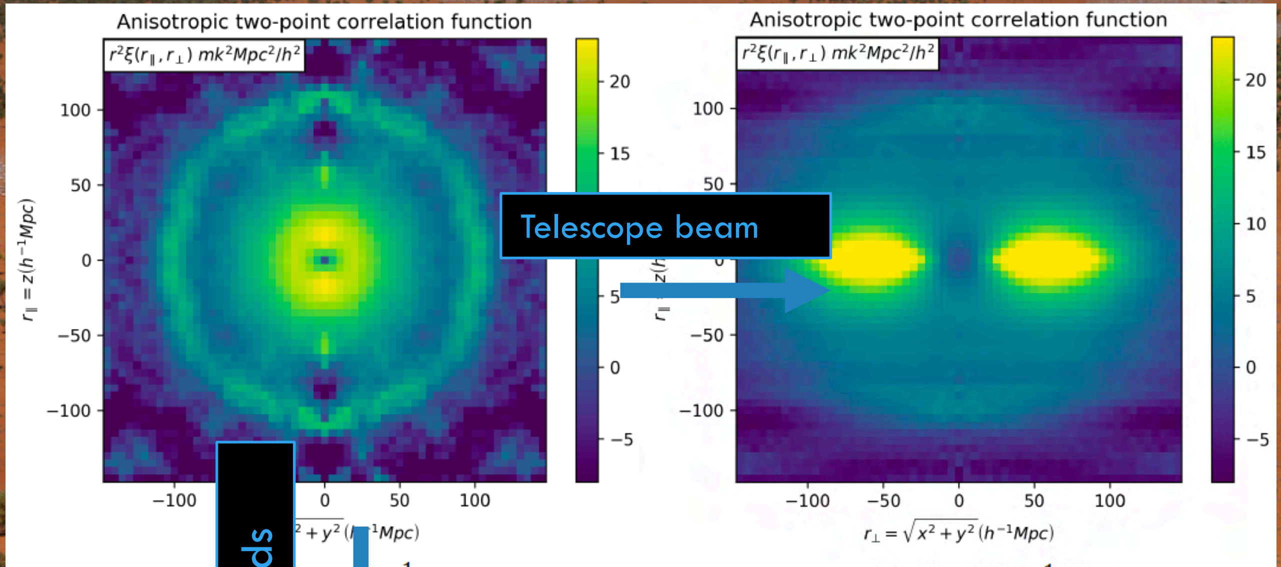

R=0 $h^{-1}Mpc$

(c) R=25 $h^{-1}Mpc$

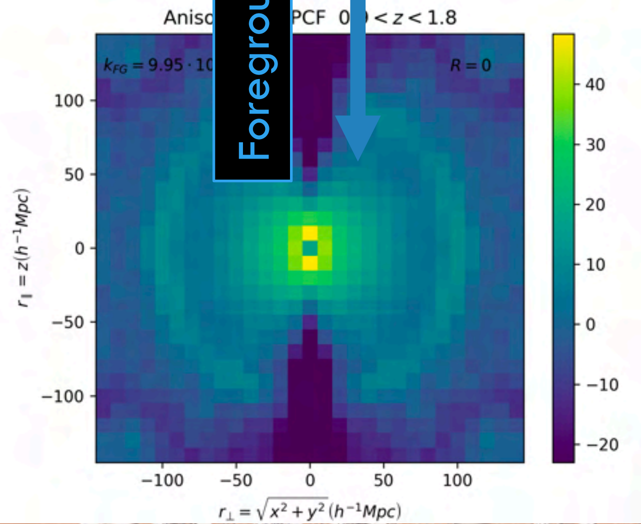

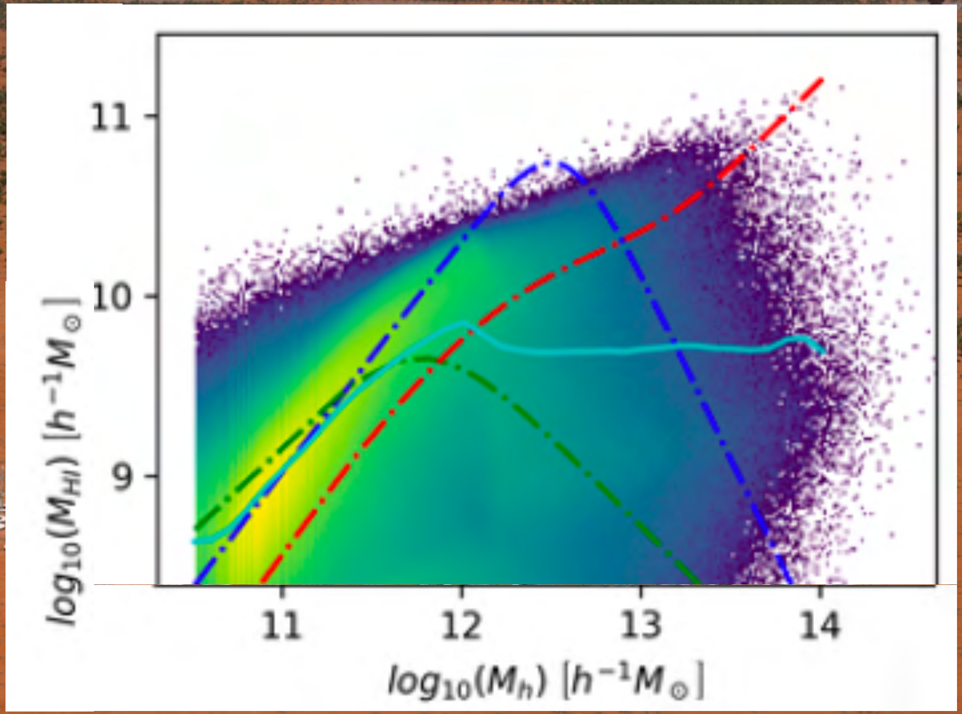

SKA starting construction
But precursor MeerKAT has already data!

SQUARE KILOMETRE ARRAY

CONCLUSIONS

- We dissected the assumptions that go into the HOD model for ELGs.
- We studied how the detailed choices of
  - Mean halo occupation
  - Satellite probability distribution function
  - Satellite position profiles
  - Satellite velocity profiles

affect galaxy clustering. We studied models motivated from previous studies.

- The satellite assignment choices (PDF + profiles) are found more relevant than the mean occupation
- We find strong and robust evidence for under-concentrated ELG profiles, and find this piece key in order to fit the data.
- The galaxy-halo connection is shown to affect galaxy clustering even in "Cosmological scales" and potentially cosmological inference. Although we showed this effect was subdominant for the eBOSS analysis.
- Future surveys, with increased statistical power, and planning to disentangle smaller scales will need to test their pipeline against different galaxy mocks.
- Our work is particularly relevant for Euclid and DESI, that will heavily rely on Emission Line Galaxies.

SCALE CUTS

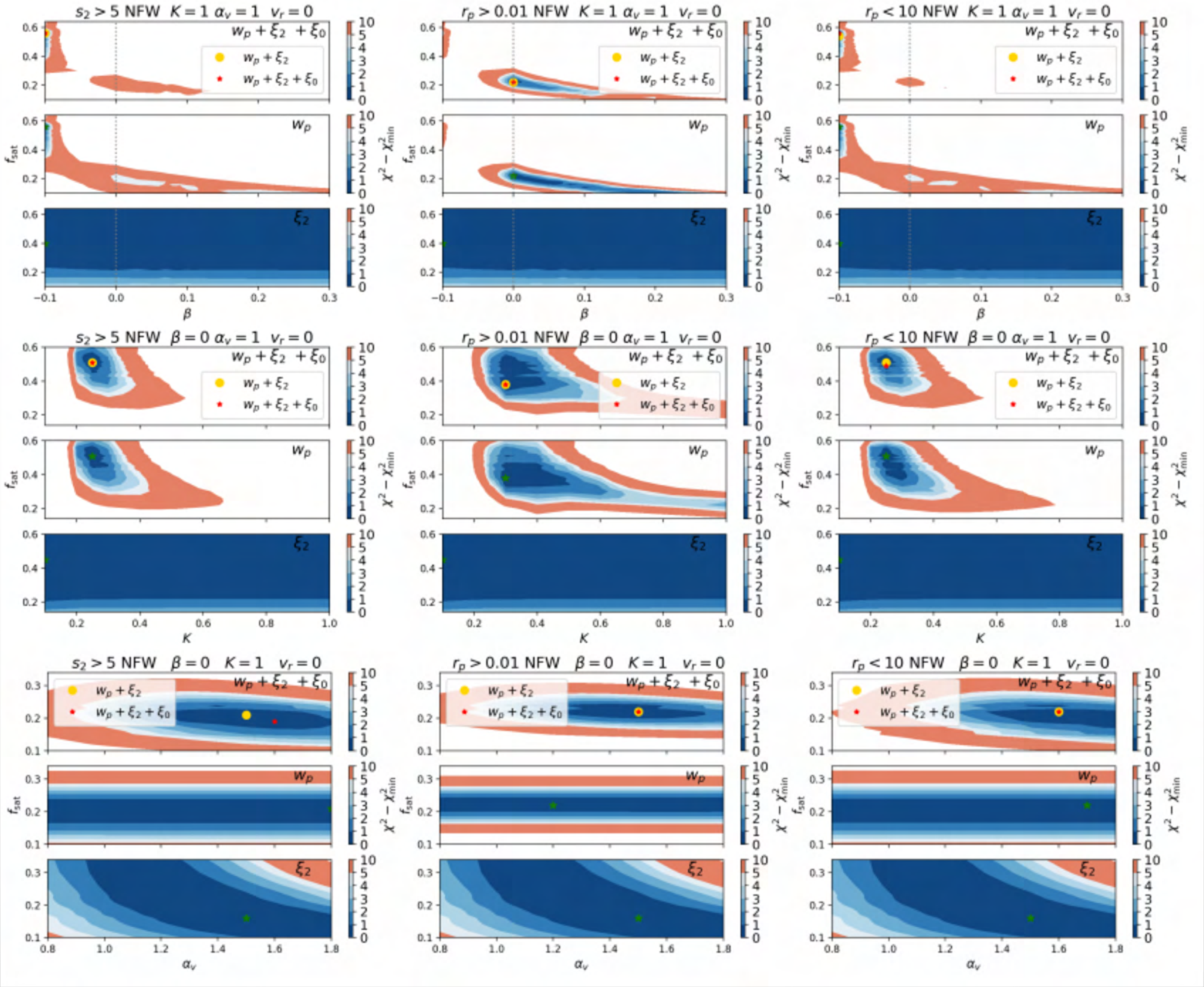
$s_2 > 5$ NFW $K=1$ $\alpha_v=1$ $v_r=0$
$r_p > 0.01$ NFW $K=1$ $\alpha_v=1$ $v_r=0$
$r_p < 10$ NFW $K=1$ $\alpha_v=1$ $v_r=0$
$s_2 > 5$ NFW $\beta=0$ $\alpha_v=1$ $v_r=0$
$r_p > 0.01$ NFW $\beta=0$ $\alpha_v=1$ $v_r=0$
$r_p < 10$ NFW $\beta=0$ $\alpha_v=1$ $v_r=0$
$s_2 > 5$ NFW $\beta=0$ $K=1$ $v_r=0$
$r_p > 0.01$ NFW $\beta=0$ $K=1$ $v_r=0$
$r_p < 10$ NFW $\beta=0$ $K=1$ $v_r=0$
$w_p + \xi_2 + \xi_0$
$w_p + \xi_2$
w_p
ξ_2
f_{sat}
$\chi^2 - \chi^2_{min}$
β
K
α_v